## NEW RESULTS IN DELAYED PROTON EMISSION

by

# Ronald I. Verrall

A thesis submitted to the Faculty of Graduate Studies and Research of McGill University in partial fulfillment of the requirements for the degree of Doctor of Philosophy.

July 1968

Foster Radiation Laboratory

McGill University

Montreal

### **ABSTRACT**

The previously unidentified nuclei  $^9\mathrm{C}$ ,  $^{29}\mathrm{S}$ ,  $^{33}\mathrm{Ar}$  and  $^{37}\mathrm{Ca}$  have been observed to decay with the delayed emission of protons. Lifetimes of the nuclei and the proton energies involved were recorded. Using the relative intensities of the proton peaks,  $\log \underline{ft}$  values were measured for a number of the  $\beta^+$  decay branches of the nuclei  $^{21}\mathrm{Mg}$ ,  $^{25}\mathrm{Si}$ ,  $^{29}\mathrm{S}$ ,  $^{33}\mathrm{Ar}$  and  $^{37}\mathrm{Ca}$ .

A counter telescope for the observation of low energy protons (down to 0.8 MeV) in a large gamma ray background was designed and built, using a thin proportional counter as the dE/dx detector. With this telescope, the energies and intensities of new low energy proton peaks following the decay of <sup>21</sup>Mg and <sup>29</sup>S were measured. Log ft values for the \$\beta^+\$ transitions were estimated. The known nucleus \$\frac{40}{3}\$Sc was discovered to be a delayed proton precursor. Energies and relative intensities of eighteen peaks, all below 4 MeV, were measured.

#### AC KNOWLEDGEMENTS

I would like to thank Professor R.E. Bell, my research supervisor, for his encouragement, and for the suggestion of solutions to many problems.

I thank Professor R. Barton who, before he left McGill University, was my supervisor. His assistance and interest were appreciated.

Professor R.B. Moore has given unstintingly of his time to help me with technical problems and has had a continuing interest in the experiment, the problems and the results.

The first part of this investigation was done in collaboration with Dr. J.C. Hardy. Because of our close association and frequent discussions I learned much more than I could have, had I worked alone.

I gratefully acknowledge financial assistance in the form of a studentship from the National Research Council.

			Page
	ABST	ract	ii
	ACKI	NOWLEDGEMENTS	iii
1	INT	RODUCTION	1
2	HIST	TORICAL BACKGROUND	5
3	EXPE	RIMENTAL APPARATUS	8
	3.1	Detection Systems	8
	3.2	Electronics	9
4	GAS	COUNTER SYSTEM	14
	4.1	Introduction	14
	4.2	Choice of Gas Counter	15
	4.3	Design Criteria	16
	4.4	Description and Construction of Counter System	16
	4.5	Gas Filling	19
	4.6	Operational Values	19
5	EXPE	RIMENTAL PROCEDURES AND TECHNIQUES	25
	5.1	General	25
	5.2	Energy Determination	25
	5.3	Lifetimes	26
	5.4	Relative Intensities	27
	5•5	Particle Identification	29
	5.6	Precursor Identification	30
	5•7	Square Root Graph Paper	32
	5.8	Nomogram for Determining Log ft Values	32

6	TARGET PREPARATIONS	34
	6.1 Requirements	34
	6.2 General Method	35
	6.3 Lithium and Beryllium	35
	6.4 Boron	36
	6.5 Carbon	36
	6.6 Magnesium	36
	6.7 Phosphorus	37
	6.8 Sulfur	37
	6.9 Chlorine	38
	6.10 Potassium	38
	6.11 Calcium	38
	6.12 Titanium, Nickel and Copper	39
	6.13 Vanadium, Chromium and Manganese	39
	6.14 Composite Targets	39
7	RESULTS	40
	7.1 Using Single Counter Detection System	40
	7.2 Using the Gas Counter Telescope System	41
	7.3 Magnesium - 21	43
	7.4 Sulfur - 29	<i>5</i> 0
	7.5 Scandium - 40	56
8	SUGGESTIONS FOR FURTHER RESEARCH	69
	8.1 Apparatus and Techniques	69
	8.2 Experiments	70
9	SUMMARY	73

75
76
77
78
79
<b>3</b> 0
31
9
5
8

#### 1 INTRODUCTION

The work reported in this thesis can be divided into two distinct parts. The first part, carried out in collaboration with J.C. Hardy, was the discovery and preliminary investigation of a number of nuclides belonging to the series having the form (Z,N) = (2k + 2, 2k - 1). These are  ${}^{9}$ C,  ${}^{29}$ S,  ${}^{33}$ Ar and  ${}^{37}$ Ca. Measurements were made on the beta-delayed protons emitted in their decay. The second part of the work involved the design and construction of a counter telescope and its subsequent use to investigate low energy protons emitted from the nuclides  ${}^{21}$ Mg and  ${}^{29}$ S. Also, with the aid of the counter telescope it was found that the T = 1 nucleus  ${}^{40}$ Sc is a delayed proton emitter. This is the first example of a delayed proton precursor in this low mass region which does not belong to the previously mentioned series. When, in this thesis, work is reported which was done in collaboration with J.C. Hardy, explicit note of this fact will be made. Otherwise it is to be assumed that the research was carried out by myself.

For a complete description of the types of delayed proton emission (self-delayed, double-delayed and beta-delayed) the reader is referred to a number of articles (Barton (1963), Goldanski (1960, 1961)). These articles predict the existence of, and give a general description of these processes. To date, the only one of these which has been experimentally observed is beta-delayed proton emission, called "delayed proton emission" in what follows.

This process is depicted in fig. 1.1. The (Z,N) values represent the general case for the sequence of nuclides discussed in this thesis. The "precursor" (the name in general usage) is produced in our case by the proton bombardment of a suitable isotope, although the means by which it is created is irrevelant to its subsequent decay. The precursor decays

by beta emission to various states of the "intermediate nucleus". If the excited state of the intermediate nucleus has sufficient energy, it will be energetically possible for the nucleus to emit a proton to become what is called the "residual nucleus". It is the emitted protons which are observed.

## Measurable Quantities:

Because relatively few nuclides decay by the emission of a proton, and because it is fairly easy to detect protons in the midst of a large beta and gamma background, we have available a powerful technique of investigating these nuclides without being overwhelmed by the background of other decays taking place in the source. If these nuclides did not give rise to proton emission, it would be extremely difficult to investigate them using the more standard techniques of gamma and beta spectroscopy.

The energies of the emitted protons may be measured, giving information on the level structure of the intermediate nucleus.

A lifetime measurement may be made on the emitted protons. Since the lifetime of the intermediate nucleus is that of a compound nucleus ( $\approx$ 10<sup>-18</sup> sec), this may be considered instantaneous on the time scale involved. The half-life measured will therefore be the half-life of the precursor.

Relative intensities of the proton groups may be measured. This will give information on the beta branching ratios of the precursor.

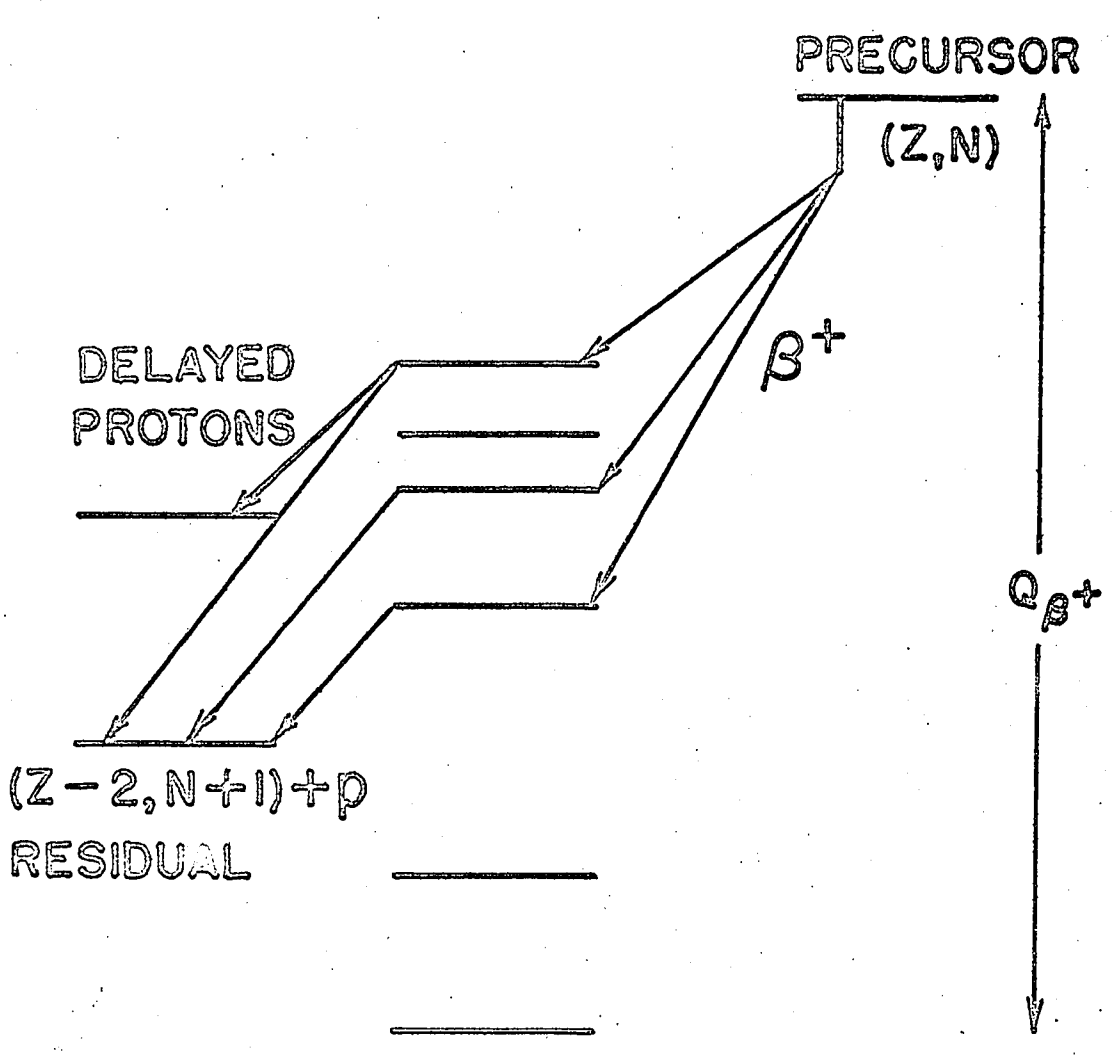
Coincidence studies and angular correlation measurements between the proton and the preceding beta particle or the following gamma ray would contribute information to the decay scheme and the spins and parities of the levels. These studies, however, are as yet impossible in practice at this laboratory. In the external beam, the counting rate would be too low

to be feasible. As for the internal beam, one has the problem of an enormous gamma background counting rate. Added to this, one has the technical problem of setting up a coincidence experiment in a very small area and in a 16 kilogauss magnetic field.

FIGURE 1.1

.

Figure 1.1: General decay sequence of delayed proton emitters.



(Z-I, N+I) INTERMEDIATE

# 2 HISTORICAL BACKGROUND

The possibility of proton radioactivity has been considered for many years. More than 15 years ago Alvarez (1950) attempted to detect proton emitters. He bombarded \$^{10}\$B\$ and \$^{19}\$F\$ with 32 MeV protons in order to produce delayed proton emitters by the reactions \$^{10}\$B(p,2n)\$^{9}\$C\$ and \$^{19}\$F(p,3n)\$^{17}\$Ne. He failed in this search, however, but discovered the delayed alpha emitters \$^{8}\$B\$ and \$^{20}\$Na in the course of this experiment. The first proton activity was seen in 1962. Between these two dates, there were a number of theoretical papers discussing the existence and nature of various types of proton decay. It is the purpose of this section to chronicle these and other papers dealing with proton decay in general and with beta delayed proton emission in particular.

The existence of a number of proton rich nuclei in the region 17< A < 40 were predicted by Baz (1959). These included the nuclei <sup>17</sup>Ne, <sup>21</sup>Mg, <sup>25</sup>Si, <sup>29</sup>S, <sup>33</sup>Ar and <sup>37</sup>Ca which have since been discovered and are known to be delayed proton precursors. Zel'dovich (1960) extended these predictions to lighter nuclei and in particular to <sup>13</sup>O. Goldanski (1960) carried out a detailed analysis of the proton stability limits and of the decay energies of neutron-deficient isotopes up to tin. He also predicted two-proton radioactivity and its main features in this paper. Karnaukhov et al (1964) extended the predictions to nuclei with Z > 50. Jaenecke (1965a) predicted that <sup>9</sup>C, <sup>17</sup>Ne, <sup>21</sup>Mg and <sup>25</sup>Si (among others) should be delayed proton emitters. Jaenecke (1965b) also proposed a formula to predict the masses of unknown isobaric states and the masses of unknown proton rich nuclei.

The first experimental results appeared in a paper by Karmaukhov et al (1962) in which they reported the observation of events which were assumed to be protons. They bombarded nickel and tantalum targets with

20Ne ions and observed delayed particles which had an energy between 3.0 and 4.5 MeV and were much less ionizing than a 4 MeV alpha particle. They were delayed by at least 0.1 sec.

Barton et al. (1963) in discovering <sup>25</sup>Si were the first to identify a delayed proton precursor. Also, they positively identified the observed radiation as protons.

Flerov et al. (1964) observed two delayed proton emitters. One was identified as a light isotope of Ne or Mg and the other as a light isotope of Br or Kr.

D'Auria and Preiss (1964) reported a 690 msec activity which they tentatively attributed to <sup>17</sup>Ne.

McPherson et al. (1964) identified <sup>17</sup>Ne, proposed a decay scheme and gave its half-life as 103 msec.

Hardy and Verrall (1964a) identified <sup>29</sup>S, proposed a decay scheme involving the analogue state in <sup>29</sup>P and gave its half-life as 195 msec.

Hardy and Verrall (1964b) and Reeder et al. (1964) in simultaneous publications reported the identification of <sup>37</sup>Ca and <sup>33</sup>Ar. Both groups gave half-lives and proposed decay schemes. The latter group also reported the observation of <sup>41</sup>Ti.

McPherson and Hardy (1965) identified  $^{21}$ Mg and gave lifetimes and proton energies for it and for  $^{25}$ Si.

Hardy et al. (1965) identified 9C and reported its lifetime and its proton decay spectra.

Siivola (1965) gave details of the decay of 108 Te by beta delayed proton emission.

Hardy and Verrall (1965) gave further details on the decay of <sup>33</sup>Ar.

Hardy and Bell (1965) gave further information on the decay of <sup>17</sup>Ne,

21<sub>Mg</sub>, <sup>25</sup>Si and extended the proton spectra up to 8 MeV.

Hardy, Verrall and Bell (1966) measured the log ft values for a number

of beta decay branches from the previously discovered nuclei  $^{21}$ Mg,  $^{25}$ Si,  $^{29}$ S,  $^{33}$ Ar and  $^{37}$ Ca. This was done by comparing the intensity of peaks in their delayed proton spectra with that of peaks in the spectrum following the decay of  $^{17}$ Ne. In conjunction with this paper, Hardy and Margolis (1965) calculated the log ft values for the superallowed beta decay branch of the same nuclei.

In a series of papers, the Brookhaven group gave new results on a number of the previously discovered isotopes. They record the new spectra with better resolution and statistics. They also quote revised half-lives. The papers are as follows:

Reeder et al (1966) -25si.

McPherson et al (1965) -130.

Poskanzer et al (1966) -33Ar, 37Ca and 41Ti.

Esterlund et al (1967) -17Ne.

Bogdanov et al (1967) observed delayed protons which they attribute to the decay of lllTe. The identification is made on the basis of the excitation function. They record with 25-30 keV resolution a complicated proton spectrum. The half-life quoted is 19.5 sec.

A more complete bibliography on proton radioactivity can be found in the review article by Goldanski (1966) where he reviews delayed proton emission as well as the other types of proton activity.

## 3 EXPERIMENTAL APPARATUS

#### 3.1 DETECTION SYSTEMS

Three detection systems were used.

- a) The first one, constructed by R. McPherson, was later used by J.C. Hardy and myself for part of the work reported in this thesis. This system consisted of a silicon surface barrier detector recessed into a solid aluminum block. The combination together with the target to be bombarded was attached to the end of a probe and inserted into the circulating beam of the McGill synchrocyclotron. (Fig. 3.1). The geometry was such that the aluminum block and the detector lay entirely below the median plane of the cyclotron. Thus the main proton beam would pass over the system without hitting it. The aluminum block was sufficiently thick, however, that any proton hitting the system could not penetrate to the detector. The target was situated in the path of the main proton beam. Beta particles emitted from the target spiral down (or up) the magnetic field. To eliminate these particles as a source of background the target was displaced horizontally far enough (\$21.5 inch) that most of these electrons could not get to the detector. Aluminum absorbers could be placed over the detector to stop alpha particles and to permit particle identification. The signal from the detector was led by a 6 foot coaxial cable down the centre of the probe to the preamplifier (Tennelec, model 100) which was mounted on the end of the probe. The detectors used were all nominally 300 mm thick, sufficient to stop a 6 MeV proton.
- b) The second system, built by J.C. Hardy and myself, was used only for the study of <sup>9</sup>C. It was a counter telescope consisting of a 50 µm totally depleted surface barrier detector (dE/dx) and a 3 mm lithium drifted detector (E). The detectors were mounted in an aluminum block very similar

to the one described in "a". The pulses from the two detectors were added and the sum was gated into the analyser only when the pulse height from the dE/dx detector fell between appropriate preset limits.

c) The third system was a telescope using a proportional counter as the dE/dx detector. A silicon surface barrier detector, identical to the one described in "a" was the E counter. The design and construction of this system are discussed in detail in Chapter 4 and it is listed here only for the sake of completeness.

### 3.2 ELECTRONICS

A block diagram of the electronics associated with detector systems "a" and "b" is shown in fig. 3.2. The lower part of this diagram shows the logic circuitry which controlled the operation of the cyclotron and the analyser during a run.

A typical cycle of operation was as follows. The cyclotron ran in its normal mode for 40 msec, after which the ion source trigger was turned off and the cyclotron oscillator continued to run for a further 60 msec. (Control not shown in fig. 3.2.) During this period, orbiting protons were swept out of the cyclotron tank. This was followed by a 40 msec delay. At this time, a gate which had been preventing pulses from getting to the analyser opened and a spectrum was collected for 32/60 sec (2<sup>n</sup> cycles of ordinary 60 cycle power). At the end of the cycle, the gate to the analyser closed and the cyclotron turned on once more. The times given above are typical but could be varied.

During the counting period, the detector pulses could be routed sequentially to the four quarters of the T.M.C. 256 channel analyser and by this means a half-life could be measured.

The routing equipment was built by Mr. K.S. Kuchela, the electronics

for system "a" is due to Drs. R. Barton and R. McPherson, and the electronics for system "b" was built by Dr. J.C. Hardy and myself.

System "c" is shown schematically in fig. 3.3. The 256 channel analyser of the earlier systems has been replaced by a 4096-channel, two-dimensional analyser. In one mode of operation, the pulses from the two detectors were fed to the analyser, the energy (E) pulses forming one dimension of the display and the dE/dx pulses forming the second dimension. In a second mode of operation the plug-in unit designated in the figure as "linear gate and A.D.C. unit B" was replaced by a multi-spectrum analyser which allowed the sequential storage of spectra in different sections of the memory. This was done for half-life determination. This unit, together with associated control electronics is shown at the bottom of the figure. The "end" pulse, signifying the completion of analysis is not a standard feature of the plug-in unit 204. It was made available for this particular set of experiments. The electronic devices in this diagram which were specially constructed were monostable flip-flops which were used as timing units and delays.

FIGURE 3.1

Figure 3.1: Experimental arrangement of the single detector system when mounted on a probe shaft and inserted into the circulating proton beam.

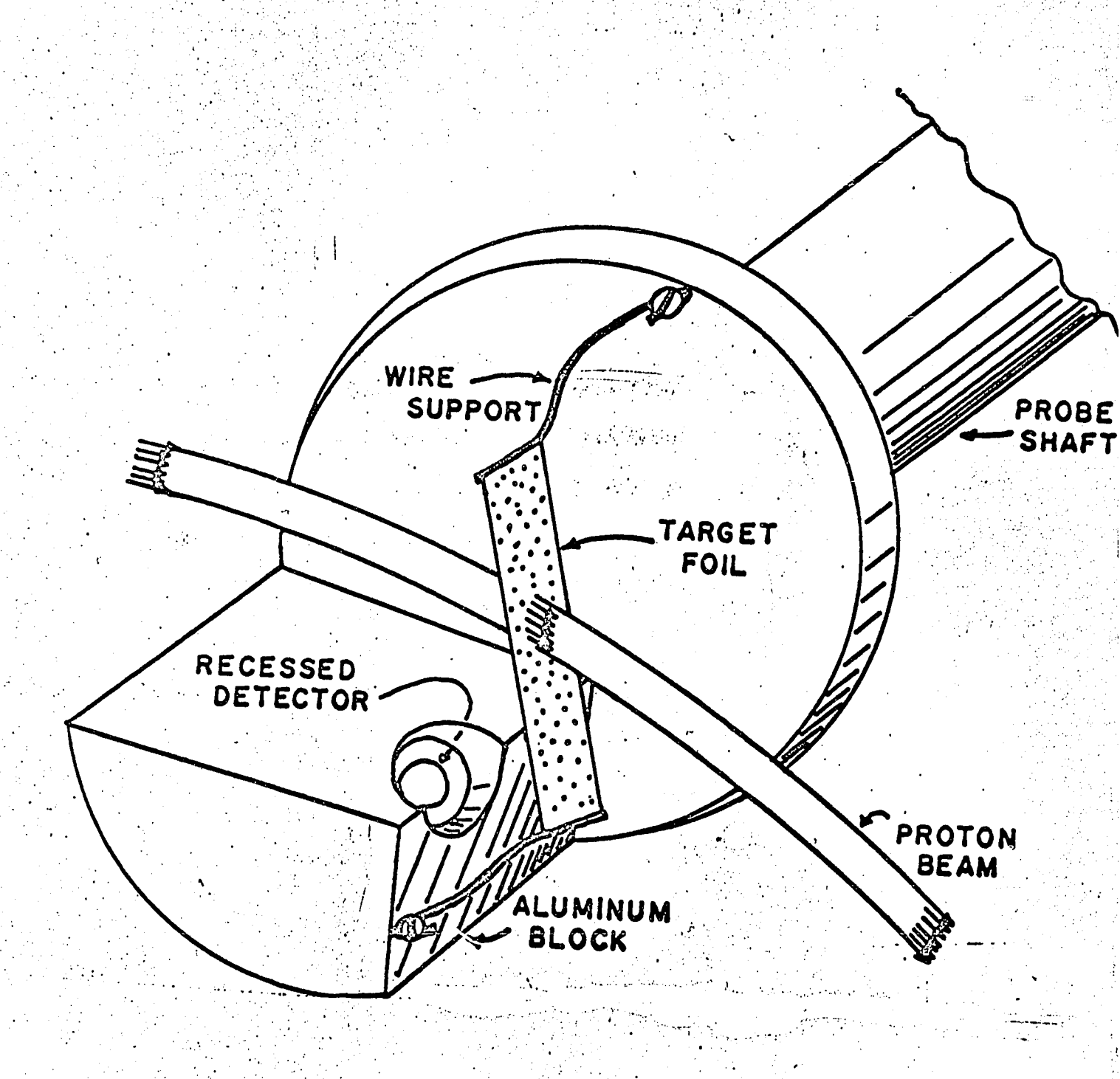
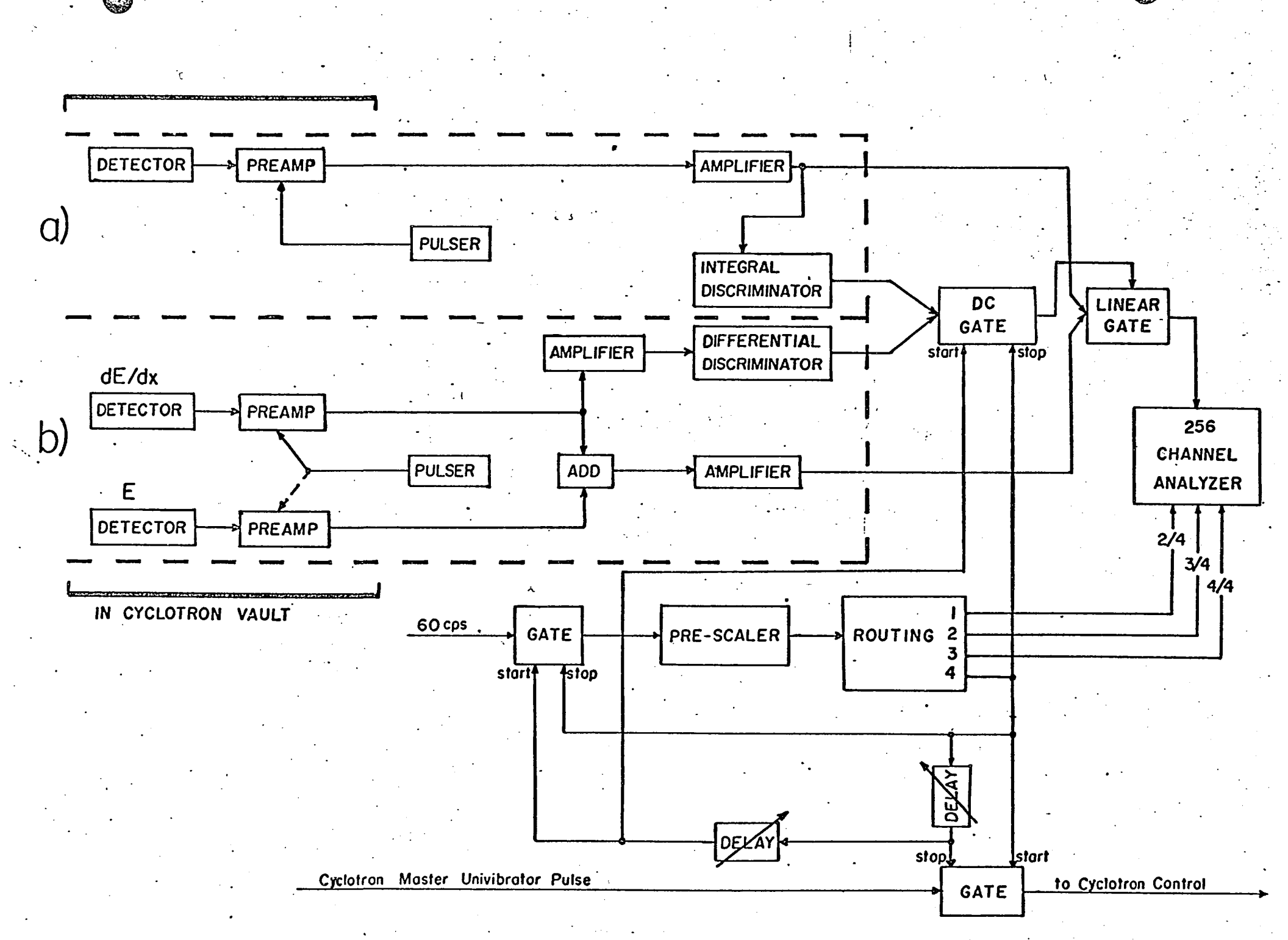


FIGURE 3.2

Figure 3.2: Block diagram of the electronics for systems "a" and "b".



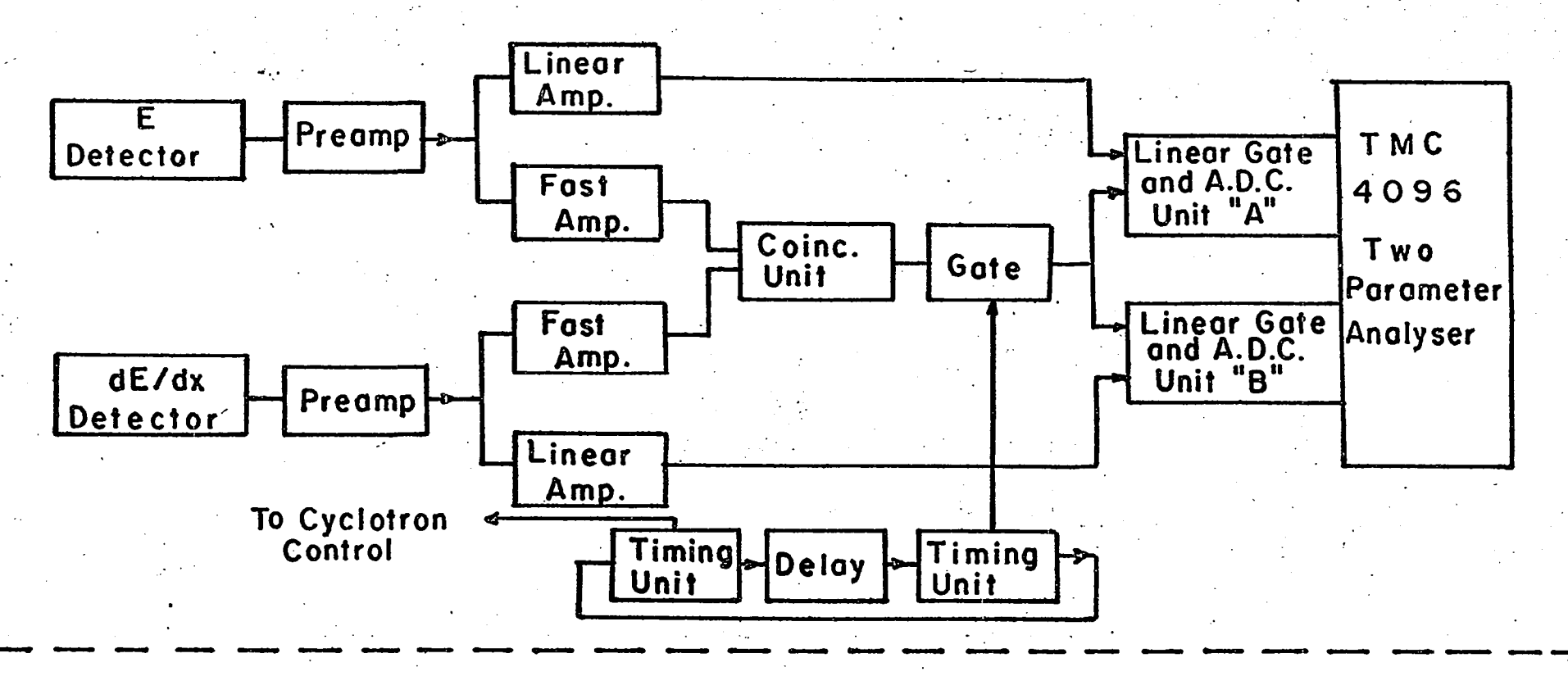
• The control of the Lorentz and the Lorentz a

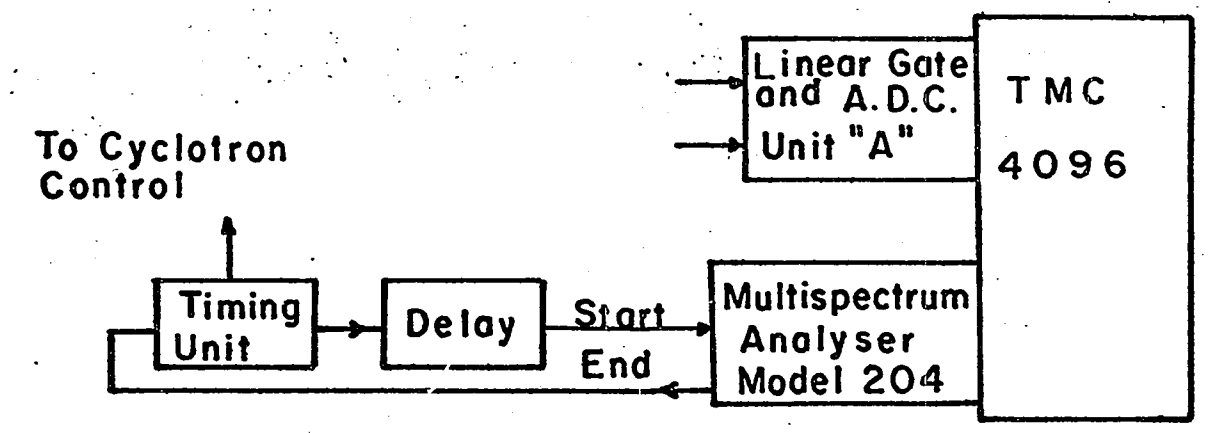
Figure 3.3: Block diagram of the electronics for system

"c". Unit "B" could be replaced by a multi
spectrum analyser as is shown in the lower

part of the diagram. This arrangement was

used for lifetime determinations.





## A GAS COUNTER SYSTEM

## 4.1 INTRODUCTION

Although the previously described single counter detection system had the advantage of simplicity, it had some very serious disadvantages. The chief fault lay in the fact that there was no way of preventing a large number of low energy background counts from being recorded. Most of these events are produced by the Compton scattering of gamma rays in the detector. The large background radiation in the cyclotron tank during a run gives rise to a counting rate of from 5000 to 10,000 counts per second in the energy region greater than 100 keV. The background spectrum, whose energy dependence is approximately exponential, precludes the observation of protons below about 3 MeV. (See, for example, any of the spectra in Appendices 1 to 4.)

Related to this is the disadvantage of having to use relatively thick targets (2 to 3 mg/cm<sup>2</sup>) in order to obtain high proton counting rates. The high rates were required to minimize the interference of the low energy background. These thick targets appreciably worsened the resolution of the proton peaks. In fact, the thick targets were the largest single contribution to the width of the peaks.

A third disadvantage of the simple detector system was the necessity of using a degrader in front of the detector to stop alpha particles. This degrader (typically 5 mg/cm<sup>2</sup> of Al) removed an appreciable amount of energy from the protons (\$\approx 350 \text{ keV}\$) and necessitated an appropriate correction for each peak. The uncertainties and errors inherent in such a correction were a definite disadvantage to be removed if possible. The degrader also has the effect of contributing to the width of the proton peaks.

All of these limitations on the use of the simple detection system are

drastically reduced by putting a thin (dE/dx) counter in front of the surface barrier (E) detector. A coincidence requirement on the two detectors prevents the recording of nearly all of the low energy Compton events. Alpha particles are easily rejected because of the large difference in dE/dx between alphas and protons of the same energy.

### 4.2 CHOICE OF GAS COUNTER

The most important consideration in the choice of a dE/dx counter is its thickness. The thinnest silicon detector commercially available at the time this project was started was 50 microns. This is sufficient to stop a 1.9 MeV proton. Only very recently have detectors as thin as 10 microns become available. This is still thicker (in terms of mass per unit area) than the gas counter used. The thin silicon detectors are small in area (25 mm<sup>2</sup>) and since counting rates are low, this is a serious disadvantage. The expense and availability are also considerations since radiation damage would render the detector useless after about 5 to 20 hours of running time.

A disadvantage of the use of a gas counter is that it is difficult to obtain good resolution with the simultaneous requirement that the detector be physically small. The 16 kgauss magnetic field also reduces the resolution of the counter. The resolution obtained, however, was quite adequate to distinguish protons from alpha particles and so the disadvantage is not at all serious.

A gas detector may be made extremely thin. The ultimate thinness is limited mainly by the film used to cover the front window. This aspect made it the logical choice for the dE/dx detector.

A counter telescope employing a proportional counter and silicon surface barrier detector has been described by Flerov et al (1965). They, however, used two windows in order to separate the gas counter from the

silicon detector. Both windows were thicker than the one used in the detector described in this thesis and they also used a greater thickness of gas.

A counter telescope of a similar type was built in this laboratory by G. Bavaria (1966) for use in the external beam. This system was also built to look for delayed protons. The proportional counter worked well and had fair resolution but the experiment suffered from a very low counting rate due to the low external beam current.

## 4.3 DESIGN CRITERIA

The design criteria for the gas counter described here were:

- 1. To make the counter as thin (in mass per unit area) as possible in order to obtain good energy determinations on low energy protons (and alphas if present).
- 2. To make the solid angle of the system as large as possible in order to look for low cross-section reactions.
- 3. To make the detector electrically stable since electrical breakdown could have a ruinous effect on the surface barrier detector.
- 4. To make a detector in which the gas purity remained high over a long period of time since it was not convenient to use continuous gas flow techniques.
- 5. To obtain as high a resolution as possible, subject to the above conditions.

## 4.4 DESCRIPTION AND CONSTRUCTION OF COUNTER SYSTEM

The gas detector is a proportional counter of a rather unusual design (fig. 4.1). To minimize the thickness of the gas detector, the silicon (E) detector is mounted inside the gas. This eliminates the need for more than one window. The window is made of 0.15 mil mylar which is glued with

epoxy resin (Techkit E-63) to an aluminum support. The inside surface of the window then has a few \(\mu\_g/cm^2\) of gold evaporated onto it to make it conductive. The gold surface forms one ground plane for the gas detector and the silicon (E) detector forms another. It was found that if the front window was not made conductive, the magnetic field drastically reduced the pulse height of the detector and worsened the resolution to such an extent that it was impossible to distinguish between protons and alpha particles.

A 10 mil tungsten wire passing between the two ground planes formed the anode of the proportional counter. A thinner wire (4 mil) was tried at first, but it was soon realized that the charge collection efficiency would be improved by using a larger wire. This is due to the fact that in order to get the same gas multiplication with a larger wire, the voltage on the wire must be greater. This increases the electric field gradient everywhere in the active volume; the result of which is to improve the charge collection. The minimum value of the electric field required at the cathode is discussed by Watt (1967). He, however, does not take into account the presence of a magnetic field, so his paper is useful only as a guide, his values forming a lower limit to the field strength required.

The wall of the gas detector is a tube of Araldite epoxy. It was made by pouring Araldite into a plastic bottle and then spinning it (1100 r.p.m.) on a lathe until it hardened. The plastic mold was cut off and the outside of the cylinder was machined to the correct size. The inside surface of the tube was not machined because the "spun" surface is very smooth and has very good outgassing properties. It is believed that machining the surface would worsen these properties. The high spinning speed is necessary to centrifuge all of the air bubbles out of the liquid

<sup>1.</sup> Araldite may be obtained from Waldor Enterprises Inc., Montreal.

Araldite.

The choice of Araldite for the chamber walls was the result of a sequence of trials and errors. Brass was tried, but its poor outgassing properties caused the pulse height to deteriorate rapidly. Aluminum was better in this regard but not good enough. A disadvantage of all conducting materials was that it was difficult to insulate the anode wire well enough; electrical breakdown involving corona and sparks was very common. By making the walls of the chamber out of an insulating material, this problem was eliminated. Conducting surfaces are placed only where they are necessary for the proper functioning of the detector. Of the various types of insulating material, epoxy seemed to be the most promising. Plexiglass, bakelite, lucite, etc. have poor outgassing properties. Glass is good in this respect, but is harder to work with than epoxy. Teflon may be satisfactory, but it is dangerous to machine and it will not seal to anything. Araldite was tried and found satisfactory.

The 10 mil tungsten wire was held in place by drilling small holes through the chamber wall, threading the wire through the holes and cementing it in place with epoxy (Techkit E-63). When the detector was completed, the wire and the chamber were cleaned with alcohol and rinsed with distilled water. The wire was then flashed red hot in a vacuum to complete the cleaning procedure.

The gas seal for the front window support was made of indium. This material was used because it forms a good seal and it has good outgassing properties. It was found that the use of a neoprene rubber 0-ring caused the gas amplification of the counter to decrease steadily, presumably because of the deterioration in the purity of the gas.

These are the main features of the detector telescope. Any other minor points of construction can be determined from the diagram in fig. 4.1.

## 4.5 GAS FILLING

Since the front window of the counter was so thin, it would withstand a gas pressure of only 60 cm of mercury. Because of its inability to take atmospheric pressure it was necessary to use a gas filling technique in which the pressure differential across the window was not allowed to become very large.

A schematic diagram of the system is shown in fig. 4.2. To evacuate the system the detector valves 1 and 2 in the diagram were opened, thus equalizing the pressure on both sides of the window. The probe was evacuated by an auxiliary forepump; then the system was opened into the cyclotron. The cyclotron itself was allowed to pump on the apparatus for 15 to 30 minutes in order to outgas the detector. Valve 1 was then closed, isolating the detector from the cyclotron vacuum. The filling gas was then allowed into the detector through valve 3, the pressure being measured by a mercury manometer (valve 4). When the gas pressure was correct, valve 2 was closed to isolate the detector from the contaminating vapours of the mercury column, the rubber hose, etc.

The valve marked "extra" in fig. 4.2 was used when a mixture of gases was required. In actual practice, pure methane ("Chemically Pure" from Mathison Inc.) was found to be adequate. No improvement in resolution was detected when various mixtures of methane and argon were tried.

### 4.6 OPERATIONAL VALUES

The pulse height response of the detector to 5.30 MeV alpha particles as a function of voltage and gas pressure is shown in fig. 4.3. It should be noted that different curves represent different amounts of energy being deposited in the gas, approximately twice as much energy being lost in the gas at 20 cm (Hg) pressure as at 10 cm pressure.

As a rule 20 cm pressure was used when protons were being observed.

When the detector was being used to look for delayed alpha emission, 2 cm pressure was used. At this pressure, the front window was much thicker than the gas and it was therefore not profitable to decrease the gas pressure further.

Sample dE/dx spectra are shown in fig. 4.4. The ThB source was placed inside the detector, the <sup>210</sup>Po source outside. Note that the spectrum from the <sup>210</sup>Po source is distorted. This is no doubt due to the bulge in the mylar window caused by the pressure differential. This bulge causes the counter thickness to be non-uniform, and a variation in the energy loss occurs.

The gas detector was very stable. The pulse height had no tendency to decrease during a run in spite of the fact that the gas was not changed or purified. The longest run without a change of gas was about 15 hours.

FIGURE 4.1

Figure 4.1: Diagram of the gas detector showing the principal points of its construction.

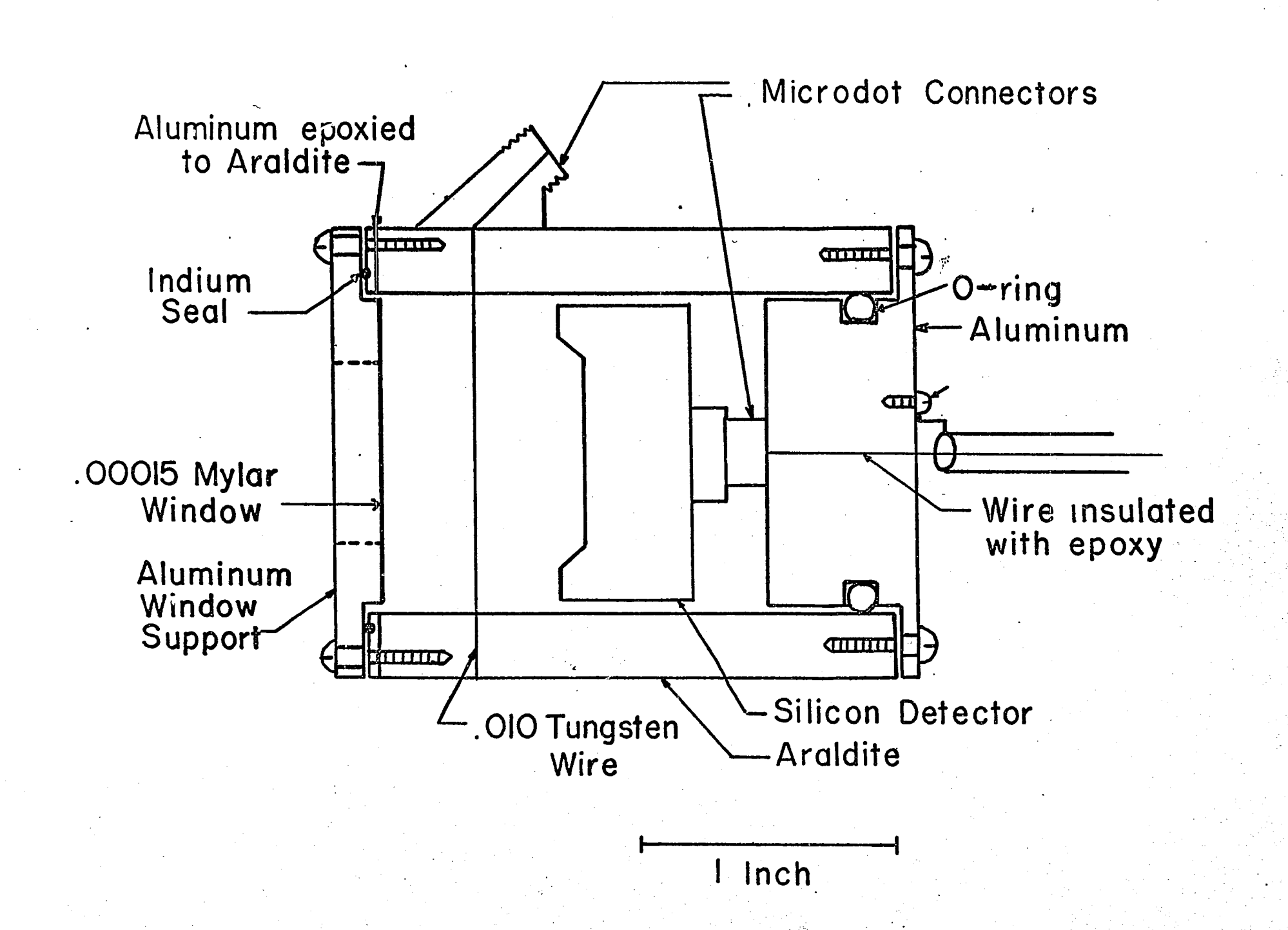


FIGURE 4.2



Figure 4.2: Schematic diagram of the gas filling arrangement for the dE/dx detector.

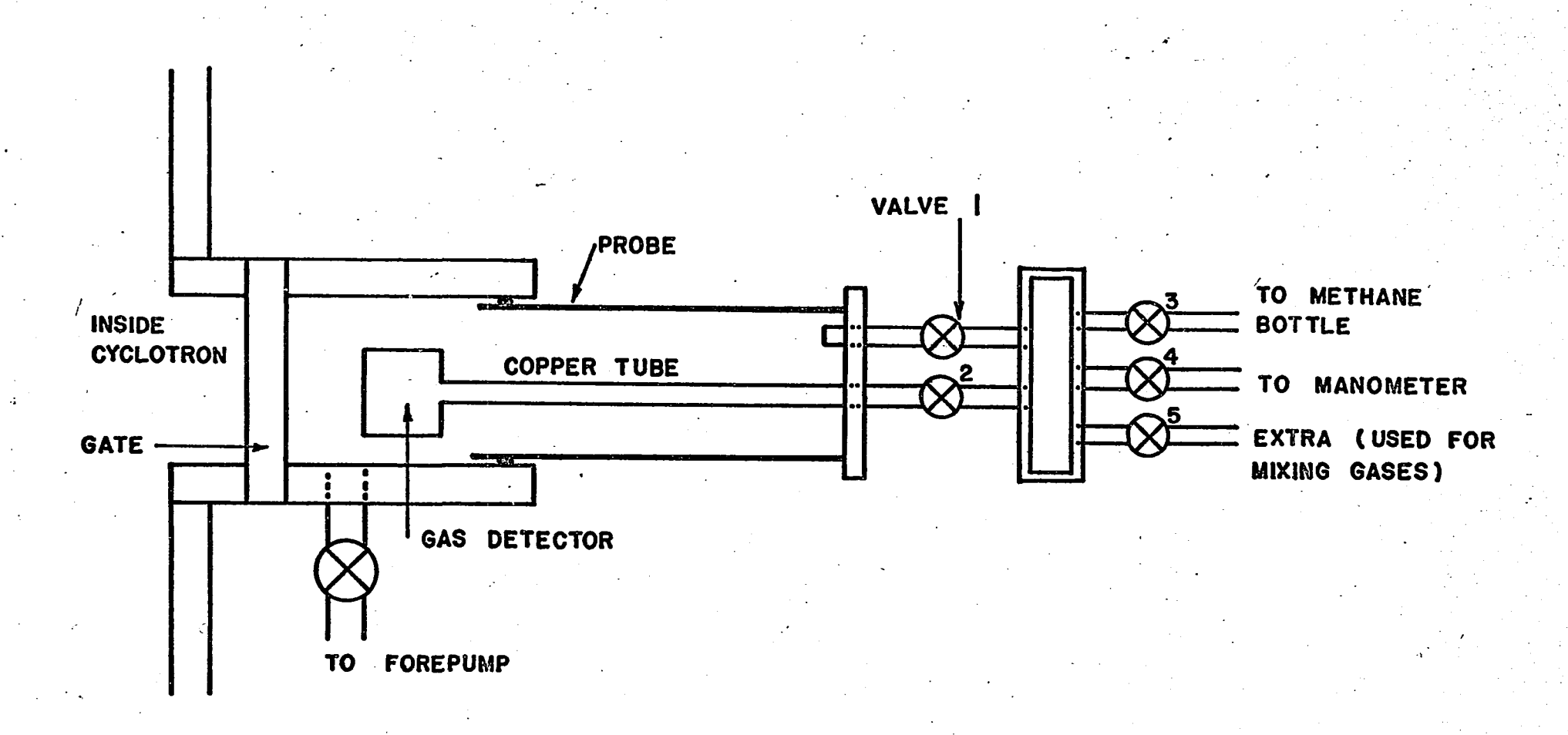


FIGURE 4.3



Figure 4.3: Pulse height response of the gas detector as a function of pressure and bias. A <sup>210</sup>Po source was used for these measurements. Note that the energy lost in the gas will change as the pressure changes.

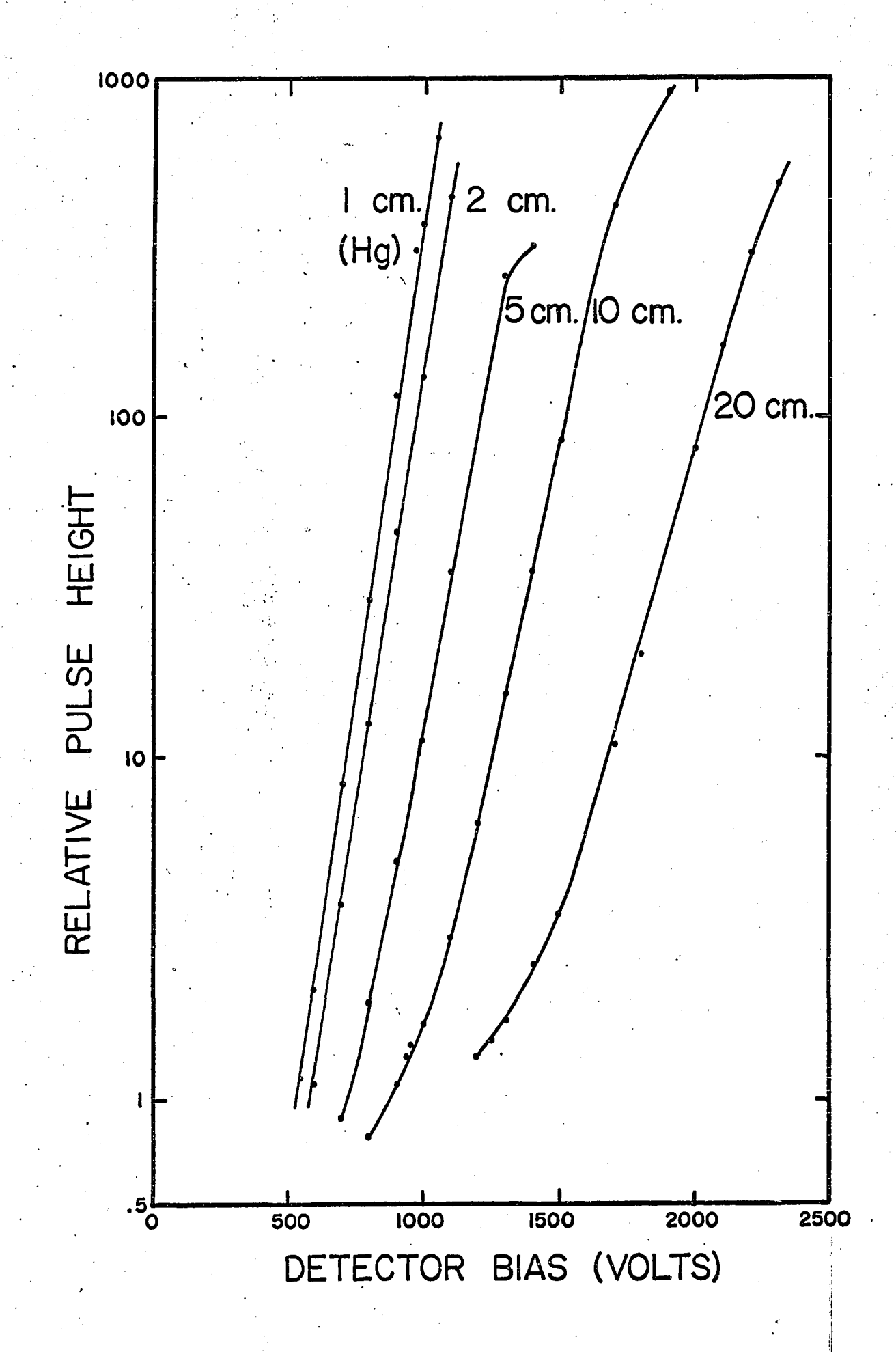




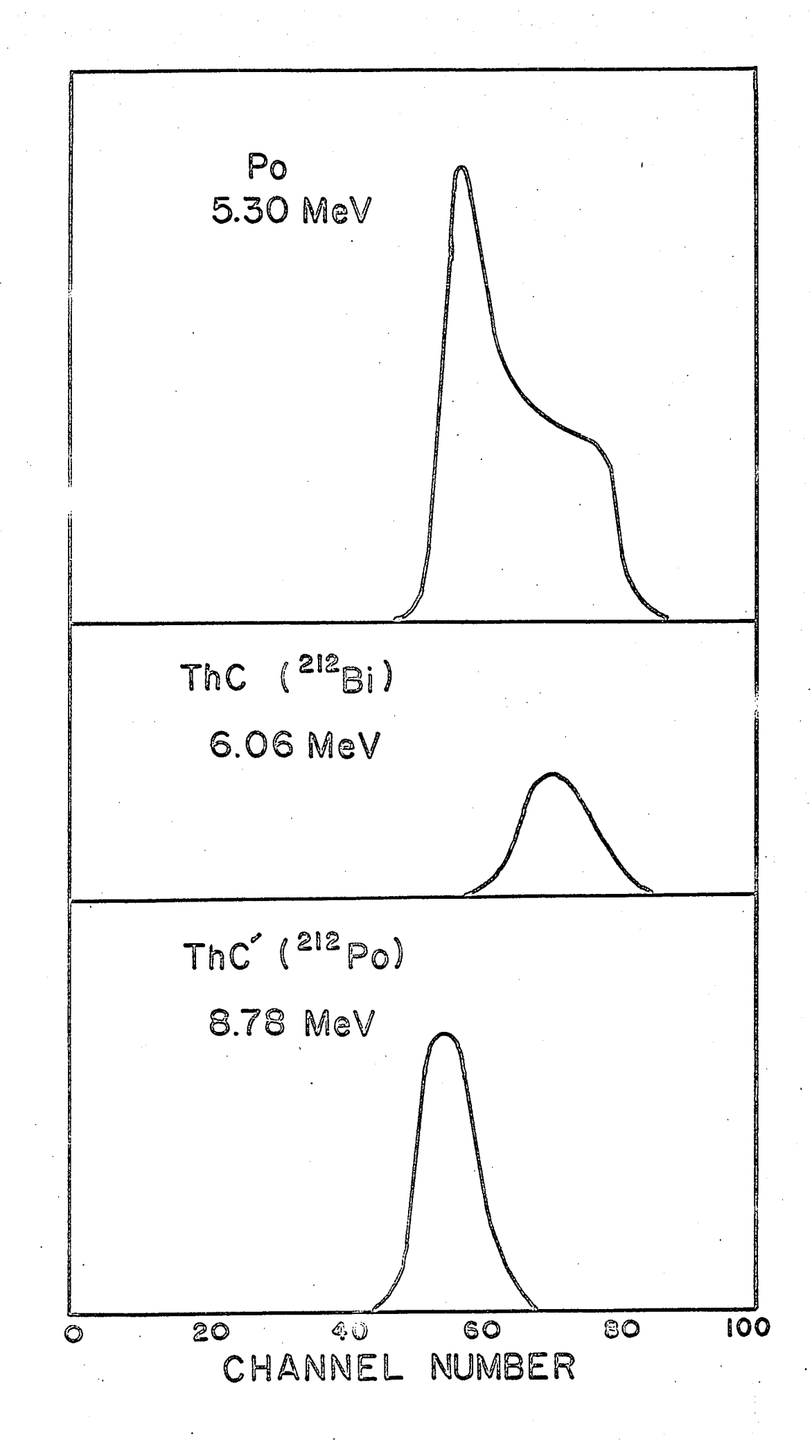
FIGURE 4.4



Figure 4.4: "dE/dx" spectra due to three alpha energies.

Only pulses in coincidence with pulses from the

"E" counter were recorded.



# 5 EXPERIMENTAL PROCEDURES AND TECHNIQUES

### 5.1 GENERAL

The basic procedure common to all experiments discussed in this thesis was to place a target in the internal circulating beam of the cyclotron, bombard it for a preset length of time ( $\approx 30$  msec), allow a delay ( $\approx 100$  msec) to let the relatively short-lived activities die away, and then detect and analyse the proton activity ( $\approx 0.5$  sec). The cycle was then repeated. The detection systems have been discussed in Chapters 3 and 4. The information sought was the energies of the proton peaks, the lifetimes of the decays, and the relative number of counts in each peak.

### 5.2 ENERGY DETERMINATION

Alpha calibration sources together with a precision pulse generator (Victoreen - Model PPG1) were used to calibrate the detector - analyser system. For the first counter systems used (the ones not employing a gas dE/dx detector), a 210 Po source was used, emitting 5.30 MeV alphas. With the system using the gas detector an extra source was used for convenience and as a cross check on energies. This was a ThB source deposited on a thin piece of aluminum foil and placed inside the gas counter. The energies of the alphas from this source are 8.78, 6.05 and 6.09 MeV. It was, however, impossible to resolve the 6.05 and 6.09 MeV lines. To find the apparent energy of the doublet, the relative intensities for the two lines were taken from the "Table of Isotopes", page 399 (C.M. Lederer et al (1967)), the known resolution of the system was used, and two normal distributions with the appropriate heights and standard deviations were added together. This procedure gives a maximum at 6.06 MeV. Using the 5.30 and 8.78 MeV lines together with the pulse generator we also obtain a maximum for the doublet at  $6.06 \pm .01$  MeV. This value, therefore, was the energy used for



calibration purposes.

Having the ThB source inside the gas counter made it possible to do an energy calibration during the actual course of a run. This eliminated the uncertainty about the effects of the intense cyclotron beam bursts on the gain and stability of the system.

The energies of the proton peaks, determined by the calibration method described above, were then corrected for energy loss due to the gas, the mylar front window, and one half of the thickness of the target. This energy was then converted to the centre-of-mass energy to determine the total disintegration energy of the proton-emitting nucleus.

The thickness of the front window and the effective thickness of the gas were determined by using the alpha sources. The alpha particle pulse heights were determined i) with no absorber, ii) with the front window in place but with no gas and iii) with the front window and the gas as absorbers. Using the measured energy losses and the range energy tables for mylar and methane given in Appendix 7, the thicknesses of these two media could be determined. The three alpha lines give three separate measurements of these thicknesses. Since the rate of energy loss of a proton (of about the same energy) is only about 0.1 of that of the alpha particles, the energy loss corrections applied to protons will be very good (the estimated error for these corrections is about 15 keV). These corrections were determined using the range energy tables for protons in mylar and methane also given in Appendix 7.

### 5.3 LIFETIMES

With the first two detector systems a 256 channel TMC analyser was used. It was arranged that the pulses from the detector would be stored in the first quarter of the memory for a fixed length of time, then in the second quarter for the same length of time and so on through the third and fourth quarter. The four spectra thus obtained were analysed to obtain the

total number of counts in each peak. The lifetime of each peak (or sum of peaks) could then be determined by plotting these totals on semi-logarithmic paper.

With the gas counter system, a 4096-channel two dimensional analyser was used. The technique was essentially the same as with the 256 channel analyser, except that one had more channels to work with; in practice, 8 groups of 512 channels were used.

The internal clock in the multispectrum analyser was checked with a precision time mark generator (Tektronix Type 181). The analyser counted the pulses from the time mark generator for a time determined by the internal clock and the number of counts was compared with the predicted number. It was found that the clock in the analyser is running about 0.5% fast. This correction was kept in mind during the analysis of results, but considering the accuracies involved ( $\approx 5\%$ ) it is not significant.

### 5.4 RELATIVE INTENSITIES

The relative intensities of different proton groups being emitted from the same source are determined simply by taking the ratio of the total number of counts under appropriate peaks in the spectrum. The intrinsic efficiency of the detector is 100% for heavy charged particles, and the solid angle is the same (to within 5%) for all energies measured. This latter statement was subject to doubt since the cyclotron magnetic field causes the proton trajectories to be curved. For instance, the radius of curvature of a 1 MeV proton moving in a plane perpendicular to the magnetic field is only 7 cm.

Since alpha particles have the same magnetic rigidity as protons it is possible to measure experimentally the effect of the magnetic field on the solid angle. The following procedure was carried out with the single counter system to check for this effect. An alpha source (210Po) was

placed at the target position and aluminum degraders were placed immediately in front of it. The counting rate of the degraded alphas was determined with the magnetic field on and then with it off. The magnetic field produced no detectable variation in counting rate down to an energy of about 2 MeV, at which point the low energy background made the technique very unsatisfactory. This energy was, however, sufficiently low for all experiments done with the single counter detector system.

The ability to detect lower energy particles using the gas counter telescope system made it necessary to look at this problem again.

Unfortunately alpha particles are not so useful to test this system since the gas counter itself will stop a 1.5 MeV alpha particle. It was necessary, therefore, to calculate the effect of the magnetic field on the effective solid angle. The geometry assumed for the calculation was that of a point source placed 5.4 cm from the detector. The source is on the detector axis of symmetry and this axis is perpendicular to the magnetic field; this geometry closely approximates the true geometry. The results are shown in fig. A8.2. The dotted line in the figure takes into account the fact that the counter support introduces a collimation effect. The details of the calculation are given in Appendix 8. The overall result is that the correction at 1 MeV, approximately the lower limit of observation, is 5% and introduces an uncertainty of 0.5%.

We now come to the problem of comparing the intensities of peaks in different spectra. This was done by using a composite target; that is, a target composed of two (or more) elements whose bombardment produces delayed proton precursors. By comparing the intensities of the proton peaks from the two different precursors, the relative cross-section for the production of the relevant peaks could be determined. One must, of course, know the relative thickness of the two elements in the target. Also, the lifetimes

of the relevant precursors must be known and taken into account.

The targets were made in two basic ways. Either one target material was evaporated onto another (e.g. sulfur onto aluminum), or a compound containing the two elements was vacuum evaporated onto thin gold foil (e.g. KF evaporated onto gold foil). Chapter 6 gives a description of target-making techniques. Appendix 5, which is a reprint of the relevant publication, enlarges on the techniques as well as giving the results of the experiment.

### 5.5 PARTICLE IDENTIFICATION

Besides protons, both alpha particles and electrons (from Compton events) are present in significant numbers. It is necessary to be able to distinguish between these particles.

## a) Single Counter System:

With this system, which had no coincidence arrangement, all electrons which left energy in the detector were counted. The detector is, however, too thin to take much energy out of most electrons and therefore the effect of the electrons was to produce a large low-energy background. Sufficient numbers of electrons are multiply scattered in the detector and lose enough energy that the observation of protons with energy below about 3 MeV is impossible. The electrons, however, do not produce peaks at higher energy.

As for alpha particles, the targets were sufficiently thick that alpha particles lines would appear extremely broad. This sort of background does appear and was eliminated in practice by placing absorbers in front of the detector to stop the alpha particles.

A double check on the identity of the protons was made by placing more absorbers in front of the detector and checking that the energy degradation of the peaks corresponded with the value predicted for protons.

## b) Gas Counter Telescope System:

Most of the counts due to electrons produced by Compton events are rejected by the coincidence condition on the two detectors. Also, the data is stored in the two dimensional mode, an example of which is shown in fig. 5.1. The energy increases along one axis and dE/dx increases along the other. In this display, the electrons, protons and alpha particles fall into distinctly different sections. For proton energies less than about 0.8 MeV, however, the electron background again interferes to the extent that the protons are no longer separable from the background.

For preliminary gain adjustment purposes, the position in the display of the <sup>210</sup>Po alpha line is noted. From this, it is a simple matter to calculate where the proton locus will lie and adjust the gain of the amplifiers accordingly.

### 5.6 PRECURSOR IDENTIFICATION

If a precursor has an atomic number Z then it can be produced plentifully by the proton bombardment of an element with an atomic number Z-1 or Z, and to a lesser extent with higher values of the atomic number. However, it is impossible to obtain the precursor by bombarding an element with an atomic number of Z-2. The identification of a precursor was carried out, therefore, by observing the existence of the appropriate proton peak after the bombardment of elements with atomic numbers Z-1 and Z; and by observing the nonexistence of the peak after bombarding an element with an atomic number of Z-2.

The mass number A was determined by measuring the apparent energy threshold for the production of the precursor from the two different targets. This threshold was compared with the calculated value obtained

by estimating the mass of the precursor. J.C. Hardy (1965) gives several formulae for making these estimations.

The threshold for a given target was obtained by bombarding the target at various energies and plotting the proton production against the bombarding energy. This, when extrapolated to zero production, gives an estimate of the threshold. Because of the radial oscillation of the internal beam, there is an appreciable energy spread ( $\approx 4$  MeV) in the beam hitting the target. Also, the shape of the excitation function at low energies is not well known. Therefore, an uncertainty of 4 MeV was assigned to all measured thresholds.

know the number of protons passing through a target. By attaching an insulated copper block on the end of a cyclotron probe and connecting it by cable to a sensitive ammeter it is relatively easy to measure the circulating proton current as a function of radius. Since the targets used were so thin, however, it is possible that a proton would lose so little energy on traversing the target that its orbit would be only slightly perturbed. When this happens, the protons can go through the target many times, thus increasing the effective current. The number of traversals for a 2.5 mg/cm<sup>2</sup> foil of magnesium was measured by J.C. Hardy (1965) for cyclotron radii varying between 22 and 34 inches and these results were used in subsequent experiments. It should be noted that the energy dependence of multiple traversals, if not taken into account, will affect the shape of the excitation function, but can have very little effect on the measured threshold value.

The identification of the precursor <sup>33</sup>Ar was slightly different in that an argon target was not made. All conclusions therefore were made from the data obtained from a chlorine (LiCl) target. (The absence of the

characteristic peaks upon bombarding a sulfur target fixed the Z value as that of argon.)

Scandium-40 is also a special case. To produce <sup>40</sup>Sc from stable scandium (100% <sup>45</sup>Sc) requires a (p,p5n) reaction. The low cross-section for this reaction accounts for the fact that very few protons were observed following the bombardment of scandium, and these few protons could be attributed to the production of <sup>41</sup>Ti, a known delayed proton emitter.

To identify  $^{40}$ Sc, use was made of the fact that the threshold for production from  $^{40}$ Ca is only 14.7 MeV. At the bombarding energy used (25 MeV), isotopes which are produced are well known. A check of their decay energies and the proton binding energy of the daughter tells us that it is energetically impossible for the nuclei to be delayed proton emitters, leaving  $^{40}$ Sc as the only possibility. Another strong piece of evidence is the fact that the observed half-life agrees very well with the previously measured  $\beta^+$ -decay half-life of  $^{40}$ Sc.

## 5.7 SQUARE ROOT GRAPH PAPER

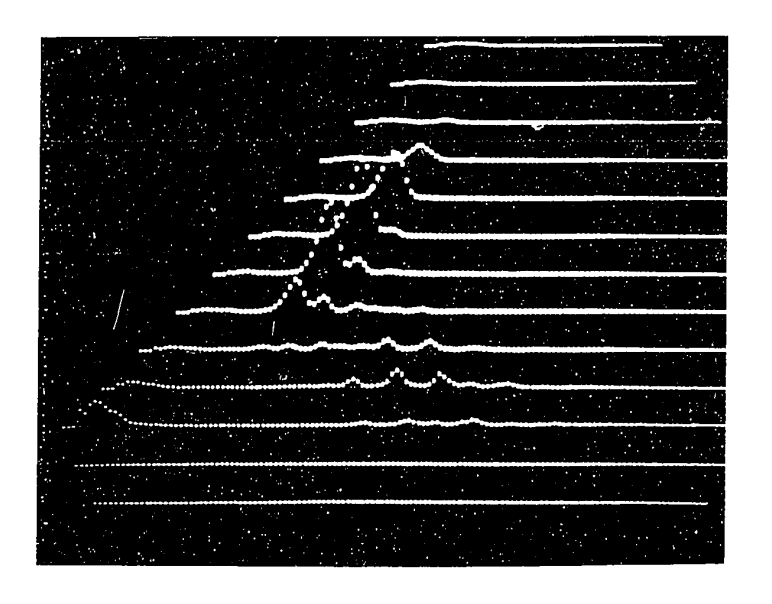
Some of the spectra in this thesis are plotted on a new type of graph paper in which the distance of a plotted point from the bottom of the graph is proportional to the square root of the number of counts being represented. The advantages of this scaling factor are discussed in Appendix 9. An example of the paper is shown there also.

### 5.8 NOMOGRAM FOR DETERMINING LOG ft VALUES

A nomogram originally constructed by Moszkowski (1951) for the rapid calculation of log ft values was extended to higher decay energies so as to be useful for this work. The nomogram and details for its use will be found in Appendix 6, which is a reprint of the publication by Verrall et al. (1966).

FIGURE 5.1

Figure 5.1: The photograph shows the mode of collection of data. The "x" axis represents energy, the "y" axis represents the dE/dx pulse size and the "z" axis corresponds to the number of counts. To obtain a final spectrum, low energy background is subtracted from each dE/dx group (when necessary) and then all the groups containing "proton" counts are summed.



## 6.1 REQUIREMENTS

Charged particle spectroscopy necessitates the use of relatively thin targets. The fact that different particles have to pass through different amounts of target material produces a spread in the energy of a peak. For best resolution, therefore, the energy broadening produced by the target should be appreciably less than the resolution of the detector-amplifier system. On the other hand, reduction in the target thickness produces a decrease in the counting rate with the result that the background problems become worse and counting times become longer. A compromise is obviously in order.

For the first detection technique described in this thesis, background was a serious problem so relatively thick targets of about 2 to 3 mg/cm<sup>2</sup> were used. Most of the energy spread observed was therefore due to the thickness of the target. For the detection technique in which a telescope was used, background was a much less severe problem and thinner targets could be used. These ranged from 0.3 to 1.0 mg/cm<sup>2</sup>. The following section is a description of the techniques used in making the targets relevant to this thesis. Most of these methods were developed by J.C. Hardy and myself. Exceptions to this are the evaporated magnesium target, the "improved" sulfur target and the targets of elements with atomic number greater than 20. These were developed for use with the gas detector system.

Other targets used in delayed proton work at this laboratory are described by J.C. Hardy (1965). The pertinent elements in these targets are oxygen, fluorine, sodium, aluminum and silicon. Since I had no part in developing these targets, I will not describe the methods here.

#### 6.2 GENERAL METHOD

The most used technique was that of vacuum evaporation, each target requiring a slight variation in the procedure. The general idea was to place the target material and backing foil in a bell jar, evacuate it, and evaporate the material onto the backing foil.

The backing foil generally used was gold leaf (200 $\mu$  g/cm<sup>2</sup>). It was relatively thin and quite easy to handle. Also, no delayed protons were observed after bombarding the foil with protons of energies up to 100 MeV.

The base plate of the vacuum evaporator (Mikras model VEIO) was fitted with insulated electrodes, used for the electrical heating of the material to be evaporated. The heating elements used were tungsten and tantalum ribbons and tungsten wire helices. The evaporation of many salts was difficult because the salt would tend to bounce off the hot ribbon before it evaporated. In some cases this was due to the violent evaporation of absorbed water or water of hydration. In other cases it was thought due to the evaporation of the salt itself. This difficulty was circumvented by having in the jar a movable hopper containing a relatively large amount of the salt. It was possible to control the hopper by external means and thus to replenish the salt on the tungsten ribbon. It was possible in this way to build up the thickness of a target through repeated evaporations without breaking the vacuum. Deliquescent salts were heated and sometimes even melted to drive off water before being introduced into the bell jar. This, of course, was done to decrease the bouncing on the hot ribbon.

The following is a short description of the target preparation for each element used.

### 6.3 LITHIUM AND BERYLLIUM

These metals were used as targets to search for delayed protons from nuclei with atomic numbers less than 6. For exploratory investigations,

thick targets (greater than the range of 5 MeV protons) were used. These were simply pieces of the metal suspended by a wire target holder. Since no protons were observed from these metals, it was not necessary to fabricate thinner targets of these elements.

### 6.4 BORON

A thick target was used for initial trials, but since delayed protons were observed (from  $^9\mathrm{C}$ ) it was necessary to make a thin target. This was done by spraying a solution of boracic acid ( $\mathrm{H_3BO_3}$ ) dissolved in distilled water onto gold foil and evaporating the water with a heat lamp. The spray was formed by a perfume atomizer. If care was taken to make a fine spray, and the procedure was not hurried, very uniform targets could be made. Targets as thick as 2.5 mg/cm<sup>2</sup> were made.

The oxygen in the target also gives rise to delayed protons (from <sup>13</sup>0) but these can easily be discriminated against since the half-life of <sup>13</sup>0 is only about one tenth the half-life of <sup>9</sup>C.

### 6.5 CARBON

Strips of 2.4 mg/cm<sup>2</sup> polyethylene (CH<sub>2</sub>) were used as a carbon target.

It might be mentioned here that when one is looking for proton or alpha activities with low yields, it is carbon which is the most obnoxious impurity. Targets must be kept very clean, since a smear of finger grease, vacuum grease, etc., will give rise to a proton and alpha particle background sufficient in many cases to obscure the desired spectrum. The protons arise from the decay of <sup>9</sup>C and the alpha particles are emitted following the  $\beta^+$ decay of <sup>8</sup>B.

### 6.6 MAGNESIUM

In the original work on magnesium, carried out by R. McPherson and

J.C. Hardy, the target used was a thin (2.3 mg/cm<sup>2</sup>) magnesium foil. For my investigation of the low energy proton peaks a still thinner target was needed. The following vacuum evaporation technique was used. Lengths of magnesium wire were placed on a tungsten ribbon situated inside the bell jar. The gold backing foil was attached to an aluminum plate and the assembly was placed about 6 inches above the tungsten ribbon. The aluminum plate acted as a heat sink for the gold foil; without it, the foil tended to curl during or after evaporation.

It was found that very little magnesium evaporated onto the gold foil unless the foil was attached to a -2000 volt supply. The actual voltage was not critical, but it had to be negative. Very little current was taken from the supply; much less than if the process was one of simple ion collection. The effect is an interesting one and bears further investigation.

Using this technique, targets of magnesium as thick as 0.5 mg/cm<sup>2</sup> were easily made.

## 6.7 PHOSPHORUS

Straightforward attempts to vacuum-evaporate phosphorus result in the deposition of films of yellow phosphorus which ignites spontaneously on contact with air. The method of B.W. Hooton (1964) was used to circumvent this problem. The bell jar was evacuated and then isolated from the pump. Phosphorus was evaporated into the vacuum in the normal way. Then a second tungsten sheet placed over the target backing was heated to a red glow. At this higher temperature the gaseous  $P_4$  molecules (yellow phosphorus) are dissociated into  $P_2$  molecules which then condense as red phosphorus. Targets with thickness up to 0.7 mg/cm<sup>2</sup> were produced.

## 6.8 SULFUR

A beaker of sulfur was set boiling by a small electric heater. Next to this was set a small stand on which a gold foil backing was placed. A bell jar was then placed over the whole apparatus. The jar filled with sulfur fumes and sulfur was deposited on everything and in particular on the gold backing.

Targets made in this way tend to "burn" off when being bombarded in the cyclotron. It was found that by vacuum evaporating a small amount of gold (about  $10\mu\,\mathrm{g/cm^2}$ ) ento the target, this burn-off was prevented. During the evaporation of the gold, some of the sulfur was evaporated from the target, so it was necessary to start with a thicker target than was ultimately required. The amount of gold deposited was monitored by measuring the increase in weight of a piece of gold foil placed next to the target.

### 6.9 CHLORINE

The salt LiCl made a good chlorine target. It is, however, deliquescent and the vacuum evaporation technique for deliquescent salts described in section 6.2 was used. The target was stored in a desiccator. Targets were made as thick as 2.5 mg/cm<sup>2</sup>.

### 6.10 POTASSIUM

The compound KOH was used. It is deliquescent and was prepared and stored in the same way as LiCl.

#### 6.11 CALCIUM

Calcium metal turnings were placed on the tungsten ribbon in the vacuum evaporator and were evaporated onto a gold backing. It was found that a single large piece of calcium was easier to evaporate than a number of small pieces. The resulting targets were kept in a desiccator to prevent the formation of Ca(OH)<sub>2</sub>. Targets of 1 mg/cm<sup>2</sup> were used for the original

work on <sup>37</sup>Ca and targets of 0.5 mg/cm<sup>2</sup> were used with the gas detector telescope system.

## 6.12 TITANIUM, NICKEL AND COPPER

Metallic foils, each about 2.5 mg/cm<sup>2</sup> in thickness were used. These were obtained from A.D.Mackay Inc., 198 Broadway, New York.

## 6.13 VANADIUM, CHROMIUM, AND MANGANESE

These elements were vacuum evaporated onto a gold foil backing using the standard techniques. A tungsten wire coil was used as the heating element. A high temperature was required, and it was necessary to provide a heat sink for the gold foil. This was done by mounting the gold foil on an aluminum plate. Two aluminum sheets pressed against the edges of the foil holding it in contact with the block and preventing it from curling. A target made in this fashion did not tend to twist or curl after being removed from its mount.

#### 6.14 COMPOSITE TARGETS

In order to make relative cross section measurements (Appendix 5), it was necessary to make targets containing two (or more) of the elements which give rise to delayed proton emission. Some of the targets are simply composed of one of the previously mentioned elements or compounds evaporated onto aluminum or magnesium foil instead of onto gold foil. The techniques for making these targets are the same as have been described using gold foil. Other targets were made using compounds such as AlF<sub>3</sub>, NaF, KF, and CaSO<sub>4</sub> which contain two of the pertinent elements. They were evaporated onto gold foil using the techniques for salts described in section 6.2.

### 7 RESULTS

### 7.1 USING SINGLE COUNTER DETECTOR SYSTEM

The work done with this detection system was carried out in collaboration with J.C. Hardy. Briefly, the results of this work were as follows. The first observation of the decays of  $^9$ C,  $^{29}$ S,  $^{33}$ Ar and  $^{37}$ Ca was made. The spectra of delayed protons resulting from their decays were measured in the energy region greater than about 3.0 MeV. The half-lives of these nuclei were measured. The T = 3/2 states in  $^{29}$ P,  $^{33}$ Cl and  $^{37}$ K, analogues of the ground states of  $^{29}$ S,  $^{33}$ Ar and  $^{37}$ Ca were observed for the first time and their excitation energy was measured. Relative crosssections were measured for the production of the proton peaks in the decay of  $^{17}$ Ne,  $^{21}$ Mg,  $^{25}$ Si,  $^{33}$ Ar and  $^{37}$ Ca. Using the fact that all the beta decays of  $^{17}$ Ne lead to an observable delayed proton, it is possible to obtain approximate log ft values for the observed decays in the other nuclei.

These results (as well as other investigations) are recorded in detail by J.C. Hardy in his Ph.D. thesis. Although they form part of the results of this thesis also, they will not be recorded here in such detail.

Instead, reprints of publications (of which I am co-author) describing these results will be included as appendices. The reprints in Appendices 1 to 4 describe the observation of and the preliminary work on 9°C, 29°S, 33°Ar and 37°Ca. Appendix 5 is a reprint of the paper discussing the measurement of log ft values as described briefly above. Appendix 6 is a reprint of the extended "Moszkowski" nomogram, used for calculating log ft values from the known beta decay energy endpoint and the partial half-life of the decay.

## 7.2 USING THE GAS COUNTER TELESCOPE SYSTEM

With this system it has been possible to obtain proton spectra at much lower energies. The limit now is about 0.8 MeV (versus about 3.2 MeV with the original system). For this thesis, the proton spectra following the decay of the nuclei <sup>21</sup>Mg and <sup>29</sup>S have been studied down to this energy. Energies and intensities of the newly discovered peaks have been measured and using these results, log ft values have been calculated for the corresponding beta decay. These calculations are based on estimates of the log ft values for the beta decays to the low lying states.

As well as re-examining these two nuclei, it was discovered that the nucleus 40Sc is a delayed proton emitter; its decay sequence is

These delayed protons were not observed using the simpler detection system since all the proton peaks have much too small an energy and would have been buried in the background.

The existence of <sup>40</sup>Sc is known; its mass has been measured (Bromley et al., 1966); its half-life is known (Armini et al., 1966); and several stranches together with the subsequent decays have been observed. Endt and Van der Leun (1967, page 321) give a summary of the known properties and the relevant references. Delayed alpha particles have been looked for by Glass and Richardson (1955) but none were found.

Scandium-40 is the first delayed proton emitter in the (relatively) low mass region which does not belong to the Z = 2k + 2, N = 2k - 1 sequence. A study of the systematics of the nuclear masses indicates that it is quite feasible that other members of the sequence Z = 2k + 1, N = 2k - 1 (to which Scandium-40 belongs) may also be delayed proton emitters. This is discussed in more detail in section 8.2.

Short exploratory runs (about 30 minutes each) at 85 MeV bombarding energy were performed using targets of Ti, V, Cr, Mn, Ni and Cu. There were no delayed proton peaks observed. It is estimated from the spectra observed that the proton rate (if present) from these targets is at least 20 times smaller than the rate from a sulfur or an aluminum target.

The remainder of this chapter consists of a detailed discussion of the investigation of the nuclei  $^{21}{\rm Mg}$ ,  $^{29}{\rm S}$  and  $^{40}{\rm Sc}$ .

### 7.3 MAGNESIUM - 21

# a) Observed Spectrum and Identification

A spectrum obtained by bombarding a 0.5 mg/cm<sup>2</sup> magnesium target (78.7%  $^{24}$ Mg, 10.1%  $^{25}$ Mg, 11.2%  $^{26}$ Mg) at 67 MeV is shown in fig. 7.1.

Hardy and Bell (1965) showed that in a spectrum obtained by bombarding a magnesium target the peak at 5.40 MeV is due entirely to the decay of 17Ne. There are peaks at 4.87 and 4.04 MeV which are also due to the decay of 17Ne. Using the ratio of intensities of these three peaks as indicated by Hardy and Bell (1965) and also by Esterlund et al. (1967), these two other peaks have been estimated as shown in the inset in fig. 7.1. The statistics in the 5.40 MeV peak are not as good as one would have liked and there may be considerable error in the estimate of the 17Ne background. There are, however, no 17Ne peaks below the one at 4.04 MeV (Esterlund et al., 1967) and therefore the low energy peaks in this spectrum are not from 17Ne. It is most probable that these low energy peaks result from the decay of 21 Mg. A series of bombardments at lower energies indicate that the doublet at 1.86 and 2.02 MeV has the same threshold as the main high energy peaks. Although there is no reason to doubt their assignment to 21 Mg, it is not possible to make an equally definite statement about the small peaks. It is planned that this identification procedure be carried out using the technique described in section 8.1 (suggestions for further research).

Since the new peaks cannot be from any of the known delayed proton precursors except <sup>21</sup>Mg, any anomalies would imply the existence of a new delayed proton precursor; <sup>23</sup>Al is one possibility. However, for the purpose of this analysis, all peaks will be treated as if they followed the decay of <sup>21</sup>Mg.

The proton spectrum, fig. 7.1, has slightly better resolution than the one published by Hardy and Bell (1965). Consequently, it is possible to try to separate some of the larger bumps into their component peaks. The resolution, however, is still not good enough to do this unambiguously. The attempt to separate the different peaks is indicated in fig. 7.1. It is to be emphasized that the analysis has been pushed and that in the case of small peaks or peaks very close in energy the curves as drawn in the figure are speculative. This is especially true for the peaks marked 3.71, 3.87 and 4.09.

## b) Peak Energies and Proposed Decay Scheme

Table 7.1 lists the energies of the peaks shown in fig. 7.1. The errors quoted on these energies include the uncertainties in calibration and in the corrections for energy loss in the gas counter and target. The peak position uncertainty, which is also included in the quoted error, forms the largest source of error for many of the poorly resolved peaks.

Column two in Table 7.1 gives the excitation energy of the proton emitting level in <sup>21</sup>Na assuming the proton decay to go to the ground state of <sup>20</sup>Ne; column three gives the equivalent level assuming the proton decay to go to the first excited state of <sup>20</sup>Ne. Column four lists known energy levels (Endt and Van der Leun, 1967) which are assumed responsible for the decay. These levels were assigned if the energies corresponded within the error assigned to the energy of the proton peak, and if the level's spin-parity (if known) did not forbid the decay. The level structure in <sup>21</sup>Na is not well known and several levels had to be proposed. These are listed in column five of Table 7.1.

The decay scheme shown in fig. 7.2 accounts for the observed proton spectrum, but it is, however, not unique. In some cases it is not clear to

Analysis of proton peaks assigned to the decay of the precursor  $^{21}\text{Mg}$ . Proton energies have been corrected to centre-of-mass for A = 21. The underlined value in each case indicates the level which is assigned to the decay.

•				
E <sub>p</sub> (MeV)	Possible levels in <sup>21</sup> Na		Level in <sup>21</sup> Na	
	<sup>20</sup> Ne+p+E <sub>p</sub>	<sup>20</sup> Ne <sup>#</sup> + p+E <sub>p</sub>	Known	Proposed
1.24 ± .07	3.67	<u>5.30</u>		5.30
1.32 + .04	3 <b>.7</b> 5	<u>5•37</u>		5•36
1.60 + .06	4•03	5.66	5.69	
1.86 ± .04	4.29	5•92	4.29	
2.02 ± .04	4.45	6.08	4.47	
$2.25 \pm .06$	4.68	<u>6.31</u>	6.24	
2.56 ± .04	4.99	6.62	4.99	
2.70 ± .07	<u>5.13</u>	6.76		5.13
2.91 ± .06	<u>5•34</u>	6.97		5•36
3.22 ± .07	<u>5•65</u>	7.28	5.69	
3.38 ± .07	5.81	7.44	7.43	
3.52±.07	<u>5•95</u>	<b>7.</b> 58		5.95
3.71 ± .10	6.14	7.77	6.08	•
3.87 ± .10	<u>6.30</u>	7•93	6.24	
4.09 ± .10	6.52	8.15	6.51	
4.59 ± .06	7.02	8.65		7.02
4.71 ± .06	7.14	8.77		7.14
4.84±.06	7.27	8.90	8.90	
5.03 ± .10	7.47	9.09	7.43	• .
5.63 ± .06	8.06	9•69		8.06
6.47 ± .04	8.90	10.53	8.90	

which of the two levels in <sup>20</sup>Ne the proton is going. Confirmation of the decay scheme could be carried out by measuring a proton spectrum in coincidence with the 1.63 MeV gamma ray following the decay of the first excited state of <sup>20</sup>Ne. This experiment would indicate which of the proton groups were feeding the first excited state of <sup>20</sup>Ne.

# c) Branching Ratios and Log ft Values

The relative intensities of the beta decay branches from <sup>21</sup>Mg may be determined by measuring the intensities of the appropriate proton branches. Unless, however, we can measure or at least estimate the percentage of beta transitions which go to low lying states and are not observable in a proton experiment, we cannot know absolute beta intensities and therefore cannot assign log ft values to the transitions.

It is possible to detect, with the present system, proton decays from  $^{21}$ Na levels down to the one at 3.55 MeV  $(5/2^+)$ ; a transition to this level would produce protons with an energy of 1.12 MeV. It is clear from the spectrum that there is no peak (less than 30 counts) at this energy and so less than 0.1% of all  $\beta^+$  transitions go to this level. The levels at 2.41 and 2.81 both have spins of  $\frac{1}{2}^+$ , so  $\beta^+$  transitions to these levels are forbidden. Using the mirror decay  $\beta^-$  21Ne we can estimate the transition strength to the three remaining levels, these levels being the ground state  $(3/2^+)$ , the level at 0.34 MeV  $(5/2^+)$  and the level at 1.72 MeV  $(7/2^+)$ . The decay of  $\beta^-$  was investigated by Kienle and Wien (1963) who found that of the decays to the first and second excited states, 87% went to the first excited at 0.350 MeV and 13% went to the second excited at 1.75 MeV. They did not observe decays to the ground state since they were using  $\beta^-$  coincidence techniques. An estimate of the decay intensity to the ground state may be made by assuming that the first three states with

spins of  $3/2^+$ ,  $5/2^+$ , and  $7/2^+$  form part of a rotational band with K = 3/2. Equation (15-98) in Preston (1962) gives the ratio of <u>ft</u> values for transitions from a state  $J_1$ ,  $K_1$  to two states  $J_1$  and  $J_2$ , both having the same  $K_f$ . Viz:

$$\frac{(\text{ft})_{2}}{(\text{ft})_{1}} = \left[\frac{(J_{1}nK_{1} K_{f}-K_{1} | J_{1}K_{f})}{(J_{1}nK_{1} K_{f}-K_{1} | J_{2}K_{f})}\right]^{2}$$

where n is the rank of the operator involved in the transition. Here, the matrix elements are assumed to be Gamow-Teller and therefore n=1. Putting in numbers, we find that the <u>ft</u> value to the ground state is 3/7 of the <u>ft</u> value for the decay to the first excited state.

Using these relative ft values and the measured half-life of 4.4 sec, and assuming (because of small  $\beta$  end point energies) that any other decays have negligible intensity, we find that the log ft values for the  $\beta$  decays to the ground state, the first and second excited states are 4.86, 5.23 and 5.43 respectively.

If we now assume these values are the same in the mirror decay of  $^{21}$ Mg and use a  $Q_{6}$ + of 12.8 MeV, we obtain the log <u>ft</u> values shown in Table 7.2.

These values are not very sensitive to the relative intensity of the ground state branch of <sup>21</sup>F which was estimated above. If, for example, we assume that this intensity is zero and recalculate the log ft values for the other two decays, the net result would be to increase all the log ft values in Table 7.2 by 0.27. A further source of error is the assumption of equality of the log ft values for the mirror decays. The effect of an error in this assumption can be estimated by noting that if all three mirror log ft values err in the same direction by a small amount, all the values in Table 7.2 must be changed by approximately this amount in the opposite direction. All considered, it is estimated that the systematic

TABLE 7.2

Intensities and log ft values for <sup>21</sup>Mg decay branches, estimated as described in the text (sec. 7.3c). Errors in relative intensities are as shown. The systematic error in the log ft values is probably less than 0.3. See the text for the assumptions made.

Level in <sup>21</sup> Na	Counts pertaining to this	log <u>ft</u> of preceding	
Me∇	level in the proton spectrum	B <sup>+</sup> decay branch	
4.29	3500 ± 500	5.52	
4.47	8500 ± 500	4.17	
4.99	790 <u>+</u> 30	4.97	
5 <b>.1</b> 3	280 <u>+</u> 100	5•39	
5•30	420 <u>+</u> 100	5.17	
5 <b>.</b> 36	1570 ± 80	4.57	
5.69	700 ± 200	4.82	
5•95	520 ± 150	4.87 -	
6.08	200 <u>+</u> 100	5.21	
6.24	900 <u>+</u> 300	4.50	
6.51	700 ± 200	4.57	
7.02	140 ± 50	4.99	
7.14	300 <u>+</u> 100	4.62	
7•43	750 ± 100	4.12 -	
<b>8</b> •06	. 30 ± 10	5.21	
8.90	950 ± 100	3.27	

error is less than 0.3. The errors in relative intensity in the individual branches are given in Table 7.2.

It should be noted that the log ft value in Table 7.2 for the decay to the T=3/2 level in <sup>21</sup>Na at 8.90 MeV agrees with the value calculated by Hardy and Margolis(1965), their value also being 3.27. Also to be compared with this is the experimental value of  $2.9\pm0.3$  obtained by the method of comparative cross-sections as reported in Appendix 5. These values tend to confirm the results quoted in Table 7.2. Uncertainties in the systematic error could be reduced still further by a more complete knowledge of the  $\beta$ -decay of <sup>21</sup>F.

## a) Observed Spectrum and Identification.

The proton spectrum shown in fig. 7.3 was produced by bombarding a 1 mg/cm<sup>2</sup> sulfur target (95% 32S) with 57 MeV protons. The <sup>29</sup>S is produced by the reactions <sup>32</sup>S(p,p3n)<sup>29</sup>S and <sup>32</sup>S(p,d2n)<sup>29</sup>S. At this bombarding energy very little <sup>25</sup>Si is formed; the main peak in the decay of <sup>25</sup>Si is at 4.25 MeV and would appear in channel 124 of the present spectrum, but is not present appreciably. (See Appendix 2 for a <sup>29</sup>S spectrum that contains a background of <sup>25</sup>Si.) Spectra taken at different bombarding energies indicate that the new low energy peaks, except the one at 1.04 MeV, belong to the decay of <sup>29</sup>S. As will be discussed later, there is some doubt about the 1.04 MeV peak.

The errors assigned to the peaks (as listed in Table 7.3) take into account the uncertainties in calibration, in peak determination, and in the corrections for energy loss in the gas detector and target.

A satellite peak has been indicated in the diagram, but its position and area of course have large errors attached to them. The small peaks indicated at 4.47 and 4.93 MeV had not been observed in previous work (Appendix 2) because they were masked by the <sup>25</sup>Si background. It will require increased statistics at this low bombarding energy to verify their presence and to give better estimates of their positions and sizes.

The region between channels 80 and 100 contains more counts than can be explained by the peaks which are drawn in. The statistics are not good enough, however, to do much better than note this fact.

Small peaks at higher energies reported in Appendix 2 are not identified here, partly because the statistics are not good enough, and partly because during the run the depletion depth was not always thick

enough to stop such high energy protons.

b) Peak Energies and Proposed Decay Scheme.

Table 7.3 contains a list of the observed energies. Columns two and three in the table show the proton-emitting energy levels in <sup>29</sup>P assuming the decay to go to the ground or first excited state of <sup>28</sup>Si, respectively. The underlined number corresponds with the level assigned to the decay. Column four contains the known levels in <sup>29</sup>P which are assumed to be responsible for the decay. (See Endt and Van der Leun, 1967).

TABLE 7.3

Analysis of proton peaks assigned to the decay of the precursor  $^{29}$ S.

Proton energies have been corrected to centre-of-mass for A=29. The under-lined value in each case corresponds with the level assigned to the decay.

E <sub>p</sub> (MeV)	Possible Levels in <sup>29</sup> P		Levels in <sup>29</sup> P	
	<sup>28</sup> Si + p + $E_p$	28Si <sup>*</sup> +p+E <sub>p</sub>	Known	Proposed
(1.04±.05) <sup>1</sup>	(3•79)	(5•56)		
1.32 ± .05	4.07	5.84	4.08	
2.08 + .10	4.83	6.60	6.54	
2.22 ± .04	4.97	6.74	4.97	
2.55± .04	<u>5.30</u>	7.07	5.29	
3.55±.06	6.30	8.07	8.09	
3.87±.04	6.62	8.39	8.37	
4.47± .10	7.22	8.99	7.25	
4.93±.10	<u>7.68</u>	9.45	7.64	
5.40±.10	8.15	9.92	8.09	
5.63±.04	8.38	10.15	8.37	

<sup>1.</sup> There is evidence that the 1.04 MeV peak does not belong to the decay of <sup>29</sup>S (see text).

Figure 7.4 shows the proposed decay scheme.

The peak with energy 1.04 MeV is the only one which has not been assigned to a previously known level. It does correspond to the energy of a proton decay from the 8.37 MeV level in 29P to the second excited state of <sup>28</sup>Si. However, on the basis of proton penetrabilities (G.S. Mani et al., 1963) the intensity of this decay should be a factor of 103 less than the transition to the ground state (5.63 MeV proton), but in fact it is only a factor of 3 less (fig. 7.3). This assignment therefore has not been made. Also, it is not certain that the peak follows the decay of 29S. The peak seemed to decrease in intensity relative to the other peaks at higher bombarding energies. Furthermore, it is possible that the nucleus 32Cl, formed by a (p,n) reaction on 32S, will give rise to low energy delayed protons. At higher energies, the cross-section for this reaction would increase less quickly than the cross-section for a (p.p3n) reaction, thus explaining the relative decrease in intensity. The precursor of this peak may be identified by bombarding a phosphorus target, from which it is possible to make sulfur but not chlorine isotopes. It would also, of course, be instructive to bombard a sulfur target at lower energies (\$\approx\$ 20 MeV) to determine whether or not 32Cl is a delayed proton emitter.

If, nevertheless, it turns out that this peak does come from the decay of  $^{29}\text{S}$ , it will be necessary to postulate the existence of a new level in  $^{29}\text{P}$ . This level could have been missed in previous work on this nucleus if it has a high spin. For example, if it has a spin of  $7/2^+$ , it would require an  $\ell=4$  proton to populate the state in a (p,7) experiment. This would have a small cross-section and would be easily missed.

# c) Log ft Values

It is possible from the proton spectrum to calculate the relative

intensities of beta decay branches feeding the various states. Unless one knows the percentage of the decays that are not being seen, it is not possible to calculate the partial half-lives, and thus the log ft values, for the decays.

The mirror decay <sup>29</sup>Al  $\longrightarrow$  <sup>29</sup>Si gives information on the log ft values to certain low lying states. These values for the first (1.27 MeV) and third (2.43 MeV) excited states are 5.0 and 4.9 respectively. The ground state decay is forbidden and the decay to the second excited state has a log ft greater than 6. (Endt and Van der Leun, 1967, give a list of references.) If we assume that these values can be adopted for the decay <sup>29</sup>S  $\longrightarrow$  <sup>29</sup>P we see that there are only two states, at 3.102 MeV and 3.45 MeV for which there is nothing known either from delayed proton emission or from the mirror decay. The state at 3.45 MeV is believed to have an odd parity (Endt and Van der Leun, 1967) so decays to this state would be forbidden. The state at 3.102 MeV has a spin of  $5/2^+$  and the beta decay is therefore allowed.

Neglecting this decay for the moment and using known mirror log ft values, we can calculate log ft values for the  $\beta^+$  branches observed by delayed proton emission. These values are listed in Table 7.4. To estimate the error caused by the above omission, let us assume the log ft for this decay is 5.5. In this case all the log ft values in the table must be increased by only 0.08. If, however, we assume a log ft of 5.0 for this decay, all the log ft values in the table must be increased by 0.28. It can be seen that only if the log ft value of the decay to the 3.102 MeV state is at least 5.5, no appreciable changes in the values tabulated in Table 7.4 will be necessary.

Relative branching ratios and  $\log \underline{ft}$  values estimated as described in the text (sec. 7.4c) for the decay of  $^{29}\text{S}$ . The  $\beta^+$  end points are calculated assuming a  $Q\beta^+$  of 14.0 MeV. The decay to the 3.102 MeV state in  $^{29}\text{P}$  has been ignored. The errors in the peak intensities are shown. Systematic errors in the  $\log \underline{ft}$  values are described in the text.

Level in <sup>29</sup> P (MeV)	Counts in Proton Spectrum	Log ft of Preceding
4.08	520 <u>+</u> 50	5.51
4.97	2200 <u>+</u> 60	4.74
5.29	355 ± 30	5•34
6.54	800 ± 300	4.74
7.25	100 <u>+</u> 40	5•34
7.64	70 <u>+</u> 30	5•34
8.09	400 <u>+</u> 100	4.40
8.37	1970 <u>+</u> 70	3.64

Consider now the assumption that the log ft values of mirror decays are equal. An error of 0.1 in one of these values will introduce an error of 0.04 in the tabulated values. We see, therefore, that a slight difference in the log ft values between mirror decays does not unduly affect the calculated values.

The log ft value for the decay to the T = 3/2, 8.37 MeV level in  $^{29}P$  is listed as 3.64 in Table 7.4. This value should be compared with the value 3.27 calculated by Hardy and Margolis (1965) and the value  $3.1 \pm 0.3$  as determined using the method of comparative cross-sections (Appendix 5). These values agree within their quoted errors. It is evident, however,

that improved resolution and counting statistics in the proton spectrum would substantially improve the estimates of the branching ratios. Information on the intensity of the  $\beta^+$  branch to the 3.102 MeV state will be necessary in order to reduce the uncertainty in the systematic error.

### d) Spin of Sulfur - 29

Sulfur-29 has 16 protons and 13 neutrons. On the basis of a single particle model, the configuration should be a ( $ld frac{5}{2}$ ) neutron hole below the closed shell of 14. J.C. Hardy (1965) argued that the experimental evidence supporting this was tenuous and that proton branching ratios from the analogue state in  $^{29}$ P suggested that the spin may be  $\frac{1}{2}$ .

It is now observed, however, that  $^{29}$ S beta decays to the 4.08 MeV level in  $^{29}$ P. This level is suggested by Ejiri et al. (1964) to have a spin of  $5/2^+$  or  $7/2^+$  which is incompatible with  $^{29}$ S having a spin of  $\frac{1}{2}^+$ . It is therefore reasonably certain that the spin of  $^{29}$ S is  $5/2^+$  as is predicted by the shell model.

# a) Observed Spectrum and Identification.

Figure 7.5 shows a spectrum of delayed protons obtained following the bombardment of a 0.5 mg/cm<sup>2</sup> calcium target (97% <sup>40</sup>Ca) with 25 MeV protons. At this bombarding energy, the following reactions are energetically possible: <sup>40</sup>Ca(p,n)<sup>40</sup>Sc, <sup>40</sup>Ca(p,2p)<sup>39</sup>K, <sup>40</sup>Ca(p,a)<sup>37</sup>K, <sup>40</sup>Ca(p,t)<sup>38</sup>Ca, <sup>40</sup>Ca(p,3He)<sup>38</sup>K, <sup>40</sup>Ca(p,p<sup>3</sup>He)<sup>37</sup>Ar and <sup>40</sup>Ca(p,na)<sup>36</sup>K. Of these reactions, only the first and the last produce isotopes energetically capable of giving rise to delayed protons. The last reaction, however, would have a very low cross-section since the alpha particle would be emitted below its coulomb barrier. Reactions involving the other calcium isotopes in the target are similarly energetically incapable of producing delayed proton emission. The delayed proton precursor must therefore be <sup>40</sup>Sc. The threshold for the reaction <sup>40</sup>Ca(p,n)<sup>40</sup>Sc is 14.9 MeV (lab) which is 10 MeV below the bombarding energy. The cross-section at this energy will be appreciable. A few short runs carried out at lower bombarding energies showed no observable deviations in the shape of the spectrum.

Confirmation of the identification of <sup>40</sup>Sc as the precursor was made by measuring the half-life of the emitted protons. An analysis of the peaks above 1.6 MeV (which are sitting on less background than the lower energy peaks) gives the lifetime curve shown in fig. 7.6. The half-life of 178 ± 8 msec agrees well with the best previously measured half-life of 182.7 ± 0.8 msec as determined by Armini et al. (1966).

### b) Decay Scheme and Level Agreement

Table 7.5 lists the peak energies, corrected to centre-of-mass. Column 2 gives the corresponding excitation energy of 40Ca assuming a proton decay to the ground state of  $^{39}$ K. Column 3 gives the position of the known

or proposed level which is assumed responsible for the decay (see Endt and Van der Leun, 1967). Figure 7.7 shows the proposed partial decay scheme.

It is to be noted that no proton decays to the first excited state of 39K have been proposed. The reason for this is that a proton group going to the first excited state would be much less intense than protons of about the same energy coming from lower lying levels of 40 ca and going to the ground state. These very weak branches, although they may exist, would not be seen in the proton spectrum simply because they are so weak. For example, in the region of 1. MeV in the proton spectrum, the intensity of a proton group going to the ground state of 39K would be about 100 times greater than that of a proton group going to the first excited state. This estimate is based on the assumption that the log ft values for the two relevant  $oldsymbol{eta}^{ ext{+}}$  decays are the same. It also assumes that the relevant excited state of 40ca always proton decays to the first excited state of 39K rather than to the ground state. Since this last assumption is probably quite erroneous, the above estimate is on the conservative side. When we go to higher proton energies, a similar calculation predicts even larger differences in intensity. At a proton energy of 2 MeV, for instance, the ratio becomes 3000 to 1. It is quite reasonable, therefore, to exclude proton decays to the first excited of 39K from consideration.

The errors on the energies quoted in Table 7.5 range between 30 and 50 keV. They include errors in the energy calibration, errors in peak determination and errors in the correction for energy loss in the gas counter and in the target. The larger errors are assigned to groups which are not well resolved from neighbouring peaks and to groups which have few counts in them.

The energy agreement (to within the quoted errors) with known levels is good in the region that has been studied (below 11.070 MeV excitation). The density of known levels in this region is very high, however, and the

TABLE 7.5

Analysis of proton peaks assigned to the decay of the precursor 40Sc. Proton energies have been corrected to centre-of-mass for A = 40.

E <sub>o</sub> (MeV)	39**	Levels in 40 <sub>Ga</sub>	
DD(LIGA)	<sup>39</sup> K+p+E <sub>p</sub>	Known	Proposed
1.08 ± .03	9.41	9•404	
1.27 ± .03	9.61	9.608	
1.48 ± .03	9.81	9.811	
1.58 ± .04	9•91	9.924	
1.72 ± .03	10.05	10.046	
1.88 ± .03	10.21	10.216	
2.15 ± .03	10.48		10.48
2.24 ± .05	10.57	10.535	
2.44 ± .03	10.77	10.782	
2.62 ± .03	10.95	10.927	
2.80 ± .05	11.13	11.070	
2.89 ± .03	11.22		11.22
3.12 ± .03	11.45		11.45
3.31 ± .05	11.64		11.64
3.41 ± .03	11.74		11.74
3.52±.05	11.85		11.85
•.70 ± •05	12.03		12.03
•95 ± •05	12.28		12.28

association of a proton peak with the incorrect level would be very easy.

Also, some of the peaks in the proton spectrum may be composed of two or

more unresolved peaks. The peak at 1.08 MeV is very broad and is undoubtedly
composed of several unresolved peaks.

Very few spins and parities are known in this energy region of 40ca. The spin-parity of 40Sc is 4-. Allowed beta decays will therefore pick out states in 40ca with spin parities of 3, 4 and 5. The known energy levels in this region (see Endt and Van der Leun, 1967) were measured by looking for resonances in the reaction 39K(p,8)40Ca. Since 39K has a spin-parity of  $3/2^{\dagger}$ , a proton with an  $\ell$  value of 1 is necessary to produce a 3 state and an  $\ell$  value of 3 to produce 4 and 5 states. A table of nuclear penetrabilities by Mani et al (1963) predicts that at an energy of 2 MeV, the penetrability of a proton with an & value of 1 is 400 times higher than that of a proton with an  $\ell$  value of 3. According to this, it is very possible that many of the states with the high spin values would be overlooked in a (p, ) resonance experiment. This fact increases the possibility that some of the delayed proton groups have been assigned to the wrong level in 40ca. To remove the uncertainties, more knowledge of the spin-parities is necessary. Also, a more precise energy determination of the delayed proton peaks would help to remove some of the ambiguities in level assignment.

A proton group at 2.15 MeV does not correspond to any of the known levels. Also, protons with energies of 2.80 MeV and above correspond to a region in 40Ca which has not been previously studied. Corresponding to these peaks, new levels have been proposed. These are listed in Table 7.5 and are shown as dotted levels in fig. 7.7. The peaks at 3.70 and 3.95 MeV are tentative due to the small number of counts in these peaks. Better resolution and statistics will doubtless reveal new peaks in the upper region of this spectrum.

## c) Relative Intensities and Log ft Values

The relative intensities of the observed beta decays may be measured by comparing the number of counts under each of the proton peaks. There has not yet been any comparison of the intensity of these branches with those which go to lower states of  $^{40}$ Ca. Without a knowledge of the branching ratios it is not possible to calculate  $\log \underline{ft}$  values for the transitions. For a comparison of the different decays observed here, however, we can calculate relative  $\log \underline{ft}$  values (actual  $\log \underline{ft}$  values plus some unknown constant). Table 7.6 lists the number of counts in each peak and the associated relative  $\log \underline{ft}$  value. The additive constant has been chosen by a means which, although being arbitrary, nevertheless makes the quoted values plausible. A list of known  $\log \underline{ft}$  values for allowed transitions from odd-odd nuclei in the mass region of  $^{40}$ Sc (from A = 28 to A = 62) was taken from the review by Lederer  $\underline{et}$  al. (1967). The additive constant was then chosen to make the average of the  $\log \underline{ft}$  values in Table 7.6 agree with the average of this list of known  $\log \underline{ft}$  values.

It is of interest to note the capability of delayed proton spectroscopy to pick out beta branches of very low intensity. Assuming that the log ft values listed in Table 7.6 are approximately correct, it can easily be determined that the largest peak in the spectrum represents about 0.5% of all the decays of  $^{40}$ Sc, and that the peak at energy 3.95 MeV represents a branching ratio of about 2 decays per million.

TABLE 7.6

COUNTS IN THE PROTON PEAKS AND RELATIVE LOG <u>ft</u> VALUES

Level in <sup>40</sup> Ca MeV	Counts in Spectrum	Relative log $ft$ for preceding $\beta^{\dagger}$ decay
9•404	43,400 ± 250	4.76
9.608	4,440 <u>+</u> 100	5.71
9.811	1,340 ± 80	6.11
9.924	650 ± 80	6.39
10.046	556 ± 80	6.36
10.216	1,850 ± 60	5•70
10.48	3,090 ± 70	5•38
10.535	170 ± 40	6.58
10.782	2,250 ± 60	5•20
10.927	540 ± 50	5•75
11.070	270 ± 50	5•86
11.22	900 ± 50	5.27
11.45	137 ± 20	5.87
11.64	53± 10	6.05
11.74	139± 20	5•51
11.85	34 <u>+</u> 10	5•99
12.03	34 ± 10	5•76
12.28	23 ± 10	5•33

Here is a substitute of the state of the second of the sec

FIGURE 7.1

The contract contract of selections of a contract of the contr

■2 3 3 3 3 3 3 3 3 3

Figure 7.1: Spectrum of delayed protons following the bombardment of a magnesium target (0.5 mg/cm²) with 67 MeV protons. Each peak is labelled with its energy in MeV. These energies have been corrected to centre-of-mass. The insert shows the main peaks following the decay of 17Ne drawn on the same background. The spectrum has been normalized so that the peak at 5.40 MeV has the same area as the peak in the main spectrum.

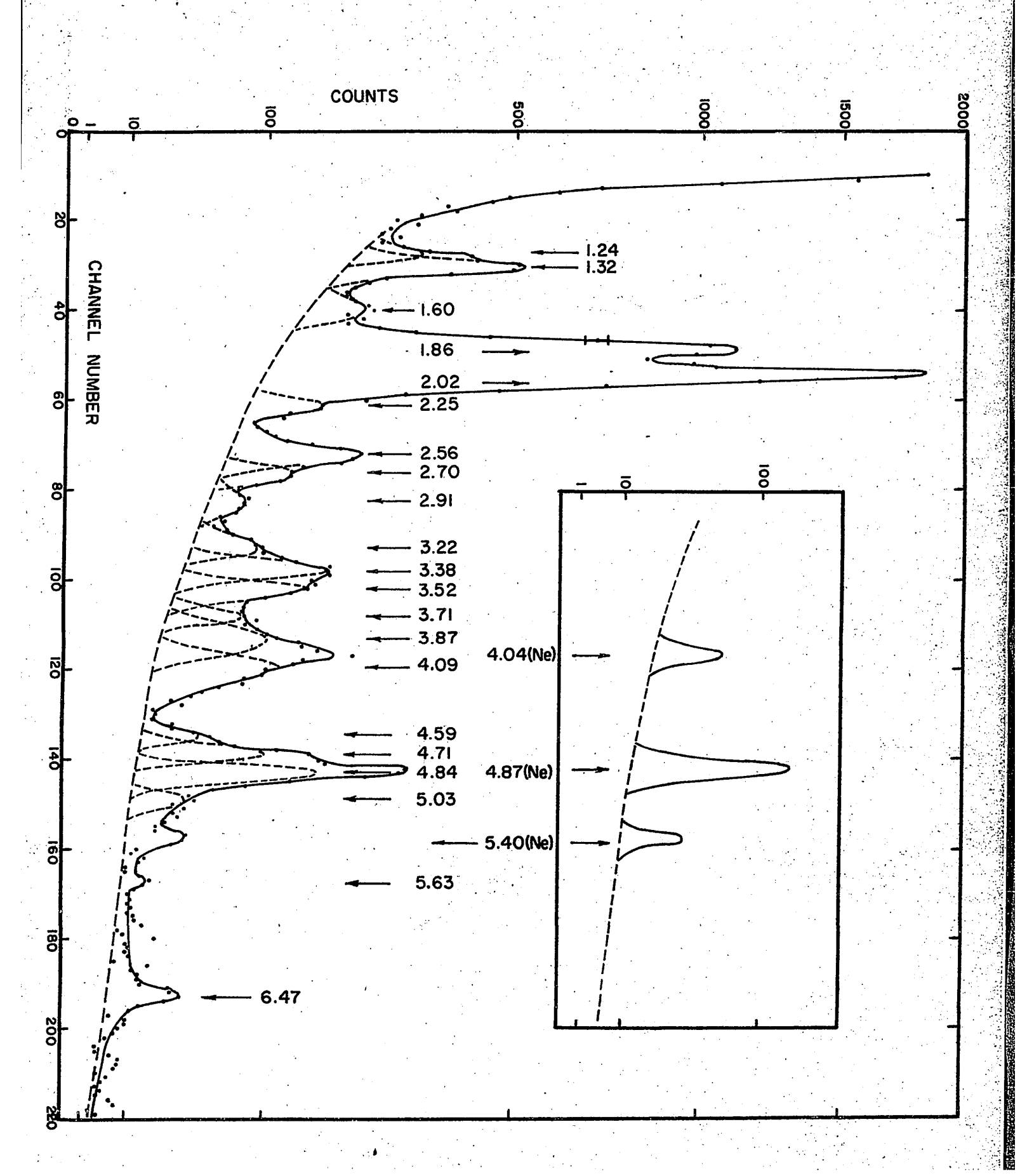
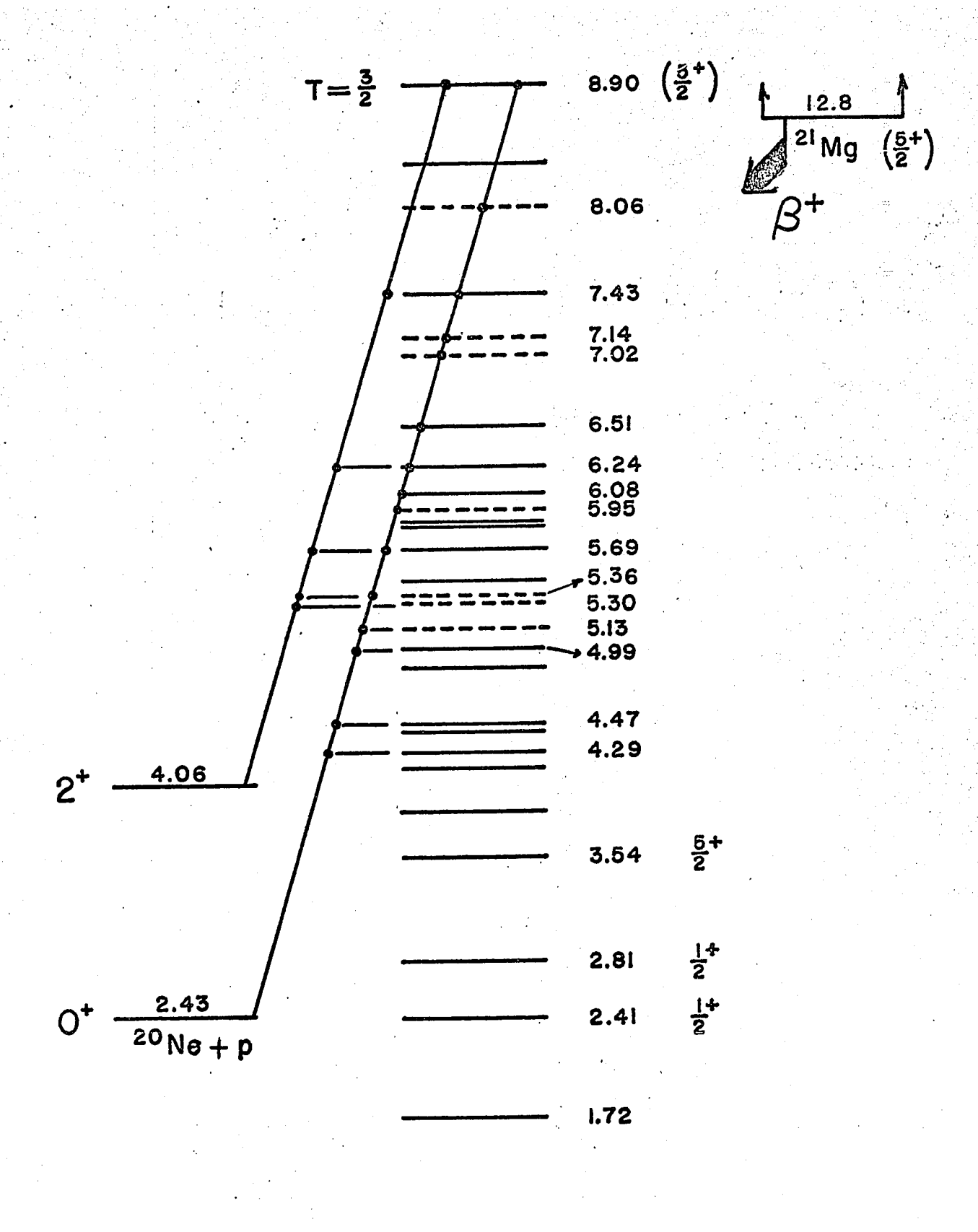


FIGURE 7.2



Figure 7.2: Proposed partial decay scheme for <sup>21</sup>Mg. The solid lines represent levels taken from the compilation of Endt and Van der Leun (1967).

The dotted levels are proposed to explain the observed spectrum.



\_\_\_\_\_ 0.338 
$$\frac{5}{2}$$
\*
\_\_\_\_\_\_ 3:
No

FIGURE 7.3

)

Figure 7.3: Spectrum of delayed protons following the bombardment of a sulfur target (1. mg/cm<sup>2</sup>) with 57 MeV protons. The peaks are labelled with their energy in MeV. These energies have been corrected to centre-of-mass.

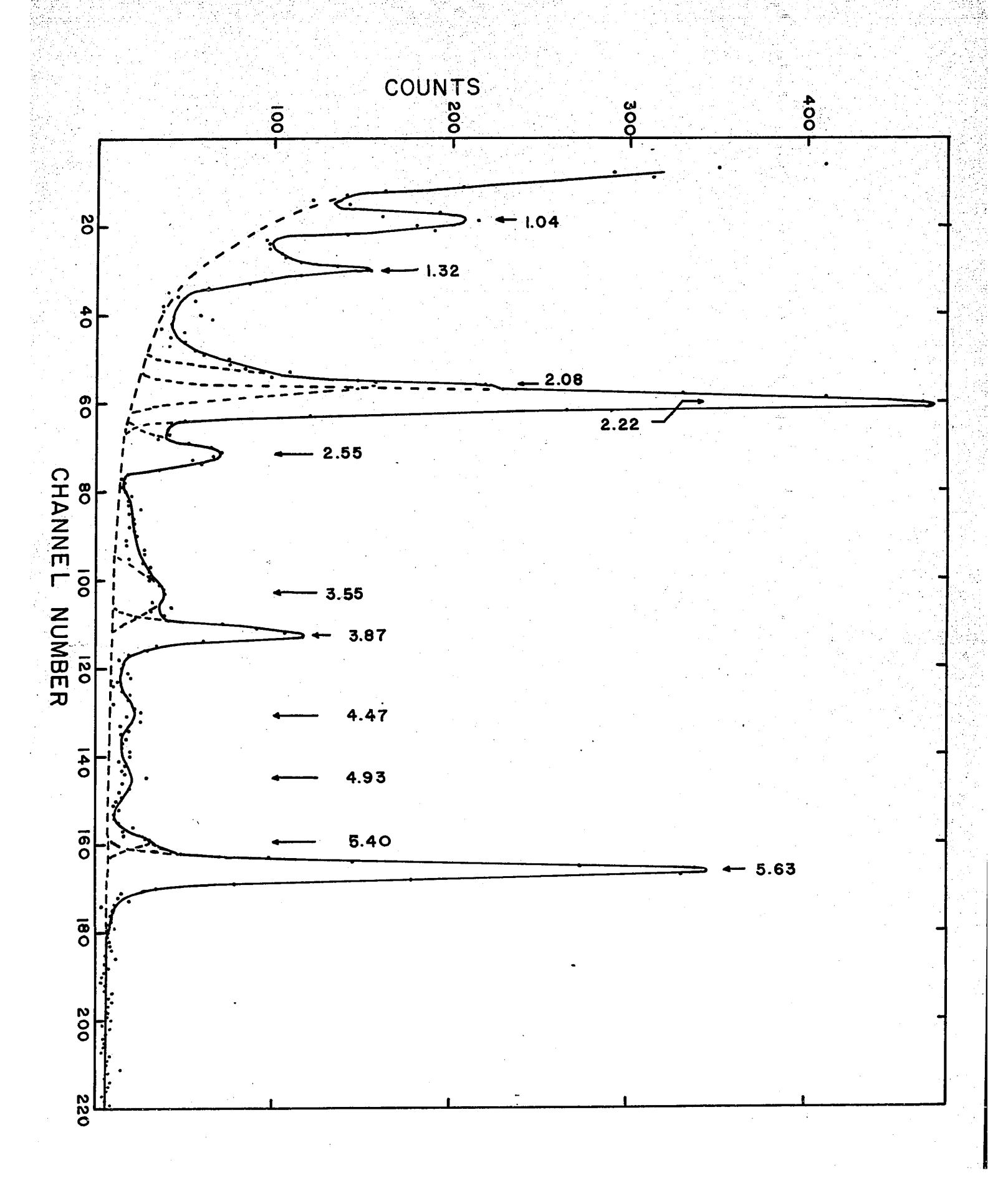
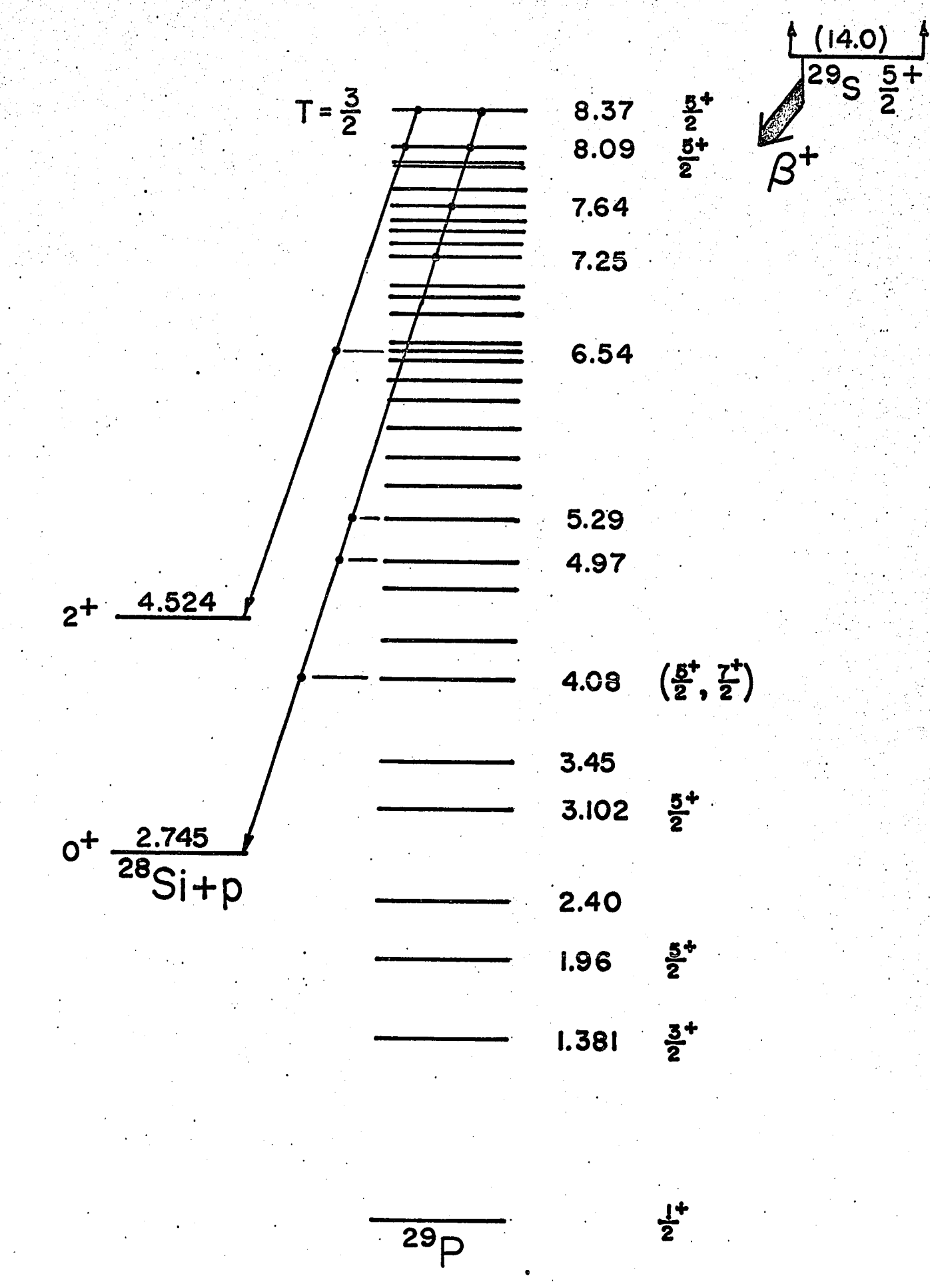


FIGURE 7.4



Figure 7.4: Proposed partial decay scheme for <sup>29</sup>S showing the transitions observed in this experiment.

The level scheme is taken from the compilation of Endt and Van der Leun (1967).



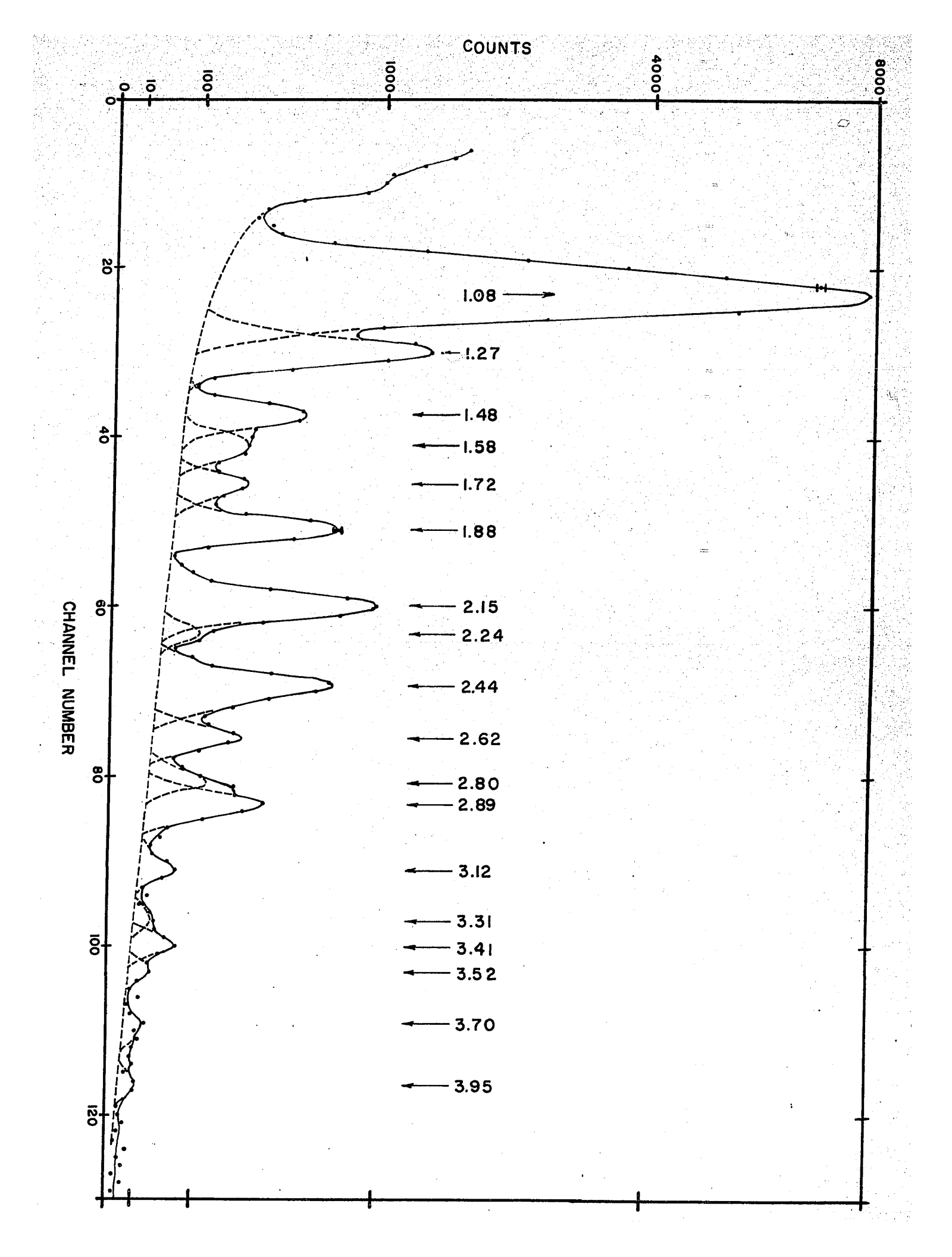
and the second of the second o

FIGURE 7.5

•Name +Sr + mar one of the Sr officer.



Figure 7.5: Spectrum of delayed protons observed following the bombardment of a calcium target (0.5 mg/cm<sup>2</sup>) with 25 MeV protons. The peaks have been labelled with their energies (in MeV) corrected to centre-of-mass.



FTCHRE 7.6



Figure 7.6: Lifetime curve for the total area of the 40Sc spectrum above 1.6 MeV.

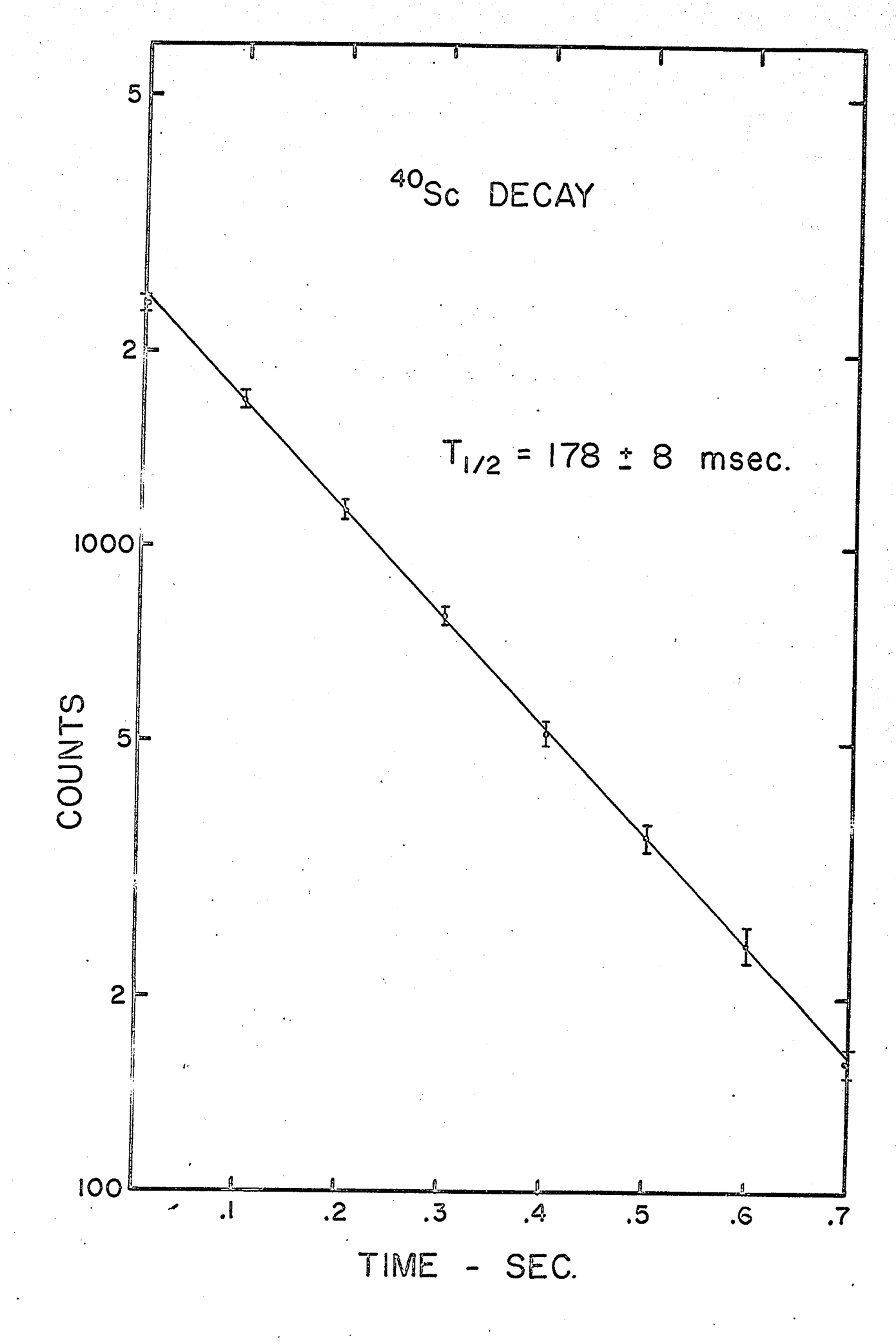
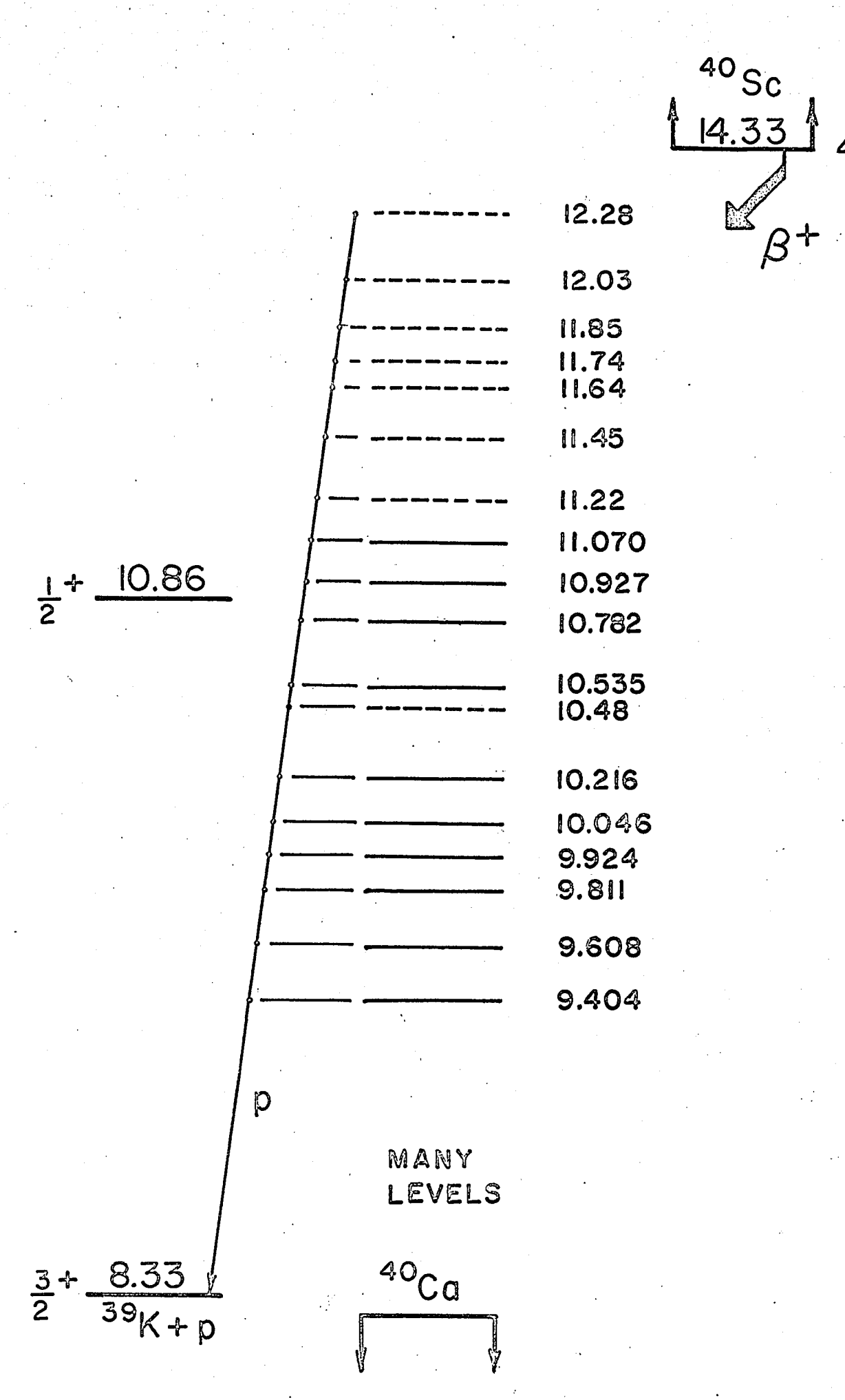






Figure 7.7: Proposed partial decay scheme for 40Sc showing the decays observed by delayed proton emission.

The levels indicated with solid lines have been taken from the compilation of Endt and Van der Leun. The dotted levels have been proposed to explain the observed spectrum.



#### 8 SUGGESTIONS FOR FURTHER RESEARCH

#### 8.1 APPARATUS AND TECHNIQUES

The ability of the gas counter telescope system to detect very low energy protons and the increased resolution due to thinner targets have resulted in the observation of many new peaks. One of the faults of the spectra is the lack of good counting statistics. This in turn is due to the rapidity at which the silicon detectors deteriorate in the cyclotron. The resolution of a typical detector is appreciably worse after  $1\frac{1}{2}$  to 2 hours of running time.

It is thought that the principal cause of radiation damage is due to protons being scattered from the target into the detector. It is proposed that a rotating wheel to act as a "chopper" be introduced between the target and the detector. This chopper would be thick enough to stop scattered protons from reaching the detector when the beam was on, and would expose the target to the detector when the beam was off. The device should appreciably extend the life of a detector. (This arrangement is presently being designed.)

Other suggestions to improve the resolution of the spectra are as follows:

- 1. Higher resolution detectors could be purchased. The resolution of the present detectors is rated as being 45 keV (FWHM). There are better detectors available, but they have not been justified because the total resolution is much worse than 45 keV, and because the resolution is so rapidly degraded by radiation damage.
- 2. Thinner targets can be made. (This entails longer counting periods, which again raises the question of radiation damage.)

- 3. An F.E.T. (field effect transistor) preamplifier could be placed close to the detector. At present, the (tube) preamplifier is approximately 6 feet from the detector, and the capacitance of the interconnecting coaxial cable worsens the resolution.
- 4. The detector could be cooled, perhaps with dry ice or liquid nitrogen, but more likely with a thermoelectric cooler.
- 5. Dr. R.B. Moore has pointed out that intensity of gamma radiation inside the cyclotron could be reduced if the parts of the machine which receive a large amount of "spilled" proton beam (e.g. the area around the channels, the dummy dee, etc.) were shielded with carbon. The activity from carbon has a half-life of about 20 minutes (11°C). Therefore it would require waiting only a few hours to obtain a relatively "cool" machine. Also, the only gamma ray in the decay of 11°C is the 0.511 MeV positron annihilation peak against which it is possible to shield the detector.
- 6. Thinner front windows for the gas counter would improve the resolution of the system, and would enable the observation of low energy alpha particles.

#### 8.2 EXPERIMENTS

An interesting problem which can now be investigated more closely involves the beta decay of <sup>17</sup>Ne to the 3.10 MeV excited state in <sup>17</sup>F. The decay should be allowed but the log ft value is very large for an allowed decay. The problem has been discussed by Margolis and de Takacsy (1965). Esterlund et al. (1967), in looking at the delayed proton decay of <sup>17</sup>Ne claim that the log ft is greater than 6.1, although they do not show the proton spectrum in the relevant region. With the telescope system described here, one should be able to push this limit to at least 7. Since the log ft of the mirror decay has been shown by Silbert and Hopkins (1964) to be 6.9,

it may be possible to make an actual observation rather than just set a limit.

With or without improvements in the experimental set-up there are a number of interesting investigations to be performed. All known delayed proton emitters could profitably be reinvestigated. The telescope system, as it now stands, can produce better spectra than any delayed proton spectra previously published. Low energy spectra for many of these nuclei were measured in Brookhaven by R. McPherson et al. (See Chapter 2). Using the telescope, I believe that all these spectra could be improved in resolution, in the low energy limit, and except perhaps in the case of <sup>25</sup>Si, in counting statistics. As an example of this, a spectrum of <sup>37</sup>Ca was obtained in which it was possible to see peaks down to about 0.9 MeV, whereas the limit in the Brookhaven spectrum was about 1.5 MeV. In this particular case, since a calcium target had been used, the low energy portion of the spectrum was badly contaminated with a <sup>40</sup>Sc background. This can be remedied, however, simply by using a potassium rather than a calcium target.

The observation of protons following the decay of  $^{40}$ Sc suggests the investigation of the series of nuclei having the structure Z = 2k + 1, N = 2k - 1. The lower members of this sequence  $^8B$ ,  $^{12}N$ ,  $^{20}Na$ ,  $^{24}Al$  and  $^{32}Cl$  are known to be delayed alpha emitters. Charged particle decay of  $^{28}P$  and  $^{36}K$  has not been observed, although it is energetically possible. Delayed proton emission is possible for all these nuclei heavier than  $^{20}Na$ , the process steadily becoming more energetically favourable as the mass increases. Except in the case of  $^{20}Na$  (Macfarlane and Siivola, 1964), no measurements of alpha spectra have been made; only the presence of alphas has been observed (Glass and Richardson, 1955). Using a thinner window on the detector, one can look for both alphas and protons from the decay of

these nuclei.

Nuclei in this series, heavier than  $^{40}$ Sc, (viz.  $^{44}$ V,  $^{48}$ Mn,  $^{52}$ Co,  $^{56}$ Cu) have not as yet been observed by any process. Mass tables calculated by Seeger (1961), predict that these nuclei are all bound and energetically capable of emitting delayed protons. These nuclei can all be produced by (p,3n) reactions on stable isotopes. It would be interesting (and quite feasible) to search for these nuclei using the present system.

### 9 SUMMARY

This thesis has reported the following:

- 1. The identification of four new nuclei ( ${}^{9}$ C,  ${}^{29}$ S,  ${}^{33}$ Ar,  ${}^{37}$ Ca) belonging to the series Z = 2k+2, N = 2k-1.
- 2. The measurement of the half-lives of these nuclei.
- 3. The observation of the high energy (above ≈ 3.2 MeV) proton peaks following the decay of these nuclei.
- 4. The location of the T = 3/2 analogue levels in nuclei which are the  $\mathcal{B}^{\dagger}$  decay daughters of  $^{29}\text{S}$ ,  $^{33}\text{Ar}$ ,  $^{37}\text{Ca}$  (i.e. in  $^{29}\text{P}$ ,  $^{33}\text{Cl}$ ,  $^{37}\text{K}$ ). Other previously unobserved levels were also located in these daughter nuclei.

The above observations were made in collaboration with J.C. Hardy, using a single counter detector system with the detector placed inside the cyclotron and the results are reported in appendices in the form of reprints of the published papers. The following work was performed after Hardy's departure.

- 5. The design and construction of a two counter telescope consisting of a silicon surface barrier (E) detector and a proportional counter (dE/dx) detector. The dE/dx detector was made very thin (≈1 mg/cm²) for the detection of low energy protons.
- 6. Use of this detector to remeasure the proton spectra following the decay of <sup>29</sup>S and <sup>21</sup>Mg with the observation of new peaks in the low energy region as well as in the region previously measured.
- 7. The discovery that the known nucleus 40 Sc was a delayed proton emitter.
- 8. A measurement of the energies and relative intensities of the proton peaks following the decay of 40Sc.

- 9. The assignment of the proton peaks from <sup>21</sup>Mg, <sup>29</sup>S and <sup>40</sup>Sc to known (or proposed) levels in the intermediate nucleus (the state decay daughter).
- 10. The estimation of  $\log \underline{ft}$  values for the newly observed transitions from  $^{21}\text{Mg}$  and  $^{29}\text{S}$ . Relative  $\log \underline{ft}$  values were calculated in the case of  $^{40}\text{Sc}$ .

"Decay of Carbon-9"

Reproduced from

Physical Review Letters

Volume 14, Number 10, 8 March 1965

Pages 376 - 378

#### **DECAY OF CARBON-9**

J. C. Hardy, R. I. Verrall, R. Barton, and R. E. Bell Foster Radiation Laboratory, McGill University, Montreal, Canada (Received 25 January 1965)

This Letter reports the results of recent measurements on delayed protons following the  $\beta^+$ decay of °C. These measurements were undertaken as part of a systematic investigation carried out at this Laboratory on the A = (4n+1),  $T_2 = -\frac{3}{2}$  series of delayed proton precursors. Carbon-9 was of particular interest not only because it was the lightest member of the series, but also because it was the lightest nuclide whose existence (i.e., particle stability) was expected, and whose decay had not been definitely detected. A few years ago, Swami, Schneps, and Fry2 interpreted a single event in a nuclear emulsion as an example of the decay of °C, and more recently Wilkinson<sup>3</sup> and Jaenecke<sup>4</sup> estimated that <sup>9</sup>C should be stable against proton emission by about 1 MeV. While the present experiment was in progress, Cerny et al.5 verified Wilkinson's estimate by measuring the energy balance in the reaction 12C(3He, 6He)9C leading to the ground state of °C.

Bombardments were carried out in the internal beam of the McGill synchrocyclotron using targets of carbon and natural boron;  $^{9}$ C was produced by the reactions (p,d2n) on  $^{12}$ C, and (p,2n) and (p,3n) on  $^{10}$ B and  $^{11}$ B, respectively.

Two alternative detection systems were used. The first was a solid-state counter telescope comprised of a  $50\mu$  totally depleted surface-barrier silicon detector (dE/dx) and a 3-mm (22-MeV for protons) lithium-drifted detector (E). The second detection system was a surface-barrier silicon detector of  $500\mu$  depletion

depth (8-MeV for protons) with absorbers to reduce the incident-proton energy. The detector system and target foil were mounted 5 cm apart on a radial probe which was inserted into the internal cyclotron beam. Counting was performed between repeated 30-msec bursts of normal cyclotron operation. The recording of pulses was interrupted during the beam burst and for 100 msec afterwards, this delay being long enough to allow the dissipation of beamstorage effects in the cyclotron. As well as proton energy spectra, time spectra could be obtained by using a 400-channel pulse-height analyzer in its scaling mode, or by sequentially directing the proton spectrum into the four quarters of the analyzer.

For the telescope system, the dE/dx and the E pulses were added, and the sum was recorded only if the dE/dx pulses fell within predetermined limits. These limits were set so as to make it possible to record protons with energies from 0.3 to 14 MeV and to exclude all  $\alpha$  particles in this range. The  $\beta$ - and  $\gamma$ -ray background, however, was not completely rejected. Figure 1 shows the spectrum obtained from a carbon target (2.4 mg/cm<sup>2</sup> polyethylene); the threshold for production of this spectrum was found to be  $52 \pm 3$  MeV. Similar peaks were obtained from a boron target (3.6 mg/cm<sup>2</sup> H<sub>2</sub>BO<sub>4</sub> sprayed on thin gold foil) bombarded at 45 MeV. No sign of a similar activity was observed in energy spectra and decay curves from thick beryllium and lithium targets. These findings

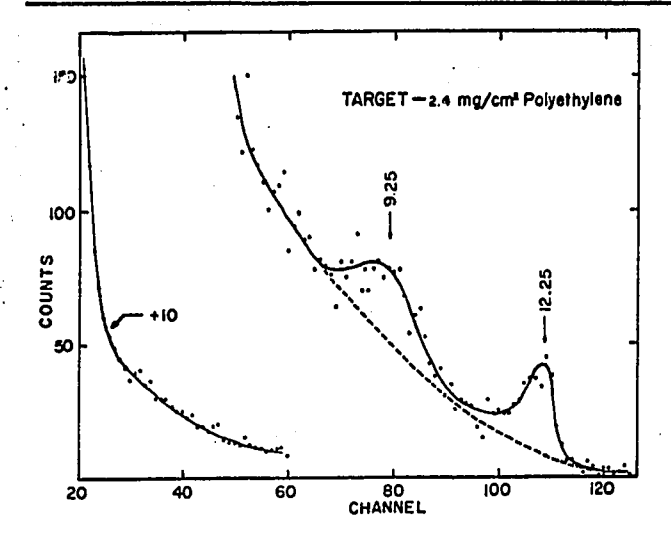


FIG. 1. Spectrum of delayed protons following the decay of  $^9$ C. The continuum contains an unknown but probably small number of  $\beta$  and  $\gamma$  counts. The peaks have been marked with their center-of-mass energies. The target was bombarded with  $\sim 10^{16}$  85-MeV protons, and the over-all detection efficiency was about 0.25%.

identify the activity as being due to  ${}^{9}$ C, whose calculated laboratory production threshold is  $55.1 \pm 0.2$  MeV for the reaction  ${}^{12}$ C(p, d2n) ${}^{9}$ C and  $28.4 \pm 0.2$  MeV for the reaction  ${}^{10}$ B(p, 2n) ${}^{9}$ C.

The two peaks in Fig. 1 were brought in turn within the range of the 8-MeV-thick detector by appropriate aluminum absorbers. This again identifies the peaks as due to protons, and gives another measure of their energies. The energies measured by the 22-MeV-thick detector involve a long extrapolation from the 5.305-MeV α-particle calibration, while those measured by the 8-MeV-thick detector involve a large absorption correction; the peaks also have substantial widths. Nevertheless, the two methods of energy measurement disagreed by only about 0.3 MeV, and we will quote average figures with appropriate error estimates. The peaks of Fig. 1 are both much wider than the resolution width (~0.25 MeV) of the target-detector system. We finally quote the measured peak energies and widths in Table I.

Table I. Peak energies corrected to center of mass, with corresponding observed widths (full width at half-maximum) corrected for resolution.

Energy (MeV)	Width (keV)	Relative intensity	
12.25 ± 0.20	800 ± 100	1 .	
$9.25 \pm 0.25$	$1400 \pm 200$	~1.5	

The time decay of the spectrum was observed in many runs, all of which gave consistent results for the half-life. Separate multiscaling runs were performed on pulses corresponding to the 12.25-MeV peak, and on those pulses in the range of 4 to 10 MeV. In the latter case a weak 800-msec component due to a mixture of <sup>8</sup>B and <sup>8</sup>Li had to be subtracted. The result for the half-life of <sup>9</sup>C is 127±3 msec.

Figure 2 shows a level scheme embodying the present results on  $^9C$ . The two peaks of Fig. 1 are attributed to proton decay from a level of  $^9B$  to the familiar ground and first excited states of  $^8Be$ . The separation of the observed peaks is  $3.0\pm0.3$  MeV in agreement with the known 2.90-MeV separation of these levels. The energy of the proton-emitting lavel of  $^9B$  is calculated to be  $12.05\pm0.2$  MeV and its width to be  $800\pm100$  keV. This is presumably the state which Dietrich and Davies $^6$  observed at  $12.3\pm0.3$  MeV with a width of  $800\pm200$  keV.

These authors also observed a level at 14.67 MeV to which they assigned  $T = \frac{3}{2}$ . Although  $\beta^+$  decay to this level from  ${}^{\theta}$ C would be superallowed, the decay energy is small, and reasonable estimates for the  $\log ft$  values lead one to expect an unobservably small number of delayed protons from this level.

With three odd particles,  ${}^{9}$ C is taken to have spin-parity  $\frac{3}{2}$ , and its allowed  $\beta^{+}$  decay to the

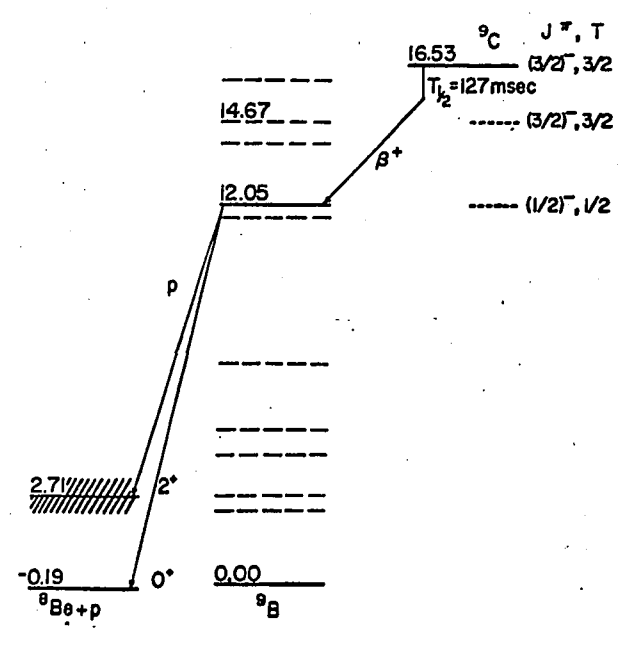


FIG. 2. Partial decay scheme of <sup>9</sup>C showing the branch identified in this experiment. All of the indicated levels for <sup>9</sup>B have been observed by previous workers.

12.05-MeV state of <sup>9</sup>B restricts that state to  $\frac{1}{2}$ ,  $\frac{3}{2}$ , or  $\frac{5}{2}$ . The nearly equal proton intensities to the 0<sup>+</sup> and 2<sup>+</sup> states of <sup>8</sup>Be favor the assignment of  $\frac{1}{2}$ .

Two of us (J.C.H. and R.I.V.) wish to thank the National Research Council for scholarships.

This work was supported by the Atomic Energy Control Board (Canada).

<sup>1</sup>See, for example, J. C. Hardy and R. I. Verrall,

Phys. Rev. Letters 13, 764 (1964), which includes further references.

<sup>2</sup>M. S. Swami, J. Schneps, and W. F. Fry, Phys. Rev. 103, 1134 (1956).

<sup>3</sup>D. Wilkinson, private communication. <sup>4</sup>J. Jaenecke, Kernforschungszentrum Karlsruhe Report No. KFK 185, 1963 (unpublished).

<sup>5</sup>J. Cerny, R. H. Pehl, F. S. Goulding, and D. A. Landis, Phys. Rev. Letters 13, 726 (1964).

<sup>6</sup>F. S. Dietrich and J. W. Davies, Bull. Am. Phys. Soc. 8, 598 (1963).

"Delayed Protons Following the Decay of  $S^{29}$ "

Reproduced from

Physics Letters

Volume 13, Number 2, 15 November 1964

Pages 148 - 149

# DELAYED PROTONS FOLLOWING THE DECAY OF S<sup>29</sup>

J. C. HARDY and R. I. VERRALL
Foster Radiation Laboratory, McGill University, Montreal

Received 15 October 1964

Delayed protons have been observed following decay of the previously unreported S<sup>29</sup>. The existence (i. e. particle stability) of S<sup>29</sup> has been predicted by Baz [1], and its expected Q<sub>β+</sub> may be estimated using the semi-empirical formula of Jaenecke [2] for Coulomb energy differences. This formula yields an energy of 8.  $2 \pm 0.5$  MeV for the first  $T = \frac{3}{2}$  level in Si<sup>29</sup>. The lowest  $T = \frac{3}{2}$  level in P<sup>29</sup> should be at about this same energy if one assumes isobaric invariance, and the Q<sub>β+</sub> for S<sup>29</sup> may be estimated at 13.8  $\pm$  0.5 MeV.

Measurements were taken using a surface barrier silicon detector of area 200 mm<sup>2</sup> and  $500 \mu$ 

depletion depth (8 MeV for protons), mounted 6 cm from the thin target foil and inserted on a radial probe into the circulating proton beam of the McGill synchrocyclotron. Counting was performed between repetitive bursts, typically 30 msec long, of normal cyclotron operation. A clock-controlled counting period was initiated following a 100 msec delay which was long enough to allow dissipation of beam storage effects in the cyclotron. This period could be accurately divided into four equal intervals, enabling the spectrum to be stored sequentially in the four quadrants of a 256 channel analyzer. Thus fourpoint decay

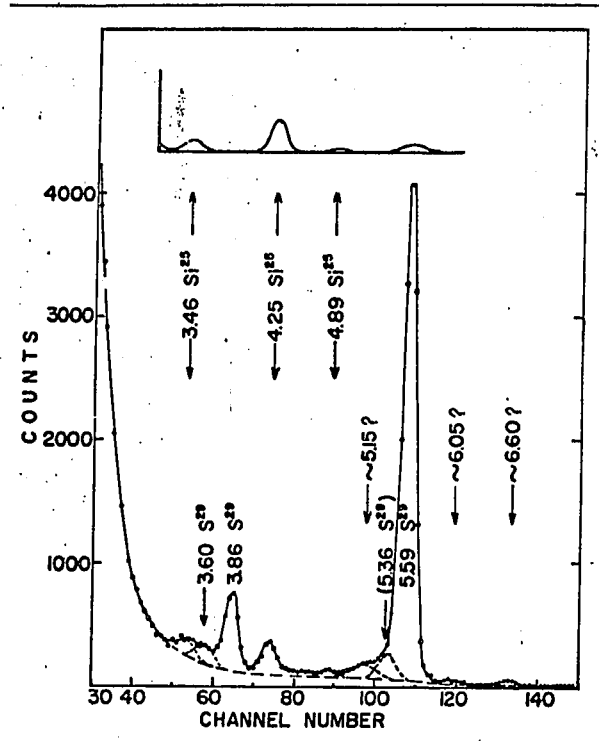


Fig. 1. Spectrum of delayed protons following the bombardment of sulfur. The energy of each proton peak is shown in MeV, corrected to centre-of-mass. The insert shows the delayed proton spectrum following the decay of  $\mathrm{Si}^{25}$ , taken from reference 4; this spectrum has been normalized so that the peak height at 4.25 MeV is the same in both spectra. The peak marked (5.36  $\mathrm{S}^{29}$ ) should be considered as less certain than the other  $\mathrm{S}^{29}$  peaks.

curves for the peaks in the spectrum could be obtained.

Fig. 1 shows the delayed proton spectrum obtained following bombardment of a 1.5 mg/cm<sup>2</sup> sulfur target evaporated on a thin (200  $\mu$ g/cm<sup>2</sup>) gold backing. A phosphorus target [3] yielded similar peaks, but the counting rate obtained was not as great.

Yield curves for the most prominent peaks could be plotted for both targets by measuring their production as a function of the target radius in the cyclotron. Radial oscillations in the cyclotron beam make the actual bombarding energy at a given target radius less than the nominal cyclotron energy at that radius by an amount not well determined (2 to 5 MeV), but relative threshold measurements are accurate to better than 2 MeV.

Spectra taken at different incident proton energies indicated that the peak in channel 74 had a higher threshold than the large peak in channel 108. Both its energy and its measured threshold indicated that it was in fact following the decay of

 $Si^{25}$ . The  $Si^{25}$  delayed proton spectrum [4] is shown as the insert in fig. 1. Other lines associated with Si<sup>25</sup> could then be identified and are seen to appear in the main spectrum with the relative intensities expected. Of the remaining lines, four were attributed to the decay of S29 by the following argument. Since these lines did not appear following bombardment of silicon, the nuclide responsible for the activity must be an isotope of phosphorus or sulfur. (Clearly there is only a small contribution to the large peak in channel 108 from the  $\mathrm{Si}^{25}$  peak at about the same energy.) Any isotope of phosphorus that can be a delayed proton precursor must have a production threshold from stable sulfur lower than that from phosphorus. In fact, however, the apparent production threshold from sulfur was 7 MeV greater than that from phosphorus, and was approximately 50 MeV. These results are compatible only with the reactions  $S^{32}(p, d2n)S^{29}$  and  $P^{31}(p, 3n)S^{29}$ whose calculated laboratory energy thresholds are  $(46.3 \pm 0.5)$  MeV and  $(39.5 \pm 0.5)$  MeV. The appearance of Si<sup>25</sup> lines in the spectrum is attributed to the reaction S<sup>32</sup>(p, \alpha d2n)Si<sup>25</sup> whose threshold, 55.8  $\pm 0.5$  MeV, is 9.5 MeV higher than the threshold for  $S^{32}(p,d2n)S^{29}$ ; this difference compares favourably with the experimental difference of about 10 MeV.

The two high energy peaks (6.05 and 6.60 MeV) were not sufficiently above background to identify their source positively, while the peak in channel 97 did not behave in a consistent manner and has not yet been identified. The energies of the peaks shown in fig. 1 are corrected to centre-of-mass. Since this correction depends upon the source, the three peaks of uncertain origin are shown only with approximate energies.

Typical decay curves for the three main peaks are shown in fig. 2. The data for the 5.59 MeV peak has been corrected for the small  $\mathrm{Si}^{25}$  peak (5.62 MeV). From such curves, the half life we adopt for  $\mathrm{S}^{29}$  is  $195 \pm 8$  msec. Incidentally, the 4.25 MeV peak is seen to have a half life consistent with its assignment to  $\mathrm{Si}^{25}$  which has a measured half life of 225 msec [4].

The proposed decay scheme appears in fig. 3. The known level at 8.08 MeV [5] would result in proton peaks at 5.33 and 3.56 MeV, agreeing within experimental error with the observed peaks at  $5.36 \pm 0.10$  and  $3.60 \pm 0.06$  MeV. The peaks at  $3.86 \pm 0.04$  and  $5.59 \pm 0.04$  MeV fit the decay of a proposed new level at  $8.36 \pm 0.03$  MeV.

proposed new level at  $8.36 \pm 0.03$  MeV. The spin-parity of  $Al^{29}$  is  $\frac{5}{2}$ , as it is for all other nuclei with 13 odd nucleons, and consequently it is likely that  $S^{29}$ , its mirror, should have the same spin-parity. On this basis, the pos-

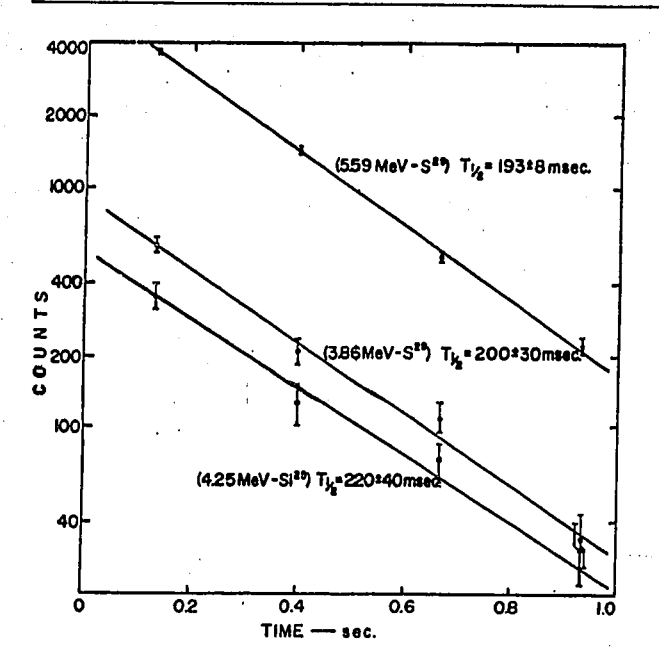


Fig. 2. Typical four-point decay curves for peaks in the spectrum of protons following bombardment of sulfur. The energy of the peak considered, its source, and its measured half life are indicated for each curve.

itron decay to the 8.08 MeV level should be allowed. If a log ft between 4.0 and 5.0 is assumed for this transition, then from the relative intensities of the proton peaks, the decay to the 8.36 MeV level has a log ft between 2.5 and 3.9, indicative of a super-allowed transition. Combining this with the fact that the expected energy of the first  $T=\frac{3}{2}$  state in  $P^{29}$  is  $8.2\pm0.5$  MeV, it is reasonable to assign this isotopic spin to the level at  $8.36\pm0.03$  MeV. Like the similar levels in  $Al^{25}$  and  $Na^{21}$  [4], this level can proton-decay only through an admixture of  $T=\frac{1}{2}$ . If this admixture is small, then it is to be expected that the level should not appear in resonance data for proton reactions on  $Si^{28}$ . This appears to be the case.

There are several other levels in  $P^{29}$  with a spin of  $\frac{5}{2}$  or  $\frac{3}{2}$  which are apparently not populated sufficiently to be observed in this experiment. This, however, is not inconsistent with these levels being fed by allowed transitions,

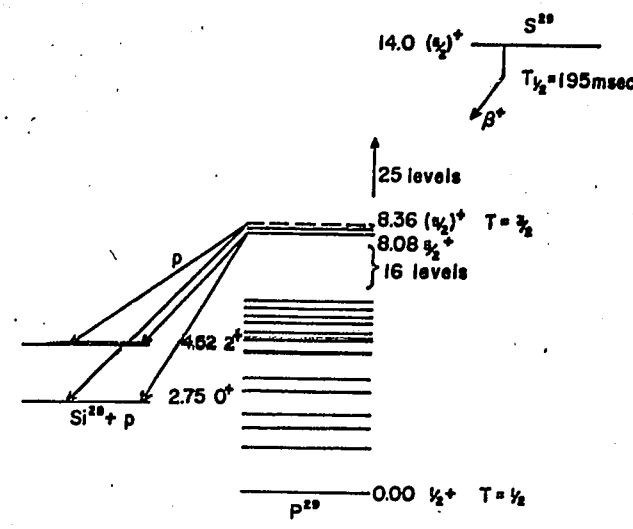


Fig. 3. Proposed decay scheme of  $S^{29}$ . The proposed  $T=\frac{3}{2}$  level is shown dashed at 8.36 MeV; all other levels and assignments are from the compilation of Endt and van der Leun [5].

since, on the basis of the range of log ft's previously assumed, transitions with high allowed log ft's could result in peaks with unobservably low intensities.

Using the value 8.36 MeV for the lowest  $T=\frac{3}{2}$  state in P<sup>29</sup> and the calculated Coulomb energy difference, a revised estimate of the Q<sub>β+</sub> for S<sup>29</sup> is 14.0 ± 0.2 MeV; this value is shown in fig. 3.

We should like to thank Professor R. E. Bell, the director of the Laboratory, and Dr. R. Barton for helpful discussions, as well as Dr. R. McPherson for assistance in the early stages of the work. We acknowledge, also, scholarships awarded by the National Research Council.

This research was supported by a grant from the Atomic Energy Control Board (Canada).

- 1. A.I. Baz, Atomnaya Energiya 6 (1959) 571.
- 2. J. Janecke, Z. Physik 160 (1960) 171.
- 3. B. W. Hooton, Nucl. Instr. and Meth. 27 (1064) 338.
- 4. R. McPherson and J. C. Hardy, Can. J. Phys, in
- P.M. Endt and C. van der Leun, Nuclear Physics 34 (1962) 1.

"Delayed Protons Following the Decay of Argon-33"

Reproduced from

Canadian Journal of Physics

Volume 43, March 1965

Pages 4.8 - 421

## DELAYED PROTONS FOLLOWING THE DECAY OF ARGON-33

J. C. HARDY AND R. I. VERRALL

Foster Radiation Laboratory, McGill University, Montreal, P.Q.

Received November 27, 1964

#### ABSTRACT

The delayed-proton precursor  $^{33}$ Ar has been produced by proton bombardment of a lithium chloride target in the internal beam of the McGill synchrocyclotron. The half-life of  $^{33}$ Ar was measured to be (178  $\pm$  10) msec. To explain the delayed proton spectrum, two new levels, at 5.55 and 7.55 MeV, in  $^{32}$ Cl are proposed. It is also proposed that the former is the expected first T=3/2 state in that nucleus.

Delayed protons have been observed following the decay of <sup>23</sup>Ar. The only previous reports of this nuclide are brief mentions by Reeder *et al.* (1964) and by us (Hardy and Verrall 1964a) in simultaneous publications that were devoted mainly to another delayed proton precursor, <sup>27</sup>Ca. We now report our results in detail; they differ somewhat from those of Reeder *et al.* 

The measurements were carried out as in previous experiments in the present series (e.g. McPherson *et al.* 1964), using thin targets bombarded in the circulating proton beam of the McGill synchrocyclotron and observed by surface-barrier silicon detectors. Figure 1 shows the delayed proton spectrum from a chlorine target (2.3 mg/cm² LiCl vacuum evaporated on a 200 µg/cm² gold backing). Shown as an inset in Fig. 1 is the spectrum of delayed protons obtained from a sulphur target, which is taken from the work of Hardy and Verrall (1964b). We now argue that in the main spectrum only the two peaks located at channels 47 and 98 can be said definitely to follow the decay of <sup>33</sup>Ar. Two other peaks, at channels 67 and 114, are too small to be identified positively, while all other peaks are attributed to <sup>29</sup>S and <sup>25</sup>Si.

The peak in channel 105 of the main spectrum was shown to follow the decay of <sup>29</sup>S by means of the following arguments. Its production threshold was found to be (50  $\pm$  5) MeV, which agrees with the calculated threshold for the reaction <sup>35</sup>Cl(p,  $\alpha$ 3n)<sup>29</sup>S. Also, the measured energy of this peak is the same as that previously found (cf. inset) for the principal proton group following the decay of <sup>29</sup>S. By comparison with the inserted spectrum, several other peaks in the main spectrum can be identified, and these are seen to appear with the relative intensities expected.

It can be seen that the predominant peak in channel 47 was not observed following proton bombardment of sulphur, and consequently the nuclide responsible for the activity must be an isotope of argon. A measurement of the threshold for its production was difficult to obtain because of the relatively high  $\beta$  background; however, an approximate value of  $(39 \pm 5)$  MeV was determined. The argon isotope must then be  $^{33}$ Ar since the observed threshold is consistent only with the reaction  $^{35}$ Cl(p,  $3n)^{33}$ Ar, whose calculated threshold is 37.8 MeV. A decay curve of the net area under this peak is shown in Fig. 2, and gives the half-life as  $(178 \pm 10)$  msec.

Canadian Journal of Physics. Volume 43 (March, 1965)

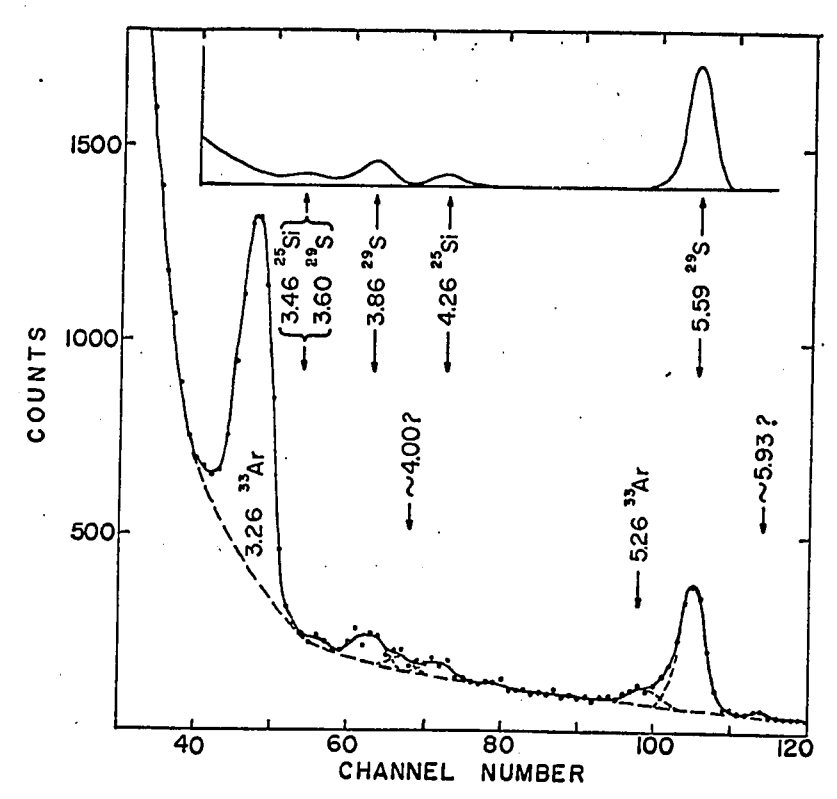


Fig. 1. Spectrum of delayed protons from a chlorine target. The energy of each proton peak is shown in MeV, corrected to center of mass. The energies of the two peaks of uncertain origin have been calculated for mass 33. The inset shows the spectrum from a sulphur target and has been normalized so that the peak height at 5.59 MeV is the same in both spectra.

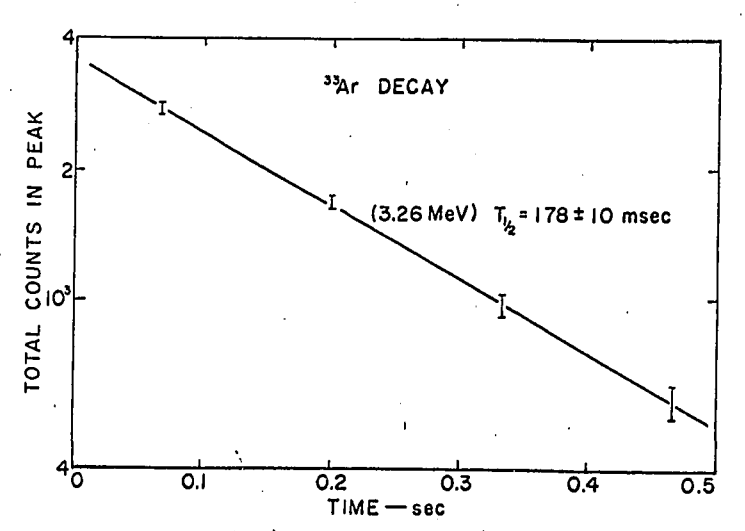


Fig. 2. Time decay of the net area under the main peak of Fig. 1, showing that the half-life of  $^{33}$ Ar is (178  $\pm$  10) msec.

From lifetime and threshold measurements, the peak in channel 98 (Fig. 1) appears also to be associated with <sup>33</sup>Ar; its intensity is about 4% of that of the main peak (3.26 MeV) of the <sup>33</sup>Ar spectrum.

The energies, corrected to center of mass, of the two peaks assigned to  $^{33}$ Ar are  $(5.26 \pm 0.1)$  and  $(3.26 \pm 0.05)$  MeV, as is indicated in Fig. 1. Figure 3 shows the proposed decay scheme of  $^{33}$ Ar and includes two new levels at  $(7.55 \pm 0.1)$  and  $(5.55 \pm 0.05)$  MeV which are introduced to explain the two observed proton peaks. The first level is in an energy region not previously explored, and the second has apparently not been observed in proton-scattering experiments.

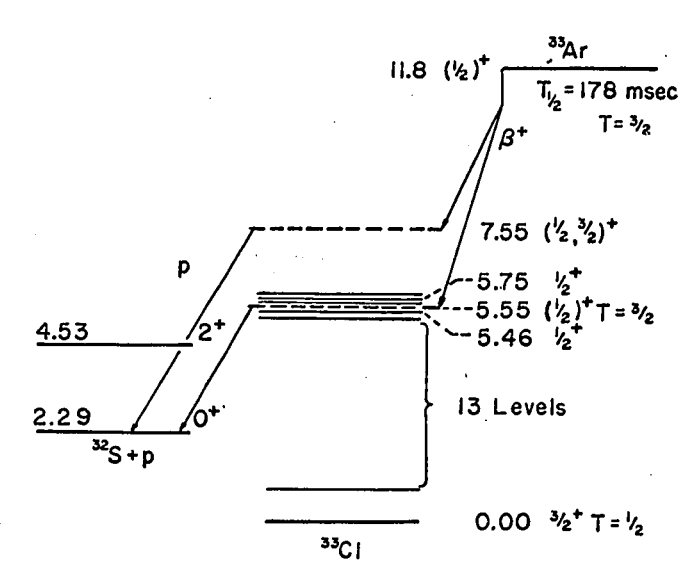


Fig. 3. Proposed decay scheme of <sup>33</sup>Ar. Previously known levels, taken from the compilation of Endt and van der Leun (1962), are shown as solid lines.

As well as observing the peak at 3.26 MeV, Reeder *et al.* observed a peak at  $(3.90 \pm 0.1)$  MeV which they attributed to <sup>33</sup>Ar. This could be the unidentified peak which we observed at about 4.0 MeV. Their measured spectrum does not extend to sufficiently high energies to include the <sup>33</sup>Ar peak at 5.26 MeV.

All known nuclei with 15 odd nucleons have an assigned spin parity of  $\frac{1}{2}$ +, and for this reason, we have assigned  $\frac{1}{2}$ + to  $^{33}$ Ar. On the basis of this assignment there are two known levels in  $^{32}$ Cl which should be fed by allowed  $\beta$  transitions and which should decay by emitting protons within the energy range of observation. Such proton groups (expected at 3.17 and 3.46 MeV) are certainly not present with an intensity comparable to that of the observed 3.26-MeV peak. This suggests that the level at 5.55 MeV is fed by a superallowed  $\beta$ + transition from the T=3/2 ground state of  $^{32}$ Ar, and is therefore the expected first T=3/2 state in  $^{32}$ Cl. This isotopic spin assignment would also account for the level's nonappearance in resonance data for proton scattering from  $^{32}$ S. Using the semiempirical formula of Jaenecke (1960) for Coulomb energy differences, and assuming isobaric invariance, the expected energy of the first T=3/2 level was calculated to be 5.54 MeV, which is in good agreement with our experimental value.

It can also be noted by comparing the relative intensities of the relevant proton peaks that the  $\log ft$  value for  $\beta$  decay to the 7.55 MeV level is only about 0.35 higher than that for the superallowed decay. It is certainly, then, a highly allowed transition, perhaps indicating that the 7.55-MeV level also has some T=3/2 admixture.

Using the value 5.55 MeV for the first T=3/2 level in  $^{33}$ Cl and a calculated Coulomb energy difference, the  $Q_{\beta^+}$  for  $^{33}$ Ar is found to be (11.8  $\pm$  0.2) MeV. This value is shown in Fig. 3.

To demonstrate the consistency of the above arguments, we now estimate the log ft value for the  $\beta^+$  decay to the 5.55-MeV level, from its energy and the experimental half-life. Correcting for  $\beta^+$  decay to the ground state of  $^{23}$ Cl, by using the known log ft value (5.0) of the mirror transition

$$^{33}P \xrightarrow{\beta} ^{33}S$$

we obtain  $\log ft = 3.0$ . Further corrections for the two or three other possible branches will raise this figure, but unless these branches themselves have unusually low  $\log ft$  values, the final result will remain in the superallowed range.

We should like to thank Professor R. E. Bell, the director of the Laboratory, and Dr. R. Barton for helpful discussions. We acknowledge, also, scholarships awarded by the National Research Council.

This research was supported by a grant from the Atomic Energy Control Board (Canada).

#### REFERENCES

ENDT, P. M. and VAN DER LEUN, C. 1962. Nucl. Phys. 34, 1.

HARDY, J. C. and VERRALL, R. I. 1964a. Phys. Rev. Letters, 13, 764.

1964b. Phys. Letters, 13, 148.

JAENECKE, J. 1960. Z. Physik, 160, 171.

MCPHERSON, R., HARDY, J. C., and BELL, R. E. 1964. Phys. Letters, 10, 65.

REEDER, P. L., POSKANZER, A. M., and ESTERLUND, R. A. 1964. Phys. Rev. Letters, 13, 767.

"Calcium-37"

Reproduced from

Physical Review Letters

Volume 13, Number 25, 21 December 1964

Pages 764 - 766

### CALCIUM-37†

J. C. Hardy and R. I. Verrall

Foster Radiation Laboratory, McGill University, Montreal, Canada (Received 13 November 1964)

This Letter reports the observation of the previously unreported  $^{87}$ Ca by measurements on the delayed protons following its  $\beta^+$  decay.

There has been much recent interest in the detection of solar neutrinos by means of the reaction  $^{37}Cl + \nu_{\rm Solar} - ^{37}Ar + e^-$ . Bahcall¹ has shown that this reaction may proceed either to the ground or to any of three excited states of  $^{37}Ar$ . The total cross section for this reaction was predicted using the measured lifetime

for the ground-state inverse transition  $^{37}$ Ar  $-^{37}$ Cl, a calculated ft value for the transition to the first  $T = \frac{3}{2}$  state of  $^{37}$ Ar, and estimated ft values for transitions to the two other excited states.

It has been pointed out<sup>2</sup> that a better estimate for branching to the latter two states can be obtained from a knowledge of the lifetime of  $^{37}$ Ca, since the positron decay of  $^{37}$ Ca $_{20}$ Ca $_{17}$ , namely  $^{37}$ Ca $_{20}$ Ca $_{37}$ K+ $e^+$ + $\nu$ , is the mirror reaction

to neutrino capture by  $^{37}_{17}\text{Cl}_{20}$ . This lifetime and other properties of the  $^{37}\text{Ca}$  decay have now been measured. The nuclide  $^{37}\text{Ca}$  is the latest one of the (4n+1) series of delayed-proton precursors studied in this Laboratory,  $^3$  the preceding members being  $^{13}\text{O}$ ,  $^{17}\text{Ne}$ ,  $^{21}\text{Mg}$ ,  $^{25}\text{Si}$ ,  $^{29}\text{S}$ , and  $^{33}\text{Ar}$ . The fact that  $^{37}\text{Ca}$  has appeared in its logical place in this series lends confidence to the results to be reported here.

Measurements were taken using a surface barrier silicon detector of 200-mm<sup>2</sup> area and 500- $\mu$  depletion depth (8 MeV for protons), mounted 6 cm from the thin target foil and inserted on a radial probe into the circulating proton beam of the McGill synchrocyclotron. Counting was performed between repetitive bursts, typically 30 msec long, of normal cyclotron operation. A clock-controlled counting period was initiated following a 100-msec delay which was long enough to allow dissipation of beam storage effects in the cyclotron. This period could be accurately divided into four equal intervals, enabling the spectrum to be stored sequentially in the four quarters of a 256-channel analyzer. Thus, four-point decay curves for the peaks in the spectrum could be obtained.

To calibrate the energy response of the system, the  $^{210}$ Po  $\alpha$  line was used in conjunction with pulses from a mercury pulse generator fed onto the input of the preamplifier. Several ten-minute counting periods were alternated with pulser calibrations in order to determine the energy of a peak.

Figure 1 shows the delayed proton spectrum obtained following proton bombardment of a 0.9mg/cm² calcium target, vacuum evaporated on a thin (200  $\mu$ g/cm<sup>2</sup>) gold backing. Similar peaks were obtained from a potassium target (KOH vacuum-evaporated on thin gold), but with a reduced counting rate. Bombardment of a chlorine target (LiCl) produced a proton spectrum which was considered to follow the decay of 33Ar; that spectrum included a peak near channel 47, but its other features indicate that its contribution to the spectrum in Fig. 1 is less than a few percent. Consequently, the nuclide responsible for the present activity must be an isotope of either potassium or calcium.

Yield curves for the prominent peak in Fig. 1 were plotted for both the calcium and potassium targets by measuring the delayed-proton production as a function of the target radius

in the cyclotron. Observations near threshold were difficult because of the  $\beta$  background under this peak; also, radial oscillations in the cyclotron beam make the actual bombarding energy at a given target radius less than the nominal cyclotron energy at that radius by an amount not well determined (2 to 5 MeV). Relative threshold measurements, however, could be made to within 2 MeV by comparing the excitation functions over a range of energies above the threshold.

The threshold for production from stable calcium (97%  $^{40}$ Ca) was found to be 7 MeV higher than that from potassium (93%  $^{50}$ K), and was approximately 47 MeV. These results are compatible only with the reactions  $^{40}$ Ca(p, d2n) $^{37}$ Ca and  $^{39}$ K(p, 3n) $^{37}$ Ca, whose calculated laboratory energy thresholds are 44.6 and 38.5 MeV. This establishes the activity as following the decay of  $^{37}$ Ca.

From decay curves of the area above background of the main proton peak, each taken over approximately five half-lives, we adopt the value  $(173 \pm 4)$  msec as the half-life of  $^{37}$ Ca.

The small peak in Fig. 1 appears to have a half-life not significantly different from that of the main peak, but threshold measurements could not be made, and positive identification was not possible. Since its intensity is only about 2 percent of that of the main peak, it is

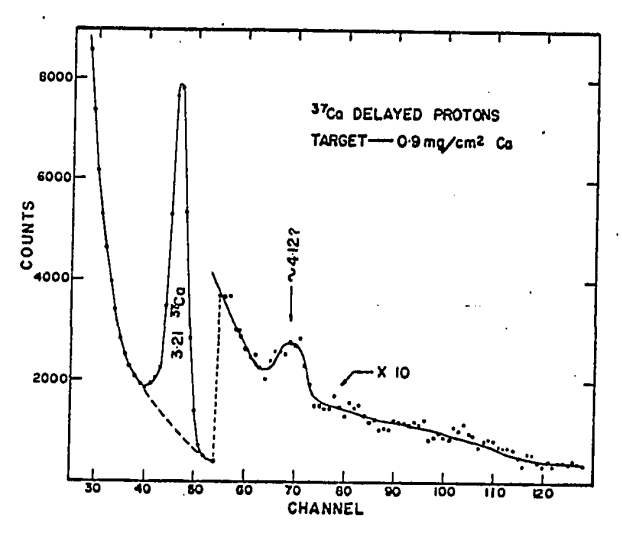


FIG. 1. The spectrum of delayed protons from a calcium target bombarded at 85 MeV in the cyclotron. The two peaks are marked with their center-of-mass energies computed for mass 37, but only the 3.21-MeV peak has been definitely assigned as following the <sup>37</sup>Ca decay.

ignored in what follows.

The energies of the peaks are shown, corrected to center of mass, in Fig. 1. The peak at  $(3.21\pm0.04)$  MeV corresponds to the decay of a level at  $(5.07\pm0.04)$  MeV in  $^{37}$ K [using Endt and van der Leun's value<sup>4</sup> of 1.86 MeV for the mass difference between  $(^{36}$ Ar +p) and  $^{37}$ K], which agrees with the predicted excitation energy (5.12 MeV) of the first  $T=\frac{3}{2}$  level in  $^{37}$ K. Such an assignment to this level would account for the fact that this peak appears with relatively high intensity, because the  $\beta^+$  decay to it from  $^{37}$ Ca would be superallowed.

Figure 2 shows the proposed decay scheme. which includes all relevant levels, and where the bracketed energies have been predicted only. The ft value for the electron capture decay  ${}_{18}^{37}\text{Ar}_{19} - {}_{17}^{37}\text{Cl}_{20}$  is known to be 1.14×10<sup>5</sup> sec, and one may assume that this value applies very nearly to the ground-state  $\beta^+$  decay  $^{37}_{20}$ Ca $_{17}$  -  $^{37}_{19}$ K $_{18}$ ; Bahcall<sup>1</sup> also calculates an ft value of  $1.9 \times 10^3$  sec for decay to the  $T = \frac{3}{2}$ level in  $^{37}\mathrm{K}$ . Using these assumptions and the measured lifetime, we have calculated approximate branching ratios for the two previously mentioned decays and the total of all other decays. Since decays to the two levels at 1.57 and 1.46 MeV are the only other ones that would contribute significantly, the branching ratios and decays should appear as in Fig. 2.

It is now possible to use these branching values for the mirror neutrino-capture reaction on <sup>37</sup>Cl. In reference 1, Bahcall made calculations concerning the cross section for the neutrino capture using estimated branching ratios. Repeating the calculation using the measured half-life and the subsequently modified ratios, a revised estimate for this cross section is obtained. This value predicts the total number of solar neutrino captures to be 3.1×10<sup>-35</sup>/(<sup>37</sup>Cl atom)-sec, a value 14%

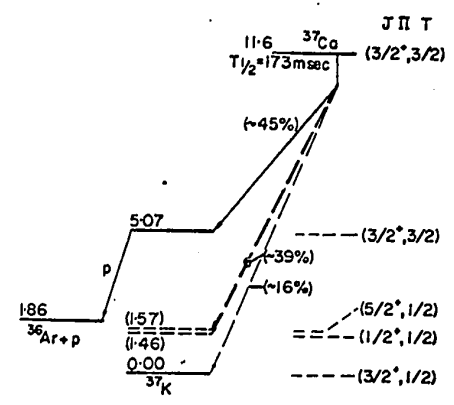


FIG. 2. Proposed decay scheme of  $^{37}$ Ca. Levels and decays that have not been directly observed are shown by dashed lines. Energies that are only estimated are shown in brackets. The  $\beta^+$  branching ratios have been estimated as described in the text.

lower than that in reference 1, Eq. (36), but well within the quoted errors.

We should like to thank Professor R. E. Bell, the director of the Laboratory, and Dr. R. Barton for helpful discussions. We acknowledge, also, scholarships awarded by the National Research Council.

<sup>†</sup>This research was supported by a grant from the Atomic Energy Control Board (Canada).

<sup>&</sup>lt;sup>1</sup>J. N. Bahcall, Phys. Rev. <u>135</u>, B137 (1964).

<sup>&</sup>lt;sup>2</sup>J. N. Bahcall and C. A. Barnes, Phys. Letters 12, 48 (1964).

<sup>&</sup>lt;sup>3</sup>R. Barton et al., Can. J. Phys. 41, 2007 (1963); R. McPherson, J. C. Hardy, and R. E. Bell, Phys. Letters 11, 65 (1964) (<sup>17</sup>Ne); R. McPherson and J. C. Hardy, to be published (<sup>21</sup>Mg and <sup>25</sup>Si); J. C. Hardy and R. I. Verrall, to be published (<sup>28</sup>S); J. C. Hardy and R. I. Verrall, to be published (<sup>33</sup>Ar).

<sup>&</sup>lt;sup>4</sup>P. M. Endt and C. van der Leun, Nucl. Phys. <u>34</u>, 1 (1962).

"Superallowed Log  $\underline{ft}$  Values for Transitions Between T = 3/2 Analogue States"

Reproduced from

Nuclear Physics

Volume 81, Number 1, 1966

Pages 113 - 119

# SUPERALLOWED $\log ft$ VALUES FOR TRANSITIONS BETWEEN $T = \frac{3}{2}$ ANALOGUE STATES

J. C. HARDY †, R. I. VERRALL and R. E. BELL Foster Radiation Laboratory, McGill University, Montreal

Received 21 December 1965

Abstract: The  $\log ft$  values have been measured for a number of  $\beta^+$ -decay branches from the delayed proton precursors  $^{21}\mathrm{Mg}$ ,  $^{25}\mathrm{Si}$ ,  $^{29}\mathrm{S}$ ,  $^{33}\mathrm{Ar}$  and  $^{37}\mathrm{Ca}$  by comparing the intensity of peaks in their delayed proton spectra with that of peaks in the spectrum following the decay of  $^{17}\mathrm{Ne}$ . In particular, each decay has a superallowed branch from the  $(T, T_z) = (\frac{3}{2}, -\frac{3}{2})$  precursor ground state to the  $(\frac{3}{2}, -\frac{1}{2})$  analogue level in its daughter nucleus. The measured log ft values for these branches agree quite well with calculations and are, in order, 2.9, 3.0, 3.1, 3.6 and 3.3, all values being  $\pm 0.3$ .

RADIOACTIVITY <sup>17</sup>F, <sup>21</sup>Na, <sup>25</sup>Al, <sup>29</sup>P, <sup>33</sup>Cl, <sup>37</sup>K [from (p,  $x\beta$ <sup>+</sup>)]; measured I (delayed protons); <sup>17</sup>Ne, <sup>21</sup>Mg, <sup>25</sup>Si, <sup>20</sup>S, <sup>33</sup>Ar, <sup>27</sup>Ca deduced log ft. Natural targets.

#### 1. Introduction

Recently, a number of new light nucleides with  $T_z = -\frac{3}{2}$  have been observed and their decay investigated  $^{1-9}$ )<sup>††</sup>. These nucleides are all delayed proton precursors. All have the form (Z, N) = (2k+2, 2k-1), all decay by the emission of positons, and in each case there are decay branches that lead to states in the daughter nucleus which are above the proton separation energy; these are characterized by the further emission of a proton. This branch of the decay may be written

$$(2k+2, 2k-1) \xrightarrow{\beta^+} (2k+1, 2k)^* \xrightarrow{p} (2k, 2k).$$
 (1)

Measurement of the energies and relative intensities of the observed proton groups yields corresponding information about the preceding  $\beta^+$ -decay branches, their energy and the relative branching intensities. However, it is only possible to obtain directly the partial half-lives, and hence  $\log ft$  values, if all branches in the  $\beta^+$ -decay of the precursor lead to proton-emitting levels, since then the total intensity of all decays can be measured.

The decay of <sup>17</sup>Ne is the only one in which this is the case. The ground state of <sup>17</sup>Ne is  $\frac{1}{2}$ , while the ground and first excited states of <sup>17</sup>F, its daughter, are  $\frac{5}{2}$  and  $\frac{1}{2}$  respectively. In fact, the lowest state in <sup>17</sup>F to which allowed decay is possible

4.C

E

<sup>†</sup> Now at Nuclear Physics Laboratory, Oxford.

<sup>&</sup>lt;sup>††</sup> Ref. <sup>1</sup>), <sup>17</sup>Ne, <sup>21</sup>Mg and <sup>25</sup>Si; ref. <sup>2</sup>), <sup>17</sup>Ne; ref. <sup>3</sup>), <sup>17</sup>Ne, <sup>29</sup>S and <sup>33</sup>Ar; ref. <sup>4</sup>), <sup>17</sup>Ne, <sup>21</sup>Mg and <sup>25</sup>Si; ref. <sup>5</sup>), <sup>21</sup>Mg and <sup>25</sup>Si; ref. <sup>6</sup>), <sup>29</sup>S; ref. <sup>7</sup>), <sup>33</sup>Ar; ref. <sup>8</sup>), <sup>37</sup>Ca and ref. <sup>9</sup>), <sup>33</sup>Ar and <sup>37</sup>Ca.

is at 3.10 MeV (2.50 MeV above the proton separation energy) and its de-excitation would result in delayed protons within the energy range of observation. The delayed proton spectrum has already been investigated  $^{1-4}$ ) between 2.5 and 8.0 MeV and, from the relative intensities of the proton groups, the log ft values for the  $\beta^+$ -decay branches have been obtained directly  $^{2,4}$ ).

The five other  $T_z = -\frac{3}{2}$  nucleides of interest here are <sup>21</sup>Mg, <sup>25</sup>Si, <sup>29</sup>S, <sup>33</sup>Ar and <sup>37</sup>Ca. The delayed proton spectra from their decays have previously been observed and investigated <sup>3-9</sup>) and consequently it has been possible to find the relative intensities of the  $\beta^+$ -decay branches from each. However, in each case allowed decay is possible to states in the daughter that are below the proton separation energy, and partial half-lives (and log ft values) could not be obtained.

It was of particular interest to measure partial half-lives for transitions from the five nucleides in question since in each case a decay branch had been observed to proceed to the lowest  $T = \frac{3}{2}$  level in the  $T_z = -\frac{1}{2}$  daughter (i.e. the analogue level); this decay branch was superallowed. Although calculations have been made for the log ft values between  $T = \frac{3}{2}$  levels <sup>10</sup>), no experimental measurements have been made of log ft values for such transitions.

#### 2. Method

It has been pointed out <sup>10</sup>) that it is possible to obtain the partial half-life of such a  $\beta^+$ -decay branch by comparing its intensity with that of a decay branch of <sup>17</sup>Ne. In practice, the total intensity of the proton groups that succeeded the unknown decay branch would be compared with that of a proton group in the <sup>17</sup>Ne spectrum.

Given two precursors X and Y, the partial half-life of a particular branch in the decay of X is related to that of one in Y by the formula

$$\frac{t(X)}{t(Y)} = C \frac{I(Y)}{I(X)} \frac{\sigma(X)}{\sigma(Y)},$$
(2)

where t is the partial half-life of the relevant transition, I the total intensity of the succeeding proton decay and  $\sigma$  the cross section for the production of the parent nucleide from the target material; C is a known factor which depends upon the total lifetimes and takes account of any differences in experimental arrangement between the two measurements, such as target thickness. Using this equation and a known half-life for <sup>17</sup>Ne, partial half-lives for transitions from other precursors may be found.

In order to make use of this formula, though, it is necessary to evaluate the ratio  $\sigma(X)/\sigma(Y)$ . Since it is possible to produce all of the previously mentioned precursors by means of (p, 3n) reactions on stable target materials, it is only necessary, therefore, to evaluate the ratio where both  $\sigma$  refer to the same type of reaction. This is done in the following manner. The six targets involved are <sup>19</sup>F, <sup>23</sup>Na, <sup>27</sup>Al, <sup>31</sup>P, <sup>35</sup>Cl and

<sup>39</sup>K. The centre-of-mass energy thresholds for (p, 3n) reactions on these nucleides all lie between 34.7 and 38.2 MeV, and the thresholds for other proton-induced reactions lie within equally narrow limits. At a bombarding energy well above thresholds, one is then justified in taking the ratio of (p, 3n) cross sections for any two such targets as equal to the ratio of their total reaction cross sections. The present measurements were made over 40 MeV above threshold.

Recently, total reaction cross sections have been measured for incident 100 MeV protons on 39 nucleides between beryllium and uranium <sup>11</sup>). From the results it was concluded that the reaction cross section  $\sigma_R$ , varies smoothly with the atomic number and can be accurately calculated by taking into account the geometrical cross section, Coulomb penetrability and nuclear opacity. The ratio  $\sigma_R(X)/\sigma_R(Y)$  may be calculated in this way and substituted for the cross section ratio in eq. (2).

Four of the precursors have also been obtained through (p, p3n)+(p, d2n) reactions. The same arguments may be applied to these cases, and eq. (2) used with the same substitution in the cross section ratio.

## 3. Experimental Technique

#### 3.1. BOMBARDMENT PROCEDURE

What must be measured experimentally is the ratio of the intensities of proton groups from different precursors produced under the same, or at least accurately known, conditions. To avoid the uncertainties involved in separate measurements, two targets were bombarded simultaneously and peaks in the composite spectrum compared directly. Either one target material was evaporated onto another (e.g. LiF onto Al foil) or a compound of the two target elements was evaporated onto thin gold foil (e.g. NaF or NaCl). The total thickness of the composite target never exceeded 5 mg/cm<sup>2</sup>.

Proton bombardments were carried out in the internal beam of the McGill synchrocyclotron in a manner which has been described  $^5$ ). Measurements were taken using a surface barrier silicon detector which was 200 mm² in area and had a 400  $\mu$ m depletion depth (7 MeV for protons). Target and detector were mounted about 6 cm apart and inserted on a radial probe to a radius at which the circulating proton beam had an energy of 80 MeV. Counting was performed between repetitive 30 msec bursts of normal cyclotron operation, a complete cycle consisting as well of a 100 msec pause followed by 533 msec of counting time.

It is evident that in the bombardment of a composite target both target materials receive the same number of incident protons, and both subtend the same solid angle from the detector. Further, since the efficiency of the counter is 100% for all protons striking it, and since the cyclotron magnetic field does not result in any significant variation of the effective solid angle over the entire range of proton energies, the ratio of the proton intensities is simply equal to the ratio of total counts in the peaks.

Following is a list of the targets bombarded. They are divided into three groups:

those involving (p, 3n) reactions, those principally involving (p, p3n)+(p, d2n) reactions and those involving both, this group being used only to cross-check the results of group 2. A "+" denotes "evaporated onto", but where a compound appears alone in the list it is to be understood that it was prepared by evaporation onto thin (200  $\mu$ g/cm²) gold foil; in all cases except those including sulphur, evaporation was performed in a vacuum. The precursors produced from each composite target are shown after it in brackets

- (i) LiF+Al( $^{17}$ Ne,  $^{25}$ Si); AlF<sub>3</sub>( $^{25}$ Si,  $^{17}$ Ne); NaF( $^{21}$ Mg,  $^{17}$ Ne); P+Al( $^{29}$ S,  $^{25}$ Si); NaCl( $^{21}$ Mg,  $^{33}$ Ar); NaCl+Al( $^{21}$ Mg,  $^{33}$ Ar,  $^{25}$ Si); KF( $^{37}$ Ca,  $^{17}$ Ne),
- (ii)  $S + Mg(^{39}S, ^{21}Mg); S + SiO_2(^{29}S, ^{25}Si); CaSO_4(^{37}Ca, ^{29}S),$
- (iii) Mg and Al (21Mg, 25Si); S+Al(29S, 25Si); Ca+Al(37Ca, 25Si).

#### 3.2. EFFECT OF TARGET COMPOSITION

Target materials in group (i), except chlorine and potassium, are monoisotopic. Natural chlorine is composed of <sup>35</sup>Cl(75.5%) and <sup>37</sup>Cl(24.5%), and it is from <sup>35</sup>Cl that <sup>33</sup>Ar is produced by (p, 3n) reaction, the lab threshold energy being 37.8 MeV. In order to investigate the effect of the (p, 5n) reaction from <sup>37</sup>Cl (threshold 57.3 MeV) on the production of <sup>33</sup>Ar, a NaCl target was bombarded at several different energies between 45 and 80 MeV and a ratio measured in each case between the rate of production of <sup>21</sup>Mg and that of <sup>33</sup>Ar. From these measurements, it was concluded that we could neglect the effects of the <sup>37</sup>Cl(p, 5n)<sup>33</sup>Ar reaction without affecting the errors quoted for the log ft values. The <sup>41</sup>K (p, 5n) reaction was similarly neglected in the case of potassium (<sup>39</sup>K, 93.2%; <sup>41</sup>K, 6.8%).

The target materials in group (ii) are not monoisotopic, but in all cases the delayed proton precursor is produced by (p, p3n) reaction from the most abundant stable isotope (> 90% abundance for all except magnesium). If an analogy is taken to the previous argument and the effect of (p, p5n) reactions neglected compared to that of (p, p3n) reactions, then only the latter reaction need be considered for all targets in this group except magnesium. From magnesium (24Mg, 78.8%; 25Mg, 10.1%; 26Mg, 11.1%), 21Na may be produced by the (p, p4n) reaction from a reasonably abundant stable isotope, 25Mg. In this case no correction was made, but the results obtained using a magnesium target were weighted less heavily in determining log ft values for 21Na.

#### 4. Experimental Results

#### 4.1. MEASURED log ft VALUES

It is evident from the proposed decay schemes of the delayed proton precursors (e.g. that of  $^{25}$ Si in ref.  $^4$ )) that the decay branches represented by eq. (1) can proceed either to the ground state  $(0^+)$  or first excited state  $(2^+)$  of the (2k, 2k) nucleus. In most cases there are, in addition, other more highly excited states to which proton decay is energetically possible, though severely retarded by the Coulomb barrier.

Since the  $\beta$ - and  $\gamma$ -background to the recorded proton spectra becomes large below 2.5 MeV, the protons corresponding to decay to these higher excited states would not have been observed. Therefore the total number of protons actually observed from the decay of a single level sets a lower limit to the intensity of the preceding  $\beta^+$ -transition, and from this an upper limit to the log ft value for that transition may be calculated.

Table 1 Experimental log ft values for the superallowed transitions

Precursor	Daughter	Analogue level (MeV)	Experimental log ft values	Revised experimental log ft values (±0.3)
<sup>21</sup> Mg	<sup>21</sup> Na	8.90	≦ 3.0	2.9
<sup>25</sup> Si	<sup>25</sup> Al	7.91	_ = 3.0 ≤ 3.0	3.0
<sup>29</sup> S	$^{20}\mathbf{P}$	8.36	<u>=</u> 3.0 ≤ 3.1	
. <sup>33</sup> Ar	33CI	5.55	≦ 3.6	3.1 3.6
<sup>37</sup> Ca	$^{37}\mathrm{K}$	5.07	≦ 3.4	3.3

Column four of table 1 gives the experimentally measured upper limits to the  $\log ft$  values that correspond to the superallowed transition from each precursor.

## 4.2. REVISED log ft VALUES

An estimate may now be made for the intensity of unobserved proton branches from the analogue levels and a final  $\log f$  evaluated. Penetration factors, calculated using an optical model potential, have been tabulated <sup>12</sup>); these values were used to obtain the total intensity of proton decay from each level, knowing from the preceding measurements the intensity of the one or two most intense branches and knowing also the energy and possible spin-parity of those levels to which decay is possible <sup>13</sup>).

TABLE 2
Experimental log ft values for other allowed transitions

Precursor	Daughter	Energy level (MeV)	Log ft values a)
<sup>21</sup> Mg	<sup>21</sup> Na	6.52 7.45	≤ 4.4 3.7-3.9
		(8.35) b)	4.2
<sup>25</sup> Si	<sup>25</sup> AI	7.14	3.7
		(9.03)	3.6
<sup>29</sup> S	29 P	8.08	4.4
<sup>33</sup> Ar	<sup>33</sup> Cl	7.55	≤ 4.1
37Ca	<sup>37</sup> Ķ	(5.91)	≦ 4.9

a) Uncertainty in these values is  $\pm 0.1$  relative to the corresponding superallowed branch.

b) Parentheses denote levels whose identification is not certain.

Column five of table 1 lists the values calculated in this manner; it can be seen that the effect of unobserved branches should be very small.

Once the  $\log ft$  value is known for the superallowed  $\beta^+$ -decay branch from each precursor, it is possible to calculate directly the  $\log ft$  values for all other observed decay branches simply from the intensity of peaks in the delayed proton spectrum. These results appear in table 2.

### 4.3. ESTIMATED UNCERTAINTY

In order to evaluate the uncertainty in the quoted values it is necessary to take into account not only the experimental errors but also those arising from the calculation of the intensity of the unobserved proton branches and from the use of an approximation to the cross-section ratio. Purely experimental errors correspond to an uncertainty of  $\pm 0.15$  in the  $\log ft$  values, but it is more difficult to assess the effect of the other two sources of error. Where two proton branches have been observed from one level, their relative intensities have been quite well duplicated by calculation, and since the effect of the unobserved branches is expected to be small, the uncertainty introduced by the calculation of their expected intensity should in all cases be less than  $\pm 0.05$ . Finally, the results of ref. <sup>11</sup>) and the consistency of the reaction thresholds indicate that the approximation to the cross-section ratio does not introduce large error.

To take account of all contingencies, the total uncertainty that is attached to the values in column five of table 1 is  $\pm 0.30$ . It should be noted that this represents a factor of 2 in the ft value, and is intended to be, if anything, an overestimate.

The uncertainty in the values shown in table 2 are  $\pm 0.1$  relative to the  $\log ft$  value for the superallowed decay branch from the relevant precursor.

#### 5. Discussion

Calculations <sup>10</sup>) have been made for  $\log ft$  values of the superallowed transitions shown in table 1, and these predicted that all values would lie between 3.25 and 3.30. Since for transitions between  $T=\frac{3}{2}$  states the Fermi matrix element is large (=  $\sqrt{3}$ ), the  $\log ft$  value does not depend very strongly on the model-dependent Gamow-Teller matrix element; this is reflected in the similarity of the calculated values.

The experimental results shown in table 1 agree well with the calculations, all but one being within  $\pm 0.3$  of 3.3. However, the accuracy is not sufficient to test details of the model used in the calculations.

It has been pointed out that of the principal sources of error in the present measurements was the uncertainty involved in the substitution for the cross-section ratio. This error could be greatly reduced if information were available concerning the excitation functions for, say, (p, n) or (p, pn) reactions on a number of targets in this region.

We should like to thank Professor B. Margolis and Dr. R. Barton for helpful discussions. Two of us (J.C.H. and R.I.V.) wish to acknowledge Studentships from the National Research Council (Canada) held during the course of the work. This research was supported by a grant from the Atomic Energy Control Board (Canada).

#### References

- 1) R. Barton et al., Can. J. Phys. 41 (1963) 2007
- 2) R. McPherson, J. C. Hardy and R. E. Bell, Phys. Lett. 11 (1964) 65
- 3) T. H. Braid, A. M. Friedman and R. W. Fink, Bull. Am. Phys. Soc. 10 (1965) 120, 658
- 4) J. C. Hardy and R. E. Bell, Can. J. Phys. 43 (1965) 1671
- 5) R. McPherson and J. C. Hardy, Can. J. Phys. 43 (1965) 1
- 6) J. C. Hardy and R. I. Verrall, Phys. Lett. 13 (1964) 148
- 7) J. C. Hardy and R. I. Verrall, Can. J. Phys. 43 (1965) 418
- 8) J. C. Hardy and R. I. Verrall, Phys. Rev. Lett. 13 (1964) 764
- 9) P. L. Reeder, A. M. Poskanzer and R. A. Esterlund, Phys. Rev. Lett. 13 (1964) 767
- 10) J. C. Hardy and B. Margolis, Phys. Lett. 15 (1965) 276
- 11) P. Kirkby and W. T. Link, to be published
- 12) G. S. Mani, M. A. Melkanoff and I. Iori, Report CEA 2379, Centre d'Études Nucléaires de Saclay (1963)
- 13) P. M. Endt and C. van der Leun, Nuclear Physics 34 (1962) 1

"An Extended Nomogram for Log  $\underline{ft}$  Values"

Reproduced from

Nuclear Instruments and Methods

Volume 42, Number 2, 1966

Pages 258 - 260



## AN EXTENDED NOMOGRAM FOR log ft VALUES

R. I. VERRALL, J. C. HARDY and R. E. BELL

Foster Radiation Laboratory, McGill University, Montreal, Canada

Received 24 March 1965

Recent work at this laboratory has required the calculation of log ft values for beta decays with a maximum energy greater than 9 MeV. For this purpose we have extended to higher decay energies the nomogram originally constructed by Moszkowski<sup>1</sup>). We have also increased the size of the nomogram and the number of grid lines in order to make its use convenient and accurate.

The graph (fig. 2) of the Coulomb correction factor  $(\log C)$  has also been extended in the same fashion. The value of C is given by 1):

$$C = (1/f_0) \int_{1}^{W_0} F(Z, W) W(W^2 - 1)^{\frac{1}{2}} (W_0 - W)^2 dW,$$

where the notation is standard. The exact values of F(Z,W) were obtained for a point nucleus. That is,

$$F(Z,W) = \frac{1}{2p^2} (g_{-1}^2 + f_{+1}^2),$$

where g and f are the "large" and "small" radial wave functions evaluated at the nuclear radius<sup>2</sup>). The McGill IBM 7044 computer was used to facilitate evaluation of the complex gamma and confluent hypergeometric functions as well as to carry out the integrations. Because of access to this computer, we were not forced to make the approximations made by Moszkowski, thus eliminating a possible source of error. It was found, however, that our results and those of Moszkowski agree remarkably well.

In addition, an approximate correction was made to take into account the effect of screening by the atomic electrons. This was done by replacing  $F(\pm Z, W)$  by<sup>3</sup>):

$$F(\pm Z, W \mp V_0)[\{(W \mp V_0)^2 - 1\}/(W^2 - 1)]^{\pm} \times \times (W \mp V_0)/W,$$

where the upper sign refers to electrons and the lower to positrons.  $V_0$  is given by  $V_0 = 1.13 \,\alpha^2 Z^{\frac{4}{3}}$ .

The effect of the finite size of the nucleus was not included in the corrections to  $\log C$ . Rose and Holmes<sup>4</sup>) have calculated the size of this correction for various values of Z and W for an assumed nuclear charge distribution. These calculations show that for values of Z less than 60 the correction is negligible. For a Z of 60,  $\log C$  would be lowered by about 0.01 and for a Z of 96,  $\log C$  would be lowered by about 0.09. The correction is almost independent of W. It was decided that these corrections were not appreciable enough to merit the additional calculations involved.

To use the nomogram place a straight edge on the appropriate maximum energy and partial half life of a  $\beta^{\pm}$  component and read the value of  $\log f_0 t$  on the third column (fig. 1). The  $\log f t$  value is given by

$$\log ft = \log f_0 t + \log C^{1/2}$$

It is evident that the chart extends well beyond the decay energies and  $\log ft$  values likely to be encountered. However, the ease with which the extension was made once the calculation was set up and the possibility of speculative interest in these regions, led us to include these higher values.

Two of us (R.I.V. and J.C.H.) wish to thank the National Research Council for scholarships. This work was supported by a grant from the Atomic Energy Control Board (Canada).

### References

- S. A. Moszkowski, Phys. Rev. 82 (1951) 35. The nomogram is reproduced in A. H. Wapstra, G. J. Nijgh and R. Van Lieshout, Nuclear Spectroscopy Tables (North-Holland Publishing Co., Amsterdam, 1959).
- 2) M. E. Rose, Relativistic Electron Theory (Wiley and Sons Inc.) Ch. 5.
- 3) E. J. Konopinski and M. E. Rose in Alpha-, Beta- and Gammaray Spectroscopy. (ed. K. Siegbahn, North-Holland Publishing Co., Amsterdam, 1965) Ch. 23, p. 1339.
- 4) M. E. Rose and D. K. Holmes, Phys. Rev. 83 (1951) 190.

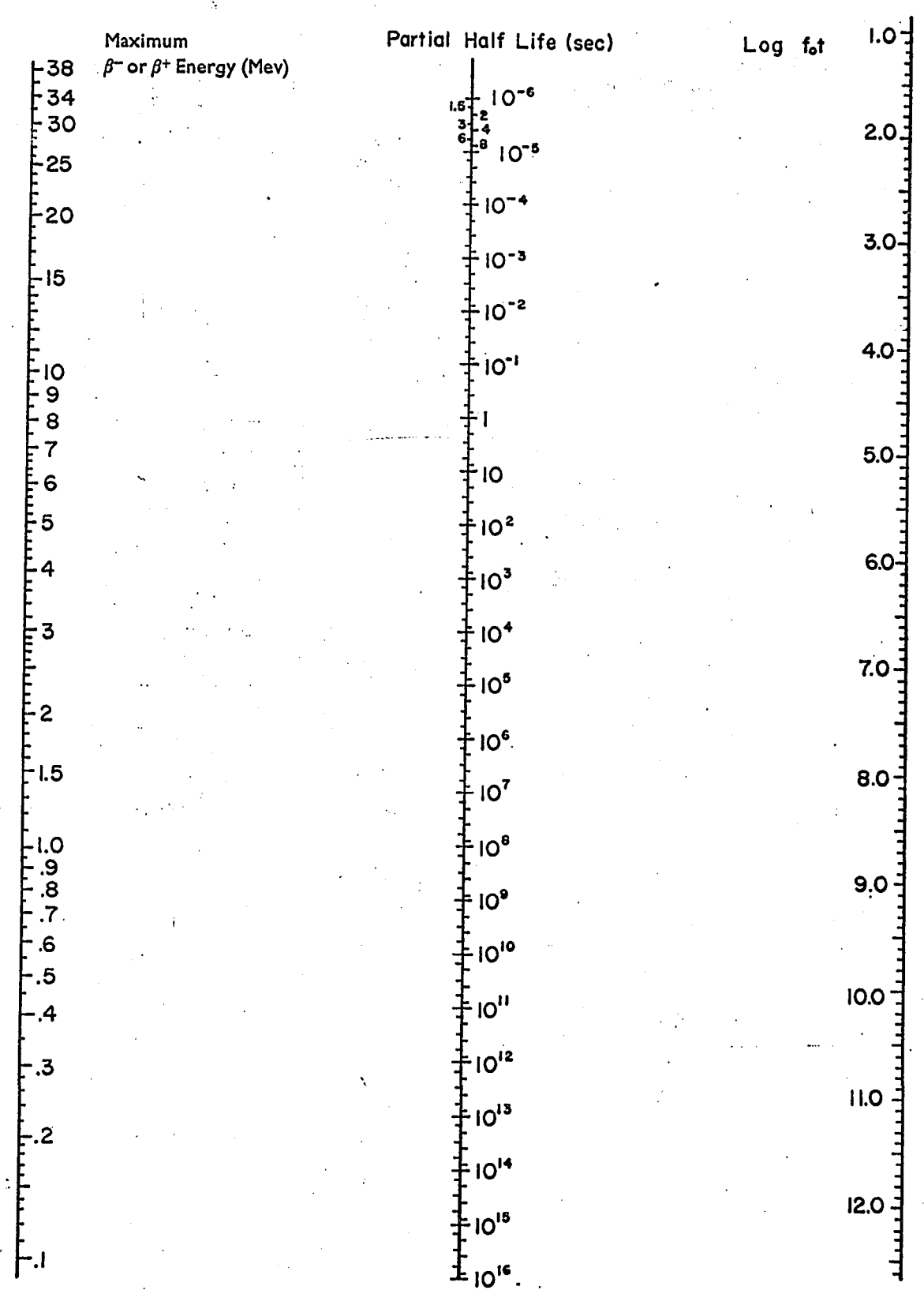


Fig. 1. Nomogram relating  $\log f_0 t$  value to the maximum  $\beta^{\pm}$  decay energy and the partial half life of the decay.

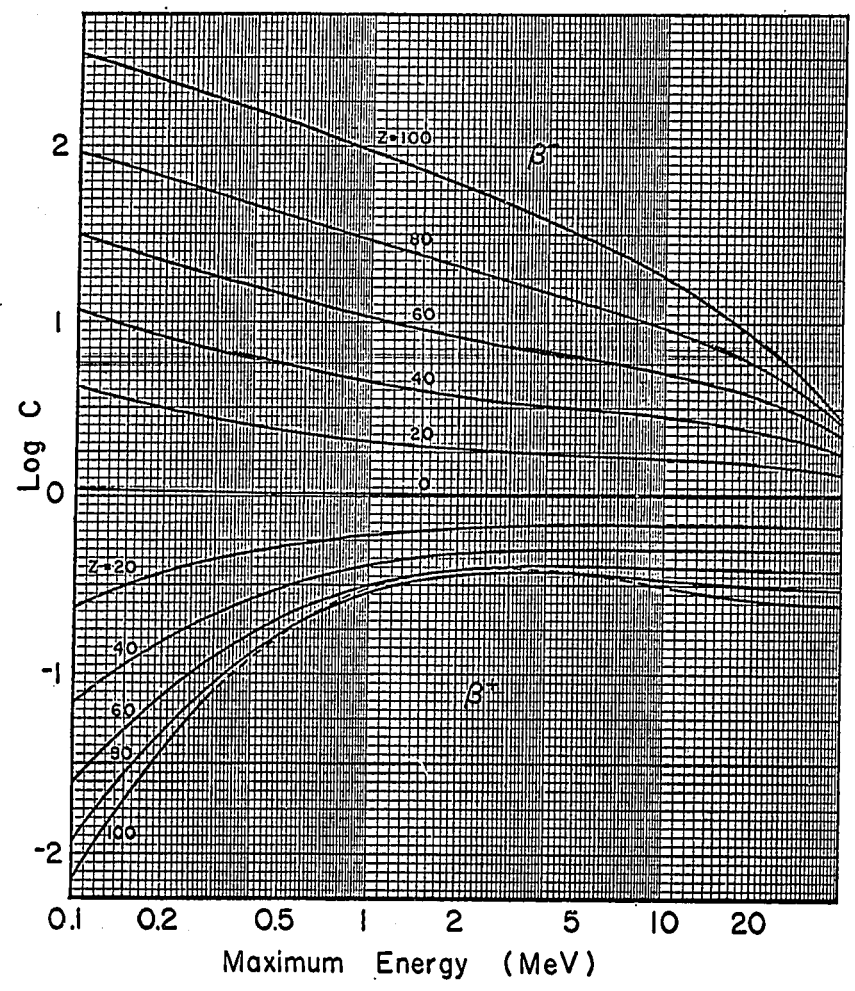


Fig. 2. Coulomb correction factor (log C). The Z value is that of the parent nucleus. Add log C to log  $f_0t$  to obtain log ft.

#### RANGE ENERGY CALCULATIONS

When the gas detector system was used, the observed protons had to pass through the mylar ( $C_{10}H_8O_4$ ) front window and the methane ( $CH_4$ ) filling gas before they were stopped in the silicon detector. In order to correct the proton energies for energy loss in these two media, it was necessary to have the appropriate range energy tables. Since these tables are not readily available, it was necessary to calculate them. Also, since alpha sources of known energies were used to determine the thickness of the window and the gas, it was necessary to calculate similar tables for alpha particles.

To calculate the dE/dx at a particular energy for a compound one uses the expression

$$\frac{dE}{dx} = \sum_{\text{compound}} f_i \frac{dE}{dx} \Big|_{i}$$

where i represents the different elements present, and fi is the fraction of the mass which that element represents. For example,

$$\frac{dE}{dx} \Big|_{CH_4} = .75 \frac{dE}{dx} \Big|_{Carbon} + .25 \frac{dE}{dx} \Big|_{Hydrogen}$$

The values of dE/dx for the elements were taken from the tables of Williamson and Boujot (1962).

Having calculated values for dE/dx for the compound we can calculate the range ( $R_0$ ) for various energies ( $E_0$ ) using the relationship

$$R_{o} = -\int_{0}^{E_{o}} \frac{dx}{dE} dE = -\int_{0}^{E_{o}} \frac{1}{\frac{dE}{dx}} dE$$

The quantity dE/dx is inherently negative; hence the appearance of the minus sign.

When l/(dE/dx) for the protons is plotted versus E, one obtains a curve which is nearly linear. For this reason a simple trapezoidal integration formula was used for the numerical integration. At the low energy end of this plot, the curve was extrapolated linearly to zero energy. Since this extrapolation is over only 50 keV, any error in this approximation will contribute negligibly to the integration.

The above procedure was also used for the alpha particle curves, except that in the low energy region, where - dx/dE is not linear, more points were evaluated and Simpson's formula was used for the numerical integration. It is felt that uncertainties in the results are due mainly to uncertainties inherent in the original tables.

The values of R and dE/dx for alphas and protons in methane and mylar are tabulated in Tables A7.1 to A7.4.

TABLE A7.1
PROTONS IN MYLAR

Energy (MeV)	$\frac{\mathrm{dE}}{\mathrm{dx}} \left( \frac{\mathrm{MeV cm}^2}{\mathrm{g}} \right)$	Range (g/cm <sup>2</sup> )
<b>.</b> 05	9.35 x 10 <sup>2</sup>	4.95 x 10 <sup>-5</sup>
•1	8.23	1.07 x 10 <sup>-4</sup>
•2	6.38	2.46
•3	5•23	4.20
•4	4.46	6.28
•5	3•90	8.68
•6	3.48	$1.14 \times 10^{-3}$
•7	3.15	1.44
<b>.</b> 8	2.88	1.78
•9	2.66	2.14
1.0	2.47	2.53
1.2	2.18	3 <b>-39</b>
1.4	1.95	4•37
1.6	1.77	5•45
1.8	1.62	6.63
2.0	1.50	7.91
2.5	1.27	1.16 x 10 <sup>-2</sup>
3.0	1.10	1.58
4.0	8.82 x 10 <sup>1</sup>	2•60
5.0	7.40	3.84
6.0	6.40	5•30
7.0	5.61	6.97
8.0	5•09	8.85
9.0	4•77	1.09 x 10 <sup>-1</sup>
10.0	4.25	1.31

TABLE A7.2

### PROTONS IN METHANE

Energy (MeV)	$\frac{\mathrm{dE}}{\mathrm{dx}} \left( \frac{\mathrm{MeV cm}^2}{\mathrm{g}} \right)$	Range (g/cm <sup>2</sup> )
•05	1.85 x 10 <sup>3</sup>	2.32 x 10 <sup>-5</sup>
•1	1.45	5•39
.2	1.04	$1.36 \times 10^{-4}$
•3	8.12 x 10 <sup>2</sup>	2.42
•4	6.74	3•78
•5	<b>5.79</b> °	5 <b>•</b> 38
<b>.</b> 6	5.10	7.23
•7	4.57	9•30
.8	4.15	$1.16 \times 10^{-3}$
•9	3.81	1.41
1.0	3.52	1.69
1.2	3.07	2.29
1.4	2.73	2•99
1.6	2.47	3.76
1.8	2.25	4.61
2.0	2.08	5•53
2.2	1.93	6.53
2.4	1.80	7.61
2.6	1.69	8.76
2.8	1.59	9.98
3.0	1.51	$1.13 \times 10^{-2}$
3•4	1.40	1.40

TABLE A7.2 (cont'd.)

Energy (MeV)	$\frac{\mathrm{dE}}{\mathrm{dx}} \left( \frac{\mathrm{MeV cm}^2}{\mathrm{g}} \right)$	Range (g/cm <sup>2</sup> )
3.8	1.25 x 10 <sup>2</sup>	1.71 x 10 <sup>-2</sup>
4.2	1.15	2.04
4.6	1.07	2.40
5•0	9.99 x 10 <sup>1</sup>	2.79
6.0	8.61	3.87
7.0	7.59	5.11
8.0	6.80	6.49
9.0	6.17	8.04
10.0	5.66	9.73

TABLE A 7.3

# ALPHAS IN MYLAR

Energy (MeV)	$\frac{\mathrm{dE}}{\mathrm{dx}} \; (\frac{\mathrm{MeV} \; \mathrm{cm}^2}{\mathrm{g}})$	Range (g/cm <sup>2</sup> )
•05	1.09 x 10 <sup>3</sup>	5.54 × 10 <sup>-5</sup>
.1	1.66	9•34
•2	2.23	1.46 x 10 <sup>-4</sup>
•3	2•45	1.89
•4	2.51	2.29
•5	2.50	2.69
•6	2.45	3.09
•7	2.38	3.51
.8	2.30	3•94
•9	2.22	4•38
1.0	2.14	4.84
1.5	1.79	7.40
2.0	1.53	$1.04 \times 10^{-3}$
2.5	1.34	1.39
3.0	1.19	1.79
4.0	9.83 x 10 <sup>2</sup>	2.72
5•0	8.40	3.82
6.0	7•37	5•09
7•0	6.58	6.53
3.0	5•96	8.13
9.0	5.46	9.88
0.0	5.04	1.18 x 10 <sup>-2</sup>

TABLE A7.4

## ALPHAS IN METHANE

Energy (MeV)	$\frac{\mathrm{dE}}{\mathrm{dx}} \; (\frac{\mathrm{MeV cm}^2}{\mathrm{g}})$	Range (g/cm <sup>2</sup> )
•05	2.32 x 10 <sup>3</sup>	2.70 x 10 <sup>-5</sup>
•1	3.42	4+51
•2	k•32	7.07
•3	4.51	9•32
•4	4.45	$1.16 \times 10^{-4}$
•5	4.30	1.38
•6	4.11	1.62
•7	3.92	1.87
•8	3•73	2.13
•9	3•55	2.41
1.0	3•38	2.69
1.2	3.09	3•31
1.4	2.83	3•99
1.6	2.62	4.73
1.8	2•43	5•52
2.0	2•28	6•37
2.2	2.14	7.27
2.6	1.91	9•26
3.0	1.73	$1.15 \times 10^{-3}$
3•4	1.58	1.39
3.8	1.45	1.65
4.2	1.35	1.94

TABLE A7.4 (cont'd.)

Energy (MeV)	$\frac{\mathrm{dE}}{\mathrm{dx}} \; (\frac{\mathrm{MeV} \; \mathrm{cm}^2}{\mathrm{g}})$	Range (g/cm <sup>2</sup> )
4.6	1.26 x 10 <sup>3</sup>	2.25 x 10 <sup>-3</sup>
5.0	1.19	2.57
6.0	1.03	3.48
7.0	$9.16 \times 10^2$	4.51
8.0	8.25	5•66
9.0	7•53	6.93
LO.0	6•93	8.32

### EFFECTIVE SOLID ANGLE OF A DETECTOR IN A MAGNETIC FIELD

When a source and detector are placed in a magnetic field, the effective solid angle for the detection of charged particles is dependent on the energy of the particles. To compare the intensities of peaks of different energies, it is necessary to know the form of this dependence.

The problem will be treated in two stages. In the first, a simple point source is assumed and collimation effects are assumed to be absent. In the second stage, an estimation is made of the effect of the collimation inherent in the detector system.

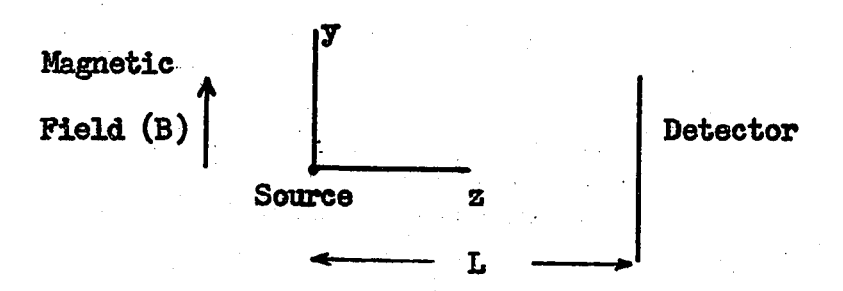


Fig. A8.1

The assumed geometry is shown in fig. A8.1. The magnetic field B is in the y direction, the detector axis lies along the z direction, and the source is at the origin of the co-ordinate system.

If a particle of mass m, charge e and initial velocity  $\overrightarrow{V} = (\overrightarrow{V}_x, \overrightarrow{V}_y, \overrightarrow{V}_z)$  is emitted from the source, its resultant motion is found to be, letting  $\omega = (Be)/m$ :

$$x = \frac{V_x}{\omega} \sin \omega t - \frac{V_z}{\omega} (1 - \cos \omega t) \qquad \qquad \dots \qquad 1$$

$$z = \frac{V_x}{\omega} (1 - \cos\omega t) + \frac{V_z}{\omega} \sin\omega t$$
 ... 2

$$y = V_y t$$
 ... 3

We now write  $(V_x, V_y, V_z)$  in terms of V and the spherical co-ordinates  $(\Theta, \phi)$ 

$$V_{x} = V \sin \theta \cos \phi$$

$$\nabla_{\mathbf{y}} = \nabla \sin \theta \sin \phi$$

Substituting these expressions into equations 1, 2 and 3 we have (x, y, z) in terms of  $(\Theta, \phi, t)$ . The problem now is to determine  $d\Omega = \sin\Theta d\Theta d\phi$  in terms of dxdy, the corresponding element of area at the target. We will then integrate the expression over the target area to determine the solid angle subtended by the detector. This is done as follows.

We write

$$dx dy dz = J(\frac{x,y,z}{\theta,\phi,t}) d\theta d\phi dt$$

$$= J(\frac{x,y,z}{\theta,\phi,t}) J(\frac{\theta,\phi,t}{\theta,\phi,z}) d\theta d\phi dz$$

where the J's are the appropriate Jacobians. Cancelling dz and rearranging we obtain

$$d\Theta d\phi = \frac{J(\underline{\Theta}, \phi, \underline{z})}{\underline{B}, \phi, \underline{t}} dx dy = \frac{\underbrace{\partial \underline{z}}{\partial \underline{t}}}{\underbrace{J(\underline{x}, y, \underline{z})}} dx dy$$

$$d \Omega = \sin\theta d \theta d \phi = \frac{\sin\theta \frac{\partial Z}{\partial t}}{J(\frac{X,Y,Z}{\theta,\phi,t})} dx dy \qquad ... 4$$

The expression multiplying dx dy must be evaluated at the detector, i.e. at z = L, and at the particular values of (x,y) in question. Since the expression can be written down most easily in terms of  $(\theta,\phi,t)$  we must solve equations 1, 2, and 3 for  $\theta,\phi$ , t, substitute the results into equation 4 and integrate the result over the surface of the detector. The equations were solved by an iterative procedure, and the numerical integration was performed using equation 25.4.61 in the "Handbook of Mathematical Functions". This numerical work was done by a computer.

For L = 5.38 cm and a circular detector of radius 0.8 cm (the standard geometry), the resulting solid angle as a function of energy is shown as the solid line in fig. A8.3.

The actual geometry is more complicated, however. The presence of the gas counter and some shielding causes an effective collimation. In the presence of a magnetic field, this collimation will shield the detector from the source to a degree depending on the energy of the proton. Fig. A8.2 shows the correct geometry with an assumed point source. The dotted curve represents the path of a proton with an energy of 0.17 MeV. It can be seen that protons with less energy than this cannot get to the detector.

Using graphical methods, an approximation was made of the amount of the detector "visible" to the target. This was used to estimate the effective solid angle. The result is shown in fig. A8.3 as the dashed line. In the region of interest, the effect is small, ( $\approx 5\%$  correction at 1 MeV).

<sup>1.</sup> U.S. Dept. of Commerce, Series 55 (1965), Edited by M. Abramowitz and I.A. Stegun.

Therefore the accuracy of the calculation is sufficient for the purpose of this thesis. The fact that the source has a small finite area is estimated to have a negligible effect on the above calculations.

Line of the Figure A8.2 . At the

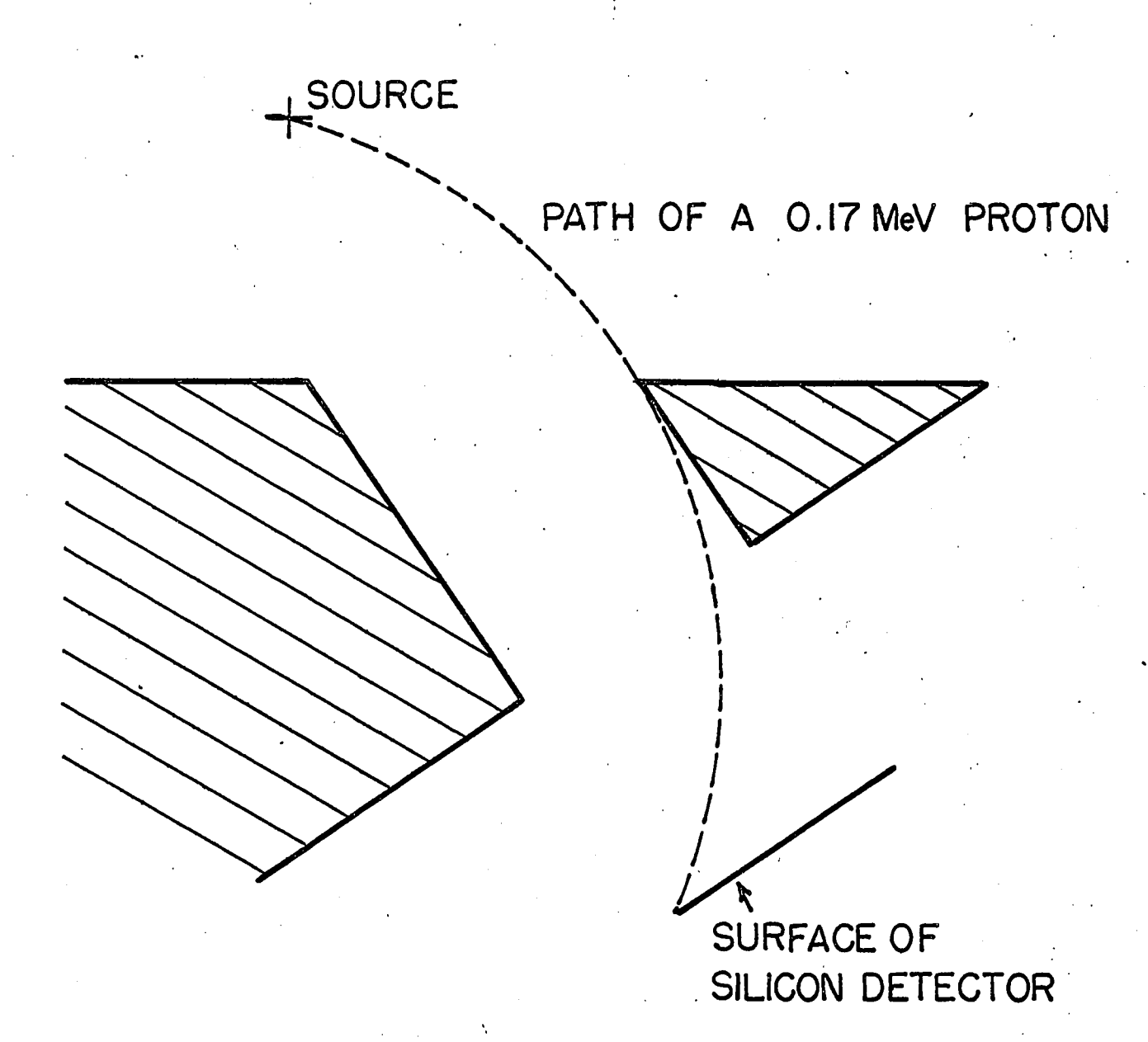
Sometimes of the State of the S

where the end of the the miles of the end of the end

instance of a decision of the second of the

Figure A8.2: Scale diagram of the source-detector geometry showing the collimation effect of the supporting structure. The path of the proton with the smallest observable energy (0.17 MeV) is shown.

(The magnetic field is normal to the diagram.)



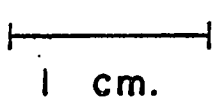


FIGURE A8.3

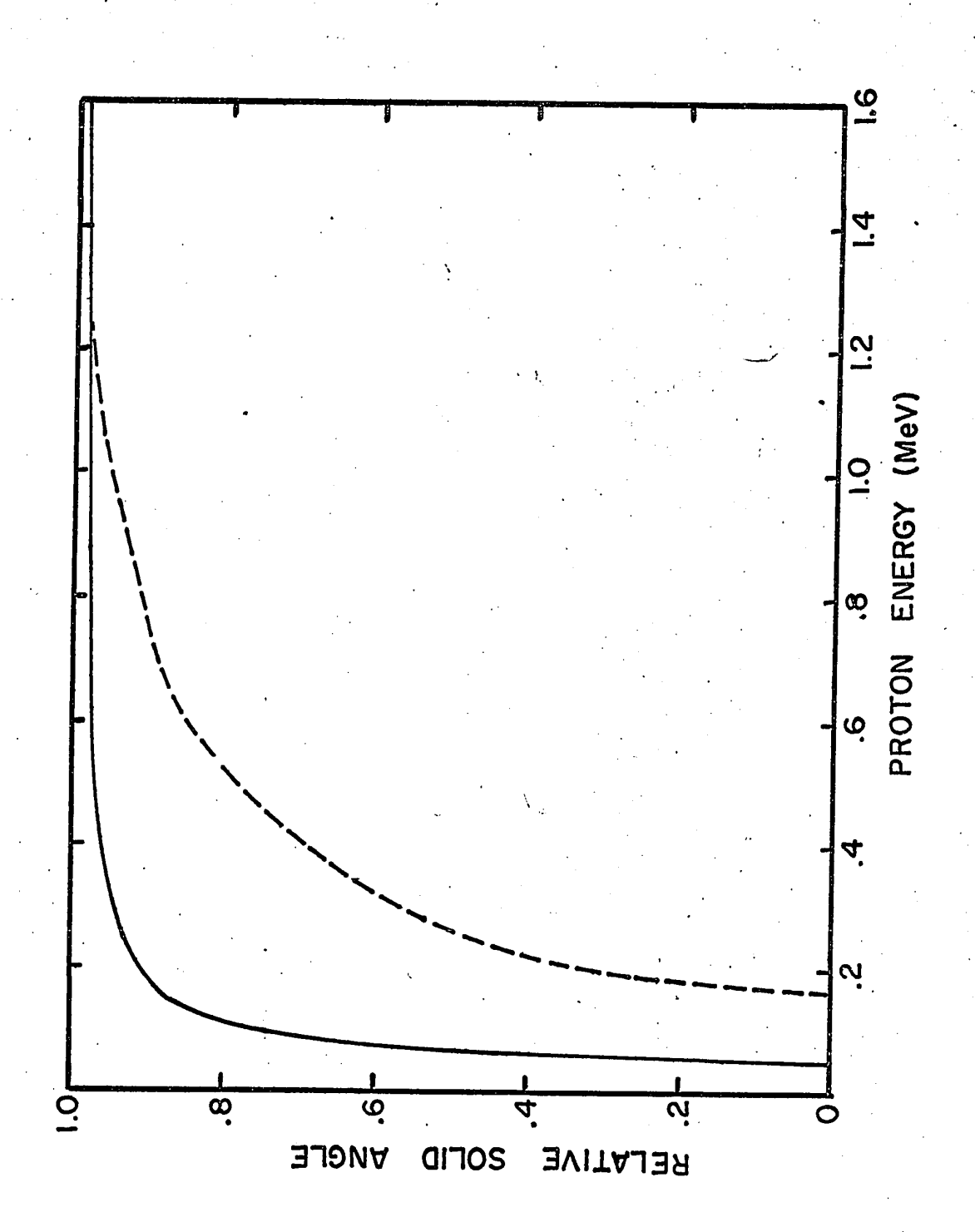
· n to one of the stag and

Control of the contro

in the control of the section of the control of the

There was a decidence of wage with when

grison ititum (e. 19<mark>44) est e est e</mark>, a lug dan lu <mark>kil</mark> sala . Mest kanste it tirom e til viga men (e. 1985) lukti. Figure A8.3: Effective solid angle of the standard sourcedetector geometry as a function of proton
energy. The curve is normalized to the solid
angle with the magnetic field off. The solid
line does not take into account the collimating
effect of the apparatus. The dotted curve does
take this into account.



#### APPENDIX 9

SQUARE ROOT GRAPH PAPER1

Some of the proton spectra in this thesis are plotted on a new type of graph paper in which the distance above the base line at which a number is plotted is proportional to the square root of the number. The paper was designed after seeing a publication by Hooton (1967) in which this kind of scale was suggested for the oscilloscope display of spectra accumulated in a multichannel analyser. Hooton's motive was to provide a display in which the scatter of the points due to their ordinary Poisson errors would be independent of the position of the points on the display. This property follows so long as the variance of an observed number N is proportional to N, as in Poisson statistics. A plotted multichannel spectrum having a large number of channels should then appear as a band of points having a constant vertical width. This is an obvious convenience in the analysis of spectra.

Square root graph paper (or a square root display) also has advantages for showing a spectrum whose intensity covers a wide range. Linear paper overemphasizes the high intensity region with the result that low intensity peaks tend to disappear. A multi-cycle logarithmic scale, on the other hand, overemphasizes the low intensity region and compresses the high intensity peaks. On a 4-cycle logarithmic scale, for example, three-quarters of the area of the graph is devoted to the intensities lying below 10% of full scale. In addition, the value zero cannot be plotted on a logarithmic scale. Square root paper lies between the extremes of these two commonly used scales.

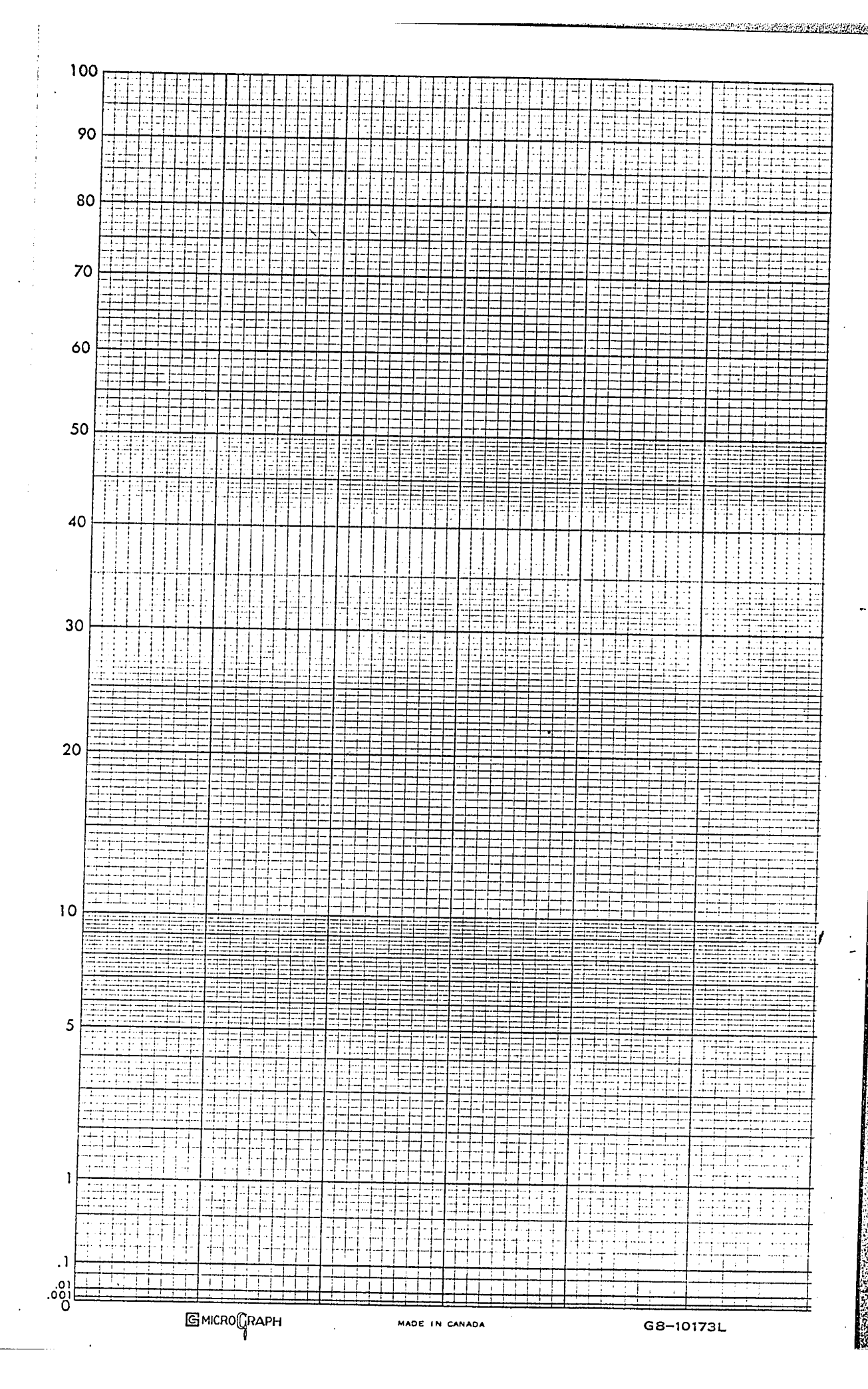
Available in 11" x 17" sheets from Graphic Controls Inc., Montreal, Number G8 - 10173L.

A note is presently in preparation for submission to "Nuclear Instruments and Methods" describing the graph paper and mentioning its availability.

An  $8^{n} \times 11^{n}$  facsimile of the paper is shown in fig. A9.1.

FIGURE A9.1

Figure A9.1: A reproduction of the "Square Root" graph paper which is now commercially available.



ALVAREZ, L. (1950) Phys. Rev. 80, 519.

ARMINI, SUNIER and RICHARDSON (1966) Bull. Amer. Phys. Soc. 11, 909.

BARTON, R. 1963 Ph.D. Thesis, McGill University (unpublished).

BARTON, R., McPHERSON, R., BELL, R.E., FRISKEN, W.R., LINK, W.T. and MOORE, R.B. (1963) Can. J. Phys. 41, 2007.

BAVARIA, G.K. (1966) M.Sc. Thesis, McGill University (unpublished).

BAZ, A.I. (1959) Atomnaya Energia 6, 571.

BOGDANOV, D.D., DAROTSI, Sh., KARNAUKHOV, V.A., PETROV, L.A. and TER-AKOP'YAN, G.M. (1967) Report JINR (Dubna) E6-3142.

BROMLEY, D.A., OVERLY, J.C. and PARKER, P.D. (1966) Phys. Rev. Letters 17, 705.

D'AURIA, J.M. and PREISS, I.L. (1964) Phys. Letters 10, 300.

ENDT, P.M. and VAN DER LEUN, C. (1967) Nucl. Phys. AlO5, 1.

EJIRI, H. et al. (1964) Nucl. Phys. 52, 561.

ESTERLUND, R.A., McPHERSON, R., POSKANZER, A.M. and REEDER, P.L. (1967)

Phys. Rev. 156, 1094.

FLEROV, G.N., KARNAUKHOV, V.A., TER-AKOP'YAN, G.M., PETROV, L.A. and SUBBOTIN, V.G. (1964) Nucl. Phys. 60, 129.

FLEROV, G.N., KARNAUKHOV, V.A., TER-AKOP'YAN, G.M., PETROV, L.A. and SUBBOTIN, V.G. (1965) Soviet Physics, JETP 20, 278.

GLASS, N.W. and RICHARDSON, J.R. (1955) Phys. Rev. 98, 1251.

GOLDANSKI, V.I. (1960) Nucl. Phys. 19, 482.

GOLDANSKI, V.I.(1961) Nucl. Phys. 27, 648.

GOLDANSKI, V.I. (1966) Ann. Rev. Nucl. Sci. 16, 1.

HARDY, J.C. (1965) Ph.D. Thesis, McGill University (unpublished).

HARDY, J.C. and BELL, R.E. (1965) Can. J. Phys. 43, 1671.

HARDY, J.C. and MARGOLIS, B.M. (1965) Phys. Letters 15, 276.

HARDY, J.C. and VERRALL, R.I. (1964a) Phys. Letters 13, 148.

HARDY, J.C. and VERRALL, R.I. (1964b) Phys. Rev. Letters 13, 764.

HARDY, J.C. and VERRALL, R.I. (1965) Can. J. Phys. 43, 418.

HARDY, J.C., VERRALL, R.I., BARTON, R. and BELL, R.E. (1965) Phys. Rev. Letters 14, 376.

HARDY, J.C., VERRALL, R.I. and BELL, R.E. (1966) Nucl. Phys. 81, 113.

HOOTON, B.W. (1964) Nucl. Inst. and Methods 27, 338.

HOOTON, I.N. (1967) Nucl. Inst. and Methods 56, 277.

JAENECKE, J. (1965a) Nucl. Phys. 61, 326.

JAENECKE, J. (1965b) Nucl. Phys. 73, 97.

KARNAUKHOV, V.A., TER-AKOP'YAN, G.M. (1964) Phys. Letters 12, 339.

KARNAUKHOV, V.A., TER-AKOP'YAN, G.M. and SUBBOTIN, V.G. (1962) Report JINR (Dubna) Plo72. Also, Soviet Physics, JETP 18, 879 (1964).

KIENLE, P. and WIEN, K. (1963) Nucl. Phys. 41, 608.

LEDERER, C.M., HOLLANDER, J.M. and PERLMAN, I. (1967) Table of Isotopes, Sixth Edition, John Wiley and Sons, Publishers.

MacFARLANE, R.D. and SIIVOLA, A. (1964) Nucl. Phys. 59, 168.

MANI, G.S., MELKANOFF, M.A. and IORI, I. (1963) Rapport C.E.A. 2379, Centre d'Etudes Nucleaires de Saclay.

MARGOLIS, B. and de TAKACSY, N. (1965) Phys. Letters 15, 329.

McPHERSON, R., ESTERLUND, R.A., POSKANZER, A.M. and REEDER, P.L. (1965)

Phys. Rev. 140, B1513.

McPHERSON, R. and HARDY, J.C. (1965) Can. J. Phys. 43, 1.

McPHERSON, R., HARDY, J.C. and BELL, R.E. (1964) Phys. Letters 11, 65.

MOSZKOWSKI, S.A. (1951) Phys. Rev. 82, 35.

POSKANZER, A.M., McPHERSON, R., ESTERLUND, R.A. and REEDER, P.L. (1966)

Phys. Rev. 152, 995.

PRESTON, M.A. (1962) Physics of the Nucleus, page 451. Addison-Wesley Publishing Co. Inc.

REEDER, P.L., POSKANZER, A.M. and ESTERLUND, R.A. (1964) Phys. Rev. Letters 13, 767.

REEDER, P.L., POSKANZER, A.M., ESTERLUND, R.A. and McPHERSON, R. (1966)

Phys. Rev. 147, 781.

SEEGER, P.A. (1961) Nucl. Phys. 25, 1.

SIIVOLA, A.T. (1965) Phys. Rev. Letters 14, 140.

SILBERT, H.G. and HOPKINS, J.C. (1964) Phys. Rev. 134, B16.

VERRALL, R.I., HARDY, J.C. and BELL, R.E. (1966) Nucl. Inst. and Methods 42, 258.

WATT, D.E. (1967) Nucl. Inst. and Methods 50, 353.

WILLIAMSON, C.F. and BOUJOT, J.P. (1966) "Tables of Range and Rate of Energy Loss of Charged Particles of Energy 0.5 - 150 MeV." Rapport CEA - R3042, Centre d'Etudes Nucleaires de Saclay.

ZEL'DOVICH, Ya.B. (1960) JETP 11, 812.